REVIEWS OF
MODERN PHYSICS

VOLUME 38, NUMBER 4 OCTOBER 1966

Quantization of Macroscopic Motions and Hydrodynamics of Rotating Helium II

E. L. ANDRONIKASHVILI, YU. G. MAMALADZE
Institute of Physics, Academy of Sciences of the Georgian SSR, Tbilissi, U.S.S.R.

This paper is a review of experimental data and theoretical studies devoted to the rotating helium II problem. The problem arose when helium II appeared to be rotating as a whole in a uniformly rotated container, while dragging of its superfluid component into rotation of a cylindrical vessel seemed impossible due to the absence of viscosity and Landau's requirement curl $\mathbf{v}_s=0$. Later it was found that imitation of a solid body rotation by helium II is realized by means of Onsager–Feynman's vortex lines which possess quantized circulation. In a uniformly rotating vessel they are distributed approximately uniformly along its cross section, aligned parallel to the axis of rotation, and cause a complicated velocity distribution at which $\operatorname{curl}\mathbf{v}_s=(2\pi\hbar/m)\Sigma_v\delta(\mathbf{r}-\mathbf{r}_v)$, that is, Landau's requirement is valid everywhere excluding singular lines where the curl is equal to infinity ($\mathbf{r}_v$ is a two-dimensional radius vector of a vortex line in an arbitrary plane perpendicular to the axis of rotation).

In the review the experiments are described in which both an averaged picture of the joint rotation of the superfluid and the normal components is displayed and the studies in which the existence of vortex peculiarities is manifested in a clear manner. The measurements of the meniscus of rotating helium II and its angular momentum belong to the first group of these experiments ("integral" ones). Propagation of second sound, oscillations of solid bodies immersed into helium II, passage of negative ions, and different relaxation processes (acceleration and deceleration of the vessel, changes of temperature, etc.) form the second group ("local" experiments). The experiments in which the superfluid performs potential rotation, which can be persistent in the vessel at rest are also described. Vortex lines are absent there and the circulation of velocity can reach the value equal to a lot of elementary circulations.

Special attention is devoted to the problem of the nature of the phase transition helium I–helium II (and back) in the state of rotation.

The properties of rotating helium II illustrate brightly the main peculiarity of a quantum liquid, i.e., its complete inability to perform nonpotential motions. They show that Landau's requirement curl $\mathbf{v}_s=0$ remains valid even when the thermodynamical condition of the free-energy $(E-L\omega_0)$ minimization gives preferrence to the velocity distribution of the type $v=\omega_0 r$.

CONTENTS

1. THE ORIGIN OF THE ROTATING HELIUM II PROBLEM

1.1. How the Problem of Rotating Helium II Has Arisen

While explaining the experiments of Kapitza (1938a, b, 1941a, b), who discovered and studied the phenomenon of superfluidity, Landau (1941) suggested the two-fluid theory of a quantum liquid (see, also, Landau, 1944, 1947; Lifshitz and Andronikashvili, 1959). Using not quite rigorous, but very convenient, and therefore widely spread, terminology for the physical interpretation of the experimental facts, we can describe the main principles of this theory in the following way. Helium II consists of two fluids, one of them is a normal (n) component, which is an ordinary viscous liquid. The properties of this liquid depend on the existence of thermal excitations in helium, which are called rotons and phonons (in accordance with the different types of energy dependence on the momentum in different parts of the dispersion curve). The other one is a superfluid (s) component with zero viscosity and zero entropy. In addition, it cannot perform nonpotential motions. The character of motion of each of the components can be quite different. In other words, one can axcribe two celocities $\mathbf{v}_n$ and $\mathbf{v}_s$ and two densities ρ_n and ρ_s to each point of space, so that $\rho_n+\rho_s=\rho$. Here ρ is an ordinary density of the liquid, while ρ_n and ρ_s are the effective densities of motions performed with the velocities $\mathbf{v}_n$ and $\mathbf{v}_s$, respectively. With a rise in temperature, elementary excitations (phonons and rotons) involve larger and larger parts of the liquid in thermal motion, and thus the normal component density is increased, while that of the superfluid one is decreased: $\rho_n/\rho=0$, when $T=0°\mathrm{K}$ and $\rho_n/\rho=1$, when $T=T_\lambda=2.17°\mathrm{K}$. The latter temperature corresponds to the point of the phase transition.

Simultaneous with the creation of his theory, Landau suggested some experiments to test its validity. One was an experiment in which the properties of helium II in a rotating vessel would be studied. It was assumed that, because of the absence of viscosity and the necessity of maintaining the condition curl $\mathbf{v}_s=0$, the superfluid component would not take part in the rotation of the vessel and only the normal component would be rotated.

Such an experiment, the aim of which was to show directly the possibility of the simultaneous existence of two independent fields of velocities $\mathbf{v}_s$ and $\mathbf{v}_n$, was really performed by Andronikashvili (1946, 1948a), but in quite a modified form. Axial oscillations of a vessel with a pile of closely spaced parallel thin disks, suspended in helium II by means of an elastic thread, were realized instead of rotation. The normal component was dragged into the motion of the disks completely, while the superfluid one did not take any part in it. One could detect this phenomenon by measurements of the period of oscillations of the suspended system, determined by its moment of inertia. This moment of inertia consisted of the moment of inertia of the vessel and that of the normal component. The investigations performed allowed confirmation of the existence of the two components in helium II and the possibility of the simultaneous realization of two different motions in this liquid, as well as establishing the temperature dependence of ρ_n.

At that time, the difference between rotation and axial oscillations seemed quite unessential. But soon, when Andronikashvili (1948b, published in the paper of Andronikashvili and Kaverkin, 1955) performed an experiment with really rotating helium, the result was

quite different. Helium II seemed to rotate like a solid body.

1.2. The First Observations of Rotating Helium II

The idea of the experiment mentioned above, as well as that of the similar Osborne's experiment (1950), was the following. As is well known, a rotating viscous liquid eventually forms a parabolic meniscus, the shape of which depends on the force of gravitation and on centripetal force. Because of that, in particular, the depth of the meniscus h is equal to

$$h=\omega_0^2R^2/2g, \qquad (1.2.1)$$

where ω_0 is the angular velocity of rotation, R is the radius of the vessel, and g is the acceleration of gravity. It would seem that in the case of helium II the whole thing would be quite different. In this case the force of gravity acts on the whole bulk of the liquid, while the centripetal force would have to act only on its normal component, since it is assumed that the superfluid component does not rotate. Therefore, one should expect that the shape of the meniscus would depend on the amount of the superfluid component, i.e., on temperature, and its depth would be determined by the formula

$$h=(\rho_n/\rho)(\omega_0^2R^2/2g). \qquad (1.2.2)$$

In both experiments described, vessels with a radius of the order of centimeters were used and the velocity of rotation was about some tens of radians per second. There was no difference in the depths of the meniscus of helium I and helium II at any temperature and velocity of rotation. Formula (1.2.1) was always rigorously maintained, which gave an impression that helium rotated like a solid body.

Thus, in these experiments helium II behaved as if it were rotating as a classical liquid. The only small difference which could be noticed at maximum velocities of rotation was that a small conic pit appeared at maximum velocities of rotation on the lower part of the parabolic meniscus (Andronikashvili and Kaverkin, 1955).

Participation of the superfluid component in rotation of the vessel was also found in the experiments of Hall (1955; see, also, Hall and Vinen, 1955), who used a vessel filled with closely spaced disks for this purpose, which dragged the normal component into motion completely. The angular momentum of helium II was measured by determination of the torsion effect, which was required to accelerate and slow down the liquid.

In addition, Hall and Vinen (1955) have shown that rotating helium II renders an additional resistance to propagation of thermal waves called second sound. Attenuation of these waves in their propagation perpendicularly to the axis of rotation depended on velocity, increasing linearly with an increase of ω_0. For propagation of second sound along the rotation axis, its attenuation was the same as in helium II at rest.

1.3. Is Rotating Helium II a Superfluid?

At the time when nothing was known about the physical nature of critical phenomena in helium II, any interaction of the superfluid component with the walls of the vessel or with the normal component caused an idea of the breakdown of superfluidity. Such a possibility was foreseen by Landau's theory, according to which a body moving in helium II with the velocity of about 60 m/sec could generate thermal excitations (rotons) there. In this way, the liquid lost the ability to flow without friction. The idea of the breakdown of superfluidity also appeared in the association of the establishment of a solid-body rotation of helium. But it was found (Andronikashvili and Kaverkin, 1955) that the fountain effect[1] continued to exist in rotating helium II and had the same value as in helium II at rest. This fact was an obvious demonstration of the existence of the superfluid, which, being a liquid with zero entropy, flows towards a source of heat to get entropy and become normal. Moreover, it was also established that the relative content of the superfluid and normal components did not depend on the velocity of rotation.

We have already mentioned the experiments performed by Hall and Vinen (1955). In them the existence of the superfluid component in rotating helium II and the independence of its amount on the velocity of rotation were displayed in the absence of any dependence of the velocity of second-sound propagation u on ω_0 (u is, as is known, a function of the ratio ρ_s/ρ_n).

1.4. Summary of the Aspects of the Rotating Helium II Problem by 1955

Thus the rotating helium II problem arose in Andronikashvili's and Osborne's experiments as early as the end of the forties, when oscillating disk experiments were already finished, and not in 1941, when Landau proposed an experiment with rotating helium II. We can hardly be sorry about this delay. On the contrary, though it may sound paradoxical, one might fear that the discovery of the superfluid participation in the rotation of the container could have slowed down the development of the theory of superfluidity for several years. Fortunately, this fact was established only after the first confirmations of Landau's theory had been obtained in the experiments with a pile of oscillating

[1] The fountain effect is a phenomenon in which the superfluid component has a tendency to move through narrow pores or slits towards a source of heat. Since the normal component under such conditions cannot move towards the superfluid, a pressure difference arises on the porous partition. It is one of the particular manifestations of the thermomechanical effect which causes the superfluid component motion in the direction of the temperature gradient, while the normal component flows in the opposite direction [see Eqs. (4.2.1) and (4.2.2)].

disks and in experiments with second sound. A number of successes of the theory followed, and an unexpected result of one experiment could not have shaken the confidence in the validity of the principal ideas of the two-fluid hydrodynamics of helium II. In addition, the qualitative characteristics of many phenomena, which were specific for superfluid helium, were well studied by that time. Some of them, in particular the fountain effect and second sound, had been observed in rotating helium. This was a very essential thing, which showed that the existence of the superfluid component rotation did not mean the breakdown of superfluidity. In this respect, the experiment did not contradict Landau's theory, according to which the corresponding critical velocity was about 60 m/sec, while in the experiments of Osborne, Andronikashvili, and Kaverkin, and Hall and Vinen the maximum velocity on the periphery of the container was several orders smaller. Only the existence of the superfluid component in these experiments showed that the nature of the critical phenomena is not connected with the breakdown of superfluidity spoken about in Landau's theory.

Nevertheless, the mechanism of dragging of the superfluid component into rotation and the very character of this rotation remained quite obscure. In particular, the question of the maintenance of the Landau condition, curl $\mathbf{v}_s=0$, remained open. It seemed that most probably this condition was broken, and the theory required an essential revision of its principles.

1.5. The Purpose and the Plan of this Review

While writing this review, the authors aimed at showing how the problems summarized in the previous paragraph were explained and at describing the further development of theoretical and experimental studies of rotating helium II. Section 2 is devoted to ideas of Onsager and Feynman, who developed Landau's theory for supercritical phenomena. The Landau–Onsager–Feynman conception is the basis of all further considerations. Then, beginning with Sec. 3, without any chronological order, the authors systematically describe the main results of practically all experimental and theoretical investigations devoted to the rotating helium problem.

However, attention is mainly devoted to those experiments, the precision and clarity of purposes of which provided the possibility of a quantitative treatment of the data obtained, or at least extraction of important qualitative conclusions from them. A similar principle has been used for the description of the results of theoretical investigations when we tried, in the main, to show clearly the physical picture of the phenomena considered. Wishing to describe all the observed phenomena from one general point of view, the authors have deliberately avoided Lin's hydrodynamics (1959, 1963), in spite of the fact that without doubt it is interesting and deserves great attention. The authors think that at present there are not sufficient data to oppose this theory to the Landau–Onsager–Feynman conception or to give a parallel interpretation of phenomena using Lin's conception. On the one hand, there are no results of some decisive experiment, which could not have been explained by the Landau–Onsager–Feynman theory. On the other hand, there are no solutions of sufficient number of concrete problems within the framework of Lin's theory, without which it is impossible to describe all or at least the most available data from the point of view of this theory.

2. PRINCIPLES OF ONSAGER–FEYNMAN THEORY

2.1. Vortex Lines in the Superfluid Component of Helium II

It has already been noted that the critical phenomena connected with the appearance of an interaction of the superfluid component and solid bodies have nothing to do with the breakdown of superfluidity. In accordance with Onsager's assumption (1949), they are connected with the appearance of vortex lines in the superfluid component of helium II. The circulation of such vortex lines is quantized in units of $\Gamma_0=h/m$ (where h is Planck's constant and m is the mass of the helium atom). In the precritical regime, the superfluid does not interact with solids (Dalamber's paradox). But in the postcritical regime, when vortex lines are present, it can have such an interaction without losing its superfluid properties. Let us recollect that a classical ideal liquid, when it has vortex lines, also breaks Dalamber's paradox (vortex resistance).

As for the circulation quantization, it explains the very fact of the critical velocity's existence. Indeed, if a vortex line cannot exist in a state with an arbitrary small intensity (circulation), then vortex formation can take place only if some minimum energy is available in the stream of fluid or in a body immersed into the liquid.

However, it is well known that the classical theorems of Helmholtz–Thomson–Lagrange forbid general vortex formation in an absolutely ideal liquid performing potential motion. Even now it is not quite clear what properties of a quantum liquid allow breaking the requirements of those theorems. Nevertheless, Feynman used quantum-mechanical ideas to explain the possibility of vortex formation and showed that a vortex hypothesis can explain the established fact of the superfluid rotation (1955, 1957).

The argument in favor of the possibility of vortex existence in a superfluid is associated with consideration of the following situation. Let helium II at the temperature absolute zero ($\rho_n=0$) be at rest in a semispace $z<0$ and in the state of uniform motion along the x axis in the semispace $z>0$. Then if the wave function of the liquid at rest is Φ_0, the wave function in the upper semispace will be $\Phi_0 \exp(ikx)$, where k is the wave number, related in the usual way to the velocity of motion. We shall question what will happen further,

whether such a state of the liquid will remain or whether an interaction between the semispaces will take place, bringing into motion the liquid in the lower semispace as well. The absence of viscosity excludes the presence of tangent forces on the interface $z=0$, and one can think that volumes of helium in the state of motion and of helium at rest are really isolated from each other and that the surface energy of the interface $z=0$ is higher, the higher is the relative velocity [Fig. 2.1(a)]. But we pay attention to the fact that the function $\Phi_0 \exp(ikx)$ turns periodically into Φ_0 with the period $\Delta x=2\pi/k$. On the corresponding lines (parallel to the y axis), the conception of the surface energy of the interface becomes senseless and nothing can prevent moving helium from flowing into the region of helium at rest and make it move to the other side of the interface. But the interface cannot exist in the form of flat strips; their cross sections are shown in Fig. 2.1(b). The surface tension should draw them up into lines (points in the section), and they would quite disappear if there were no centrifugal forces created by rotation of the liquid [Fig. 2.1(c)]. Estimation of the radius of cylinders formed in such a way, according to the equilibrium of the surface tension forces and centrifugal one, gives a meaningless value of the order of some tenths of an angstrom. It is clear that in such a case either the radius of the order of interatomic distances in helium II (Feynman used the magnitude $a_0=4$ Å) would be ascribed to this cylinder (to the vortex core) or the use of such macroscopic conceptions as surface tension or size of a hollow core in general should be renounced in favor of a more detailed description. For such a more detailed quantum description, a vortex line should be considered as a node line of the wave function, i.e., the line on which the wave function is equal to zero.[2] Then the parameter a_0 acquires the meaning of a characteristic distance from this line, within which the density of the liquid is appreciably different from its value in bulk. We return to such a description in Sec. 12.

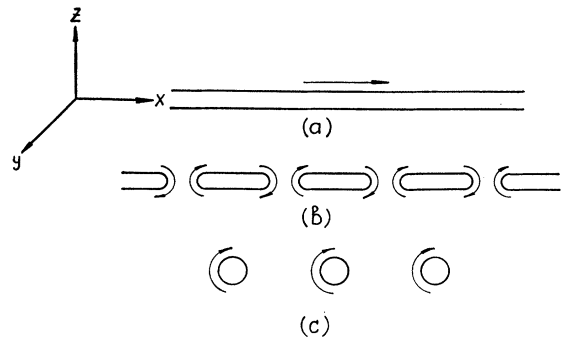

FIG. 2.1. The evolution of ideas on the nature of interface separating semispaces with helium II at rest and in the state of motion: (a) solid surface; (b) the surface torn along the lines on which wave functions of helium at rest and in motion coincide; (c) surface tension and centrifugal force make the "strips" of the interface cylindrical.

[2] It should be noted, as Feynman pointed out, that the appearance of node lines in an excited state is characteristic of the general behavior of quantum systems. Let us recollect, for instance, a harmonic oscillator. Its wave function in an unexcited state has no nodes, and each next stage of excitation increases the number of its nodes.

Though the present consideration represents a speculative experiment rather than a study of some real process, we think it has a deeper sense. Evidently it shows instability of tangent discontinuity of velocity well known in the case of a classical liquid (Landau and Lifshitz, 1953). Figure 2.1 then represents to some extent the real course of the events after a jet of superfluid flows from a hole into a large volume. Apparently the process of a vortex street formation following the motion of a body in a superfluid liquid is developed in a similar way (von Karman's chains).

2.2. Quantization of the Circulation

Having generalized the wave function of uniformly moving helium II $\Phi_0 \exp[(m/\hbar)\sum_a \mathbf{v}\cdot\mathbf{R}_a]$ (the sum is taken over all the atoms of the system), Feynman suggested writing the wave function arbitrarily moving helium II ($T=0°$K) in the form $\Phi_0 \exp(i\phi)$. The velocity of the liquid flow is related with the phase of the wave function by the expression $\mathbf{v}_s=\hbar\nabla\phi/m$. The existence of a vortex line requires a change of the wave function phase on going once round a singular point (line). However, because of the unambiguity of the wave function, the change of its phase cannot be arbitrary at one complete revolution, but should be a multiple of 2π. Considering rotation of a liquid particle round a vortex line, the phase change per revolution along the circumference with a vortex line as its center will be equal to

$$\oint \nabla\phi = d\mathbf{r}\frac{2\pi r m v_s}{\hbar};$$

hence, the condition of circulation quantization will be (n is an integer):

$$2\pi r v_s = n(2\pi\hbar/m), \qquad (2.2.1)$$

or in a more general form (for an arbitrary contour),

$$\Gamma \equiv \oint \mathbf{v}_s \cdot d\mathbf{r} = n(2\pi\hbar/m) \equiv n\Gamma_0. \qquad (2.2.2)$$

Since the circulation along any contour is equal to a sum of circulations along the contours it contains, condition (2.2.2) is valid for integration over a closed curve including a number of vortex lines. The number n in this case is a sum of integers, characterizing intensities of different vortex lines. In particular, if all the vortex lines are unit ones (with the circulation Γ_0), this number is simply equal to the number of vortex lines in the contour.

Thus the formation of superfluid vortex lines was the first phenomenon that required application of the quantization principle, similar to Bohr's postulate, to the motion the scale of which can be measured even

by centimeters. It is essential that according to (2.2.1) the distribution of the superfluid velocity round the vortex line is given by the law

$$v_s = n\hbar/mr. \tag{2.2.3}$$

It means that one of the main requirements of Landau's theory, namely, curl $\mathbf{v}_s = 0$, which remains valid over all the bulk of the liquid (because of the determination of the velocity by means of the gradient of the phase), is broken only on vortex lines themselves, where the curl is infinite but the density is equal to zero.

2.3. Energy and Tension of Vortex Lines

Now let us calculate the energy of a liquid rotating according to law (2.2.3). For unit length of a vortex line, it is

$$\epsilon = \int \frac{\rho_s v_s^2}{2} 2\pi r\, dr = \pi\rho_s \frac{\hbar^2}{m^2} \ln\frac{b}{a_0}, \tag{2.3.1}$$

where b is the effective radius of a vortex line determined by the dimensions of the vessel (if there is one vortex line) or by the vortex separation (if there are many vortex lines).

According to Bernoulli's equation, pressure in a liquid is equal to $P = P_0 - \rho_s v_s^2/2$, where, in the case of rotation according to (2.2.3), P_0 is the maximum pressure at an infinite distance from a vortex line. Nearer the core of a vortex line, the pressure decreases, creating the force with which a vortex line is attached to the surface on which it ends (Hall, 1957a). As a result, a vortex line is in a strained state and its tension force is $\int (P_0 - P)\, 2\pi r\, dr$, and according to (2.3.1) it coincides numerically with the energy ϵ of its unit length [this is clear, since its tension is equal to $\partial(\epsilon s)/\partial s$, where s is the vortex line length]. Elastic properties of vortex lines are determined by these phenomena.

2.4. Rotation of a Superfluid Liquid

The physical nature of critical phenomena in helium II is connected with the fact that a superfluid liquid, remaining superfluid, interacts, because of the existence of vortex lines, with solids or with the normal component.

Feynman has shown that the critical velocities of vortex formation are much lower than that of the breakdown of superfluidity caused by roton formation (according to Landau this velocity is 60 m/sec). It should be emphasized once more that critical phenomena at low velocities have nothing in common with the breakdown of superfluidity and, therefore, do not contradict Landau's theory.

Potential rotation, described by formula (2.2.3), is unfavorable thermodynamically. Rotation performed according to the law

$$v = \omega_0 r, \tag{2.4.1}$$

characteristic of a viscous liquid, provides a smaller value of the energy E at a given momentum $\mathbf{L}$ or, that is the same a smaller value of the free energy $F = E - \mathbf{L}\cdot\boldsymbol{\omega}_0$. But Feynman has noticed that in the presence of a great number of vortex lines, which (interacting with each other and being also attached to the bottom and top or to a free surface) rotate together with the vessel, the summary distribution of velocities in a superfluid liquid approaches closely law (2.4.1). This situation is illustrated by Fig. 2.2, which shows schematically that the mean velocity of the superfluid $\bar{v}_s$ is also determined by the formula $\bar{v}_s = \omega_0 r$ at the motion of vortex lines according to the law $v_L = \omega_0 r$. The difference between the true value of the velocity in a given point and the mean velocity is essential only in the vicinity of the considered vortex line. The existence of a number of vortex lines with unit circulation provides greater proximity of $\bar{v}_s$ to $\omega_0 r$ than the existence of a smaller number of vortex lines with great circulations. Therefore it is natural to consider that all the vortex lines have the circulation Γ_0 in uniformly rotating helium II.

2.5. Density of Vortex Lines

Let us consider some circumference with the center on the axis of rotation. The circulation of the mean velocity on it will be $2\pi r \cdot \omega_0 r$; on the other hand, as it has been already mentioned, it is equal to the number of vortex lines multiplied by Γ_0. Therefore the number

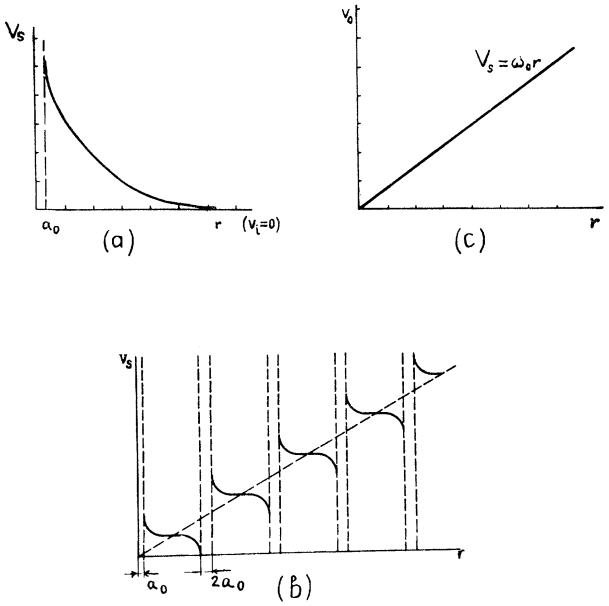

FIG. 2.2. Curl-free rotation of the liquid around vortex lines, which in their turn rotate around the common axis, leads in an average to solid-body rotation of the liquid around this axis. The figure shows: (a) the distribution of velocity around unit stationary vortex line, a_0 is the radius of the vortex core; (b) the distribution of velocities around some vortices the cores of which rotate according to the law $v_L = \omega_0 r$; (c) the distribution of velocities averaged over the volume containing several vortices.

of vortex lines piercing the unit cross section of the liquid is

$$N=2\omega_0/\Gamma_0=m\omega_0/\pi\hbar. \quad (2.5.1)$$

When $\omega_0=1$ sec^{-1}, this formula gives $N\approx 2\times 10^3$ vortex lines per square centimeter.

2.6. The Critical Velocity of Vortex Formation

The angular velocity of rotation at which the first vortex line appears on the axis of a cylindrical vessel with the radius R was calculated by Arkhipov (1957) and Vinen (1958a):

$$\omega_{c1}=[\hbar/m(R^2-a_0^2)]\ln(R/a_0). \quad (2.6.1)$$

When $\omega_0>\omega_{c1}$,[3] the contribution of a vortex line into the magnitude $E-L\omega_0$ becomes negative as the value of E for unit lengths is determined by formula (2.3.1) and $l=L/s=\pi\rho_s\hbar(R^2-a_0^2)/m$. It is easy to see by means of the direct calculation of the integral $l=\int\rho_s r v_s\cdot 2\pi r\,dr$, where v_s is determined by formula (2.2.3). Therefore, starting from this velocity, the vortex formation is favorable thermodynamically. The critical velocity ω_{c1} is very small. When $R\sim 10$ cm, it is $\omega_{c1}\sim 10^{-5}$ sec^{-1}, when $R\sim 1$ cm, it is $\omega_{c1}\sim 10^{-3}$ sec^{-1}. Hence, almost at any real velocities of the vessel, rotating helium is in the supercritical regime and contains a lot of vortex lines. The only exception arises for devices with extremely small characteristic dimensions.

When $\omega_0\gtrsim\omega_{c1}$, the number of vortex lines is not yet determined by Feynman's formula (2.5.1). Formula (2.5.1), when $\omega_0=\omega_{s1}$, gives the expression $N\cdot\pi R^2=\ln(R/a_0)$ for the total number of vortex lines in the cylinder instead of unity. This magnitude is always bigger than unity. In this connection, Kiknadze, Mamaladze, and Cheishvili have also estimated the critical velocity ω_{s1}' starting from which the presence of vortex lines with the density (2.5.1) becomes favorable thermodynamically. Such an estimation can be made proceeding from considerations similar to those used for the just mentioned formula of Arkhipov–Vinen (2.6.1). The energy of vortex lines (reduced to unit height of the vessel) is estimated in this case as $E_1=E_{sb}+E_v$; $E_{sb}=0.25\omega_0^2R^4\pi\rho_s'E_v=N\cdot\pi R^2\cdot\epsilon$, where ϵ is given by formula (2.3.1), in which the magnitude of the order of $(\hbar/m\omega_0)^{\frac{1}{2}}$ should be used as $b(\pi b^2\sim 1/N)$:

$$E_v=\omega_0R^2\pi\rho_s(\hbar/m)\ln(\hbar/m\omega_0a_0^2)^{\frac{1}{2}}. \quad (2.6.2)$$

The angular momentum of the superfluid component caused by vortex lines L_1 (also reduced to unit height), when there is a lot of vortex lines, coincides with its value at rotation of the liquid as a whole. As the contribution of each vortex line is $\pi\rho_s(\hbar/m)(R^2-r^2)$, where r is the distance from the vortex line to the cylinder axis, we have the following:

$$L_1\approx\int_0^R\pi\rho_s\frac{\hbar}{m}(R^2-r^2)\frac{m\omega_0}{\pi\hbar}2\pi r\,dr=\tfrac{1}{2}\omega_0R^4\pi\rho_s. \quad (2.6.3)$$

Hence, the contribution made by vortex lines to the magnitude $E-L\omega_0$ becomes negative when $\omega_0=\omega_{c1}'$, where $\omega_{c1}'=E_1/L_1$:

$$\omega_{c1}'=(4\hbar/mR^2)\ln(\hbar/m\omega_{c1}'a_0^2)^{\frac{1}{2}}\sim 4\omega_{c1}. \quad (2.6.4)$$

As the value of the magnitude ω_{c1} is small, one can conclude from formula (2.6.4) that the formation of vortex lines and the increase of their density until equal to the values corresponding to formula (2.5.1) takes place in a very narrow interval of angular velocities in rotating vessels, the dimensions of which are not extremely small. At the beginning of this interval, the number of vortex lines could be equal to $\ln R/a_0$, according to (2.5.1), but the presence of only one vortex line is favorable thermodynamically. At the end of this interval, the favorable number of vortex lines is equal to $2\ln(\hbar/m\omega_{c1}'a_0^2)^{\frac{1}{2}}$; that is in complete agreement with formula (2.5.1).

3. VORTEX LINES IN UNIFORMLY ROTATING HELIUM II. IMITATION OF THE SOLID BODY ROTATION OF A LIQUID

3.1. Meniscus of Rotating Helium II

It was said in the previous sections that, in the experiments of Osborne (1950) and Andronikashvili and Kaverkin (1955), the meniscus of rotating helium II was such as if the liquid rotated like a solid body.

Turkington, Brown, and Osborne (1963) reduced the minimum value of the angular velocity to $\omega_0=1.58$ sec^{-1} and used an oblique light beam, reflected from the meniscus, to measure the curvature of the free surface of the liquid. The results are shown in Fig. 3.1.

The curvature of the free surface of a thin layer of helium II at the bottom of a rotating cylindrical container was measured by a very sensitive method by Meservey (1964). The depth of the liquid layer was only 5×10^{-3} cm. The meniscus of rotating helium II, at rotation with the velocity to 0.29 sec^{-1}, at 1.1°K, was indistinguishable from the meniscus of a classical liquid. The results of Meservey are given in Fig. 3.2.

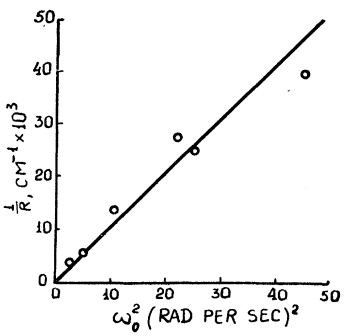

FIG. 3.1. Dependence of the meniscus curvature on the rotation velocity according to the data of Turkington, Brown, and Osborne (1963).

[3] The symbol ω_{c1} is introduced in an analogy with the first critical field H_{c1}, beginning from which Abrikosov's vortex lines are created in superconductors of the second kind.

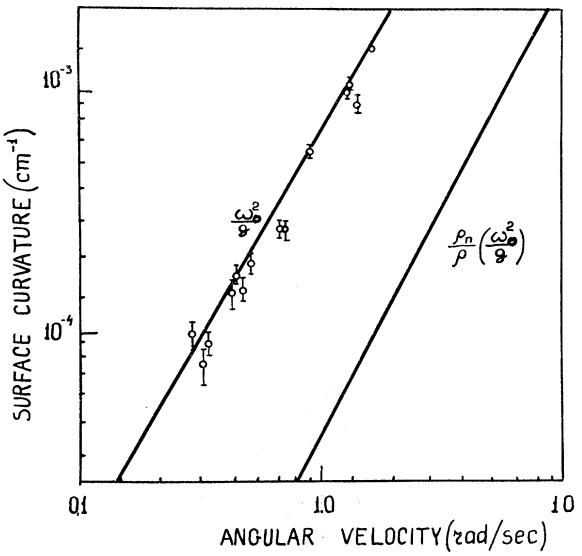

FIG. 3.2. Dependence of the meniscus curvature on the rotation velocity according to the data of Meservey (1964).

3.2. The Angular Momentum of Rotating Helium II

The experiment of Hall mentioned previously (Hall 1955, Hall and Vinen, 1955), developed in his next paper (1957), was a direct realization of Landau's suggestion on the measurement of the moment of inertia of rotating helium II. The angular momentum and, hence, the moment of inertia were found to correspond to the rigid body rotation of the liquid (see, however, Secs. 8.1, 8.6).

Reppy, Depatie, and Lane (1960) observed rotation of a transparent cylindrical vessel, filled with helium II around a vertical axis. The vessel suspended by means of a Beams type magnetic bearing, obtained suddenly an angular momentum during 0.5 sec. After that observations were made of the time dependence of the rotation velocity. It is found that the angular momentum of the liquid in these experiments is always a classical one, in other words, the liquid under all conditions performs a solid body rotation together with the vessel. In Fig. 3.3 the temperature dependence is given

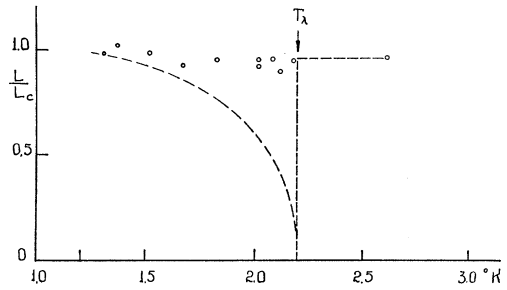

FIG. 3.3. L is the angular momentum of rotating helium II, measured by Reppy, Depatie, and Lane (1960). The velocity of rotation is about 0.2 sec^{-1}. L_c is the classical momentum of the liquid performing a solid-body rotation with the same angular velocity. The dashed line is Pellam's curve (compare Fig. 3.10).

of the ratio L/L_c, where L is the measured angular momentum and L_c is its classical value, corresponding to the solid body rotation. This ratio is equal to unity over all the range of measured temperatures.

3.3. Capture of Negative Ions by Rotating Helium II

A number of papers is devoted to ion motion in liquid helium [see, for instance, reviews of Careri (1961, 1963) and Atkins (1963)]. In particular, having studied vortex rings formed by fast moving ions in helium II, Rayfield and Reif (1963, 1965) proved quantization of their circulation and measured the radius of their core, obtaining the value $a_0 \sim 1$ Å.

The results of study of ion motion in rotating helium II were some of the serious confirmations of the existence of vortex lines in it.

Careri, McCormick, and Scaramuzzi (1962) found an appreciable decrease of the current intensity of negative

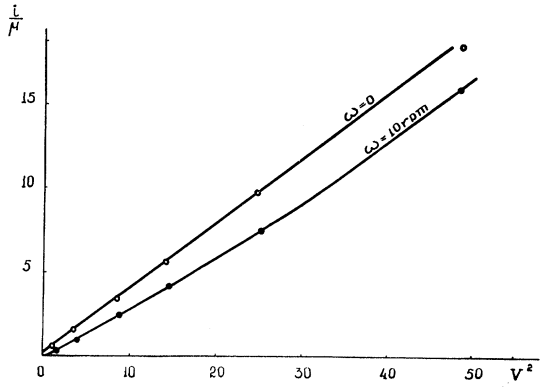

FIG. 3.4. Dependence of the negative-ion current on the voltage (in volts) in helium II at rest ($\omega_0=0$) and in rotating helium II ($\omega_0 \approx 1$ sec^{-1}) according to the data of Careri, McCormick, and Scaramuzzi (1962). i is the current intensity, μ is the mobility of ions.

ions formed by a radioactive source Po^{210} in rotating helium II at their radial motion. If the current was directed along the axis of rotation, then it did not depend at all on the angular velocity. A decrease of the current intensity of ions moving perpendicularly to the axis of rotation was found to be dependent on the angular velocity and on the temperature till the λ-point. In Fig. 3.4 the plot is given of the current intensity divided by the mobility versus the square of the applied voltage, when $\omega_0=0$ and $\omega_0 \approx 1$ sec^{-1}. Nonlinearity of the latter graph allowed the authors to make a conclusion that the effect of the current decrease cannot be explained only by a decrease of the mobility of ions, which should be connected with the appearance of new centers of scattering (vortex lines). The data obtained show the capture of a definite number of ions in the gap between the electrodes (see Fig. 3.5), i.e., formation of a space charge, caused by the capture of negative ions by vortex lines of rotating helium II. According to a widely held model of a negative ion, it is an electron

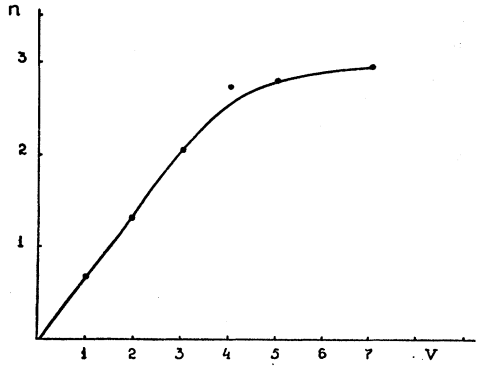

FIG. 3.5. The number of ions (in 10^6 cm^{-3}), trapped by vortex lines of rotating helium II calculated by Careri, McCormick, and Scaramuzzi (1962) according to the data represented in Fig. 3.4.

in a cavity with the diameter of several interatomic distances. Therefore, the capture of such a formation by a vortex line, which represents a node line of the wave function, i.e., the region with reduced density, is very probable. Careri *et al.* refer to a private communication of Onsager to support such a point of view.

The observations of capture of negative and positive ions in rotating helium II as well as some measurements of their mean time of capture and their mobility parallel to the axis of rotation at the temperature between 1.20° and 1.72°K were also realized by Douglass (1964). He did not find any evidence of positive ion capture. It was found that the probability of negative ion capture is proportional to the angular velocity till 45 min^{-1} and that the mean time of capture strongly depends on temperature (see Fig. 3.6). Douglass' data are described well by the relation $\tau \sim \exp(E_0/kT)$, $E_0=0.012$ eV, where E_0 is assumed to be associated with the depth of the potential well into which negative ions are trapped.

Tanner, Springett, and Donnelly (1965) have shown that the proportionality between the relative change of the negative ion current and the angular velocity of rotation is maintained at different directions of the

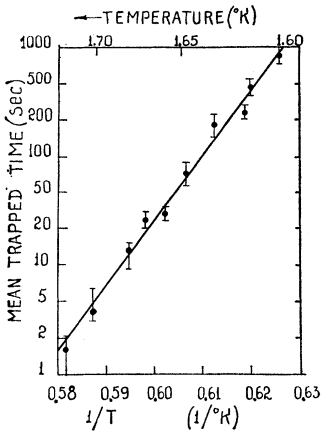

FIG. 3.6. Dependence of the trap time of negative ions on temperature according to the data of Douglass (1964).

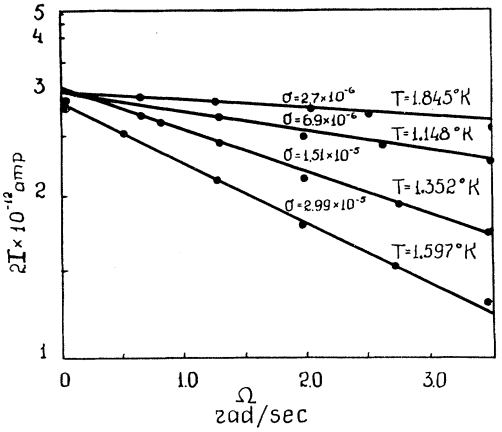

FIG. 3.7. The dependence of the negative-ion current I on the angular velocity of helium II rotation according to Springett, Tanner, and Donnelly (1965). σ is the capture cross section in cm.

current with respect to the axis of rotation. The effect disappears suddenly at an increase of temperature to $T \approx 1.6$°K. Further results of the same authors (Springett, Tanner, and Donnelly, 1965) are given in Fig. 3.7. They determined the cross section of capture σ calculated from a simple formula

$$I = I_0 \exp\left[-(m\omega_0/\pi\hbar)\sigma y\right],$$

where I is the current intensity, $m\omega_0/\pi\hbar$ is the density of vortex lines, and y is the distance passed by an ion along the applied field. σ shows a complex dependence on temperature (Fig. 3.8, a solid line). The experimentally found dependence of σ on the applied field is shown in Fig. 3.9 (also a solid line). The dashed lines are the results of the theoretical calculation made by Donnelly (1965), at the effective mass of a negative ion equal to 100 m, while its radius was 12.1 Å. The discrepancy between the theoretical and experimental results, rather considerable in Figs. 3.8, 3.9, the author explains by the presence of a space charge making the

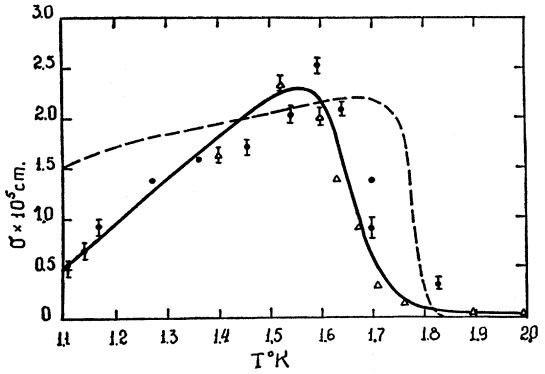

FIG. 3.8. Temperature dependence of the capture cross section of negative ions by vortex lines in rotating helium II according to the data of Springett, Tanner, and Donnelly (1965) is given by a solid line. The dashed line represents the theoretical calculations of Donnelly (1965).

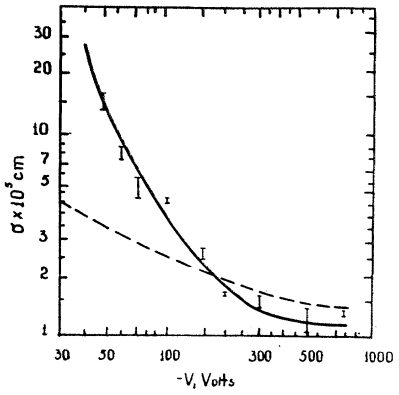

FIG. 3.9. Dependence of the negative-ion cross section on the applied voltage according to the data of Springett, Tanner, and Donnelly (1965) is given by a solid line. The dashed line is the theoretical calculation of Donnelly (1965).

electrostatic field nonuniform. The cross section of the capture for positive charges at the same mass of 100 m is somewhat smaller. However, the difference of probabilities of escaping the trap is so great for positive and negative ions that a weakening of the current of positive ions at temperatures higher than 1°K is impossible to observe. There is some probability to observe this phenomenon only when $T<1$°K.

3.4. Does Helium II Rotate as a Whole?

Perhaps the only paper stating that helium II does not rotate as a whole was that by Pellam (1960), who observed a deviation of the Rayleigh disk, suspended at an angle 45° to current lines of helium II, rotating in a cylindrical vessel. A light beam fell on the Rayleigh disk, the suspension point of which was stationary in the laboratory system of coordinates. The reflection angle of the beam served as a criterion of the moment of forces acting on the disk. It is seen in Fig. 3.10 that the effective density of a rotating liquid acting on the Rayleigh disk is equal to the total density of helium I. At the point of the phase transition, it becomes equal to zero and in helium II again increases as ρ_s at the further decrease of temperature. Thus a paradoxical conclusion is unavoidable, the normal component stops at the point of the phase transition and does not act on the disk afterwards. It is clear that nobody, including Pellam himself, could accept the conception that rotating helium II is the liquid in which only the superfluid component rotates.

The paper of Reppy, Depatie, and Lane (1960), described above, was a response to Pellam's experiment. They again confirmed that helium II rotated as a whole (Fig. 3.3).

The study of velocities inside the rotating cylindrical vessel filled with helium II was also performed by Craig (1961). With this aim a torsional balance was suspended on an elastic thread in helium II. The center of the balance suspension was stationary in the laboratory system of coordinates. The balance had a pair of disks fastened to the ends of its beam. The disks were placed so that the flow of liquid was perpendicular to their surfaces. At the constant temperature ($T<2.17$°K) the drag force acting on a disk was studied as a function of the velocity varying from 0.022 to 0.63 sec^{-1}. It was found that the drag force was proportional to the square of velocity for all the temperatures somewhat lower than the transition point. Such a dependence of the drag force on the velocity is characteristic of a classical liquid at a motion with Reynolds numbers Re >50, while in Craig's case Re >100. At a given velocity of rotation, as Fig. 3.11 shows, the drag force acting on the disks depends little on the temperature in the whole range from 1.3°K to almost the transition point. At this temperature there is no break there either.

In another paper of Craig (1964), the question was put whether Helmholtz flow could be realized under conditions of Pellam's experiment (a large angle of attack) instead of a potential flow round the disk. This hypothesis was verified and confirmed in the paper of Kitchens, Steyert, Taylor, and Craig (1965), who observed trajectories of hard particles of hydrogen–deuterium mixture suspended in liquid helium II by means of a cinema film. Helium II rotated in a cylindrical vessel, and a wing (a flat plate) was immersed in it. Under such conditions, very similar to those of Pellam's experiment, tearing away of jets behind the wing was clearly observed as well as formation of eddies. These effects were increased at an increase of the attack angle from 27° to 45° and then to 90°. Evidently, the observed phenomena were connected with the normal component motion, as the superfluid component of helium II in the similar conditions (the velocity of the flow did not exceed several centimeters per second) flows around the Rayleigh disk in a potential way (Craig and Pellam, 1957, Köeller and Pellam, 1962). In spite of the certain interest caused by the data obtained in this paper, independence of the effect on temperature made Craig *et al.* give up the hope of explaining the strange behavior of the Rayleigh disk in Pellam's experiment.

Pellam (1965) has repeated a detailed study of the Rayleigh disk behavior in rotating helium II, but he only confirmed his previous results.

The cause of Pellam's paradoxical experimental result was not clear until quite recently; Tsakadze and Shanshiashvili (1965) decided to repeat Pellam's experiment in two variants. In one case a light beam was

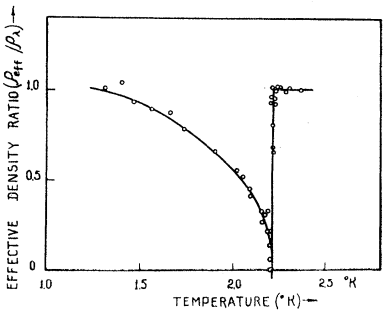

FIG. 3.10. Temperature dependence of the effective density determined by Pellam (1960) by a deflection of the Rayleigh disk, immersed into rotating helium II. ρ_λ is the density of liquid helium at the λ-point.

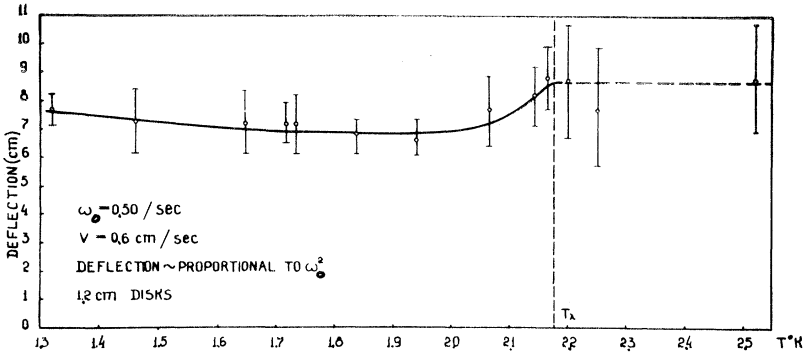

FIG. 3.11. Temperature dependence of the deflection of the disks fixed perpendicularly to the current lines of rotating helium II to the ends of the torsional balance beam (Craig, 1961).

reflected directly from the Rayleigh disk (as in Pellam's device); in the other case a mirror was placed above the rotating vessel and the light beam did not fall on the body immersed into liquid helium. In the first variant, the authors obtained a curve very similar to that of Pellam. In the second variant, the deflection of the Rayleigh disk was equal at all temperatures to that in helium I (Fig. 3.12).

Thus, at present we can definitely state that the results of Pellam's experiment were caused completely by the action of light.

3.5. Distribution of Vortex Lines over the Cross Section of a Rotating Vessel, Irrotational Regions

Usually it was thought that the distribution of vortex lines in a uniformly rotating helium II was uniform. However, Hall (1960), minimizing the free energy of the liquid, has shown that there should exist some region near the side surface of a cylinder in which there are no vortex lines and the motion is determined by the law $v_s = \Gamma/2\pi r$. Here Γ is the sum of circulations of all the vortex lines existing in the vessel. It is natural to call such a region "irrotational," as then not only the curl of the local velocity, but also that of the mean velocity is equal to zero.

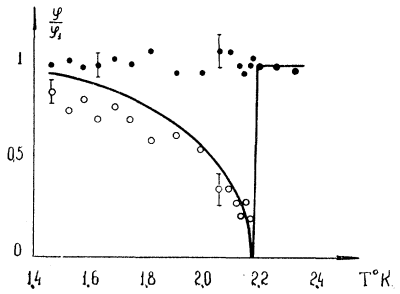

FIG. 3.12. Temperature dependence of the angle of the Rayleigh disk deflection in rotating helium II according to the data of Tsadakze and Shanshiashvili (1965). The points were obtained when a mirror placed above the liquid level was illuminated; circles when the Rayleigh disk was illuminated; the solid line is Pellam's curve (1960) shown in Fig. 3.10. φ_1 is the angle of deflection in helium I. ($\varphi/\varphi_1 = \rho_{eff}/\rho_\lambda$.)

Bendt and Oliphant (1961) have shown that an irrotational region should be created round the inner cylinder at rotation of helium II in an annulus between two coaxial cylinders moving with the common angular velocity. Proceeding from the minimization of the free energy $E - L\omega_0$, they have calculated the velocity dependence of the irrotational region radius and the value of the circulation in this region (Figs. 3.13, 3.14). It was found that the velocity circulation Γ round the inner cylinder can reach hundreds of thousands of quanta h/m. It is more favorable thermodynamically to allow the possibility of the existence of such values of Γ which are incompatible with the continuity of the mean velocity on the boundary between the region occupied by vortex lines and the irrotational region (sliding).

Formation of an irrotational region round the inner

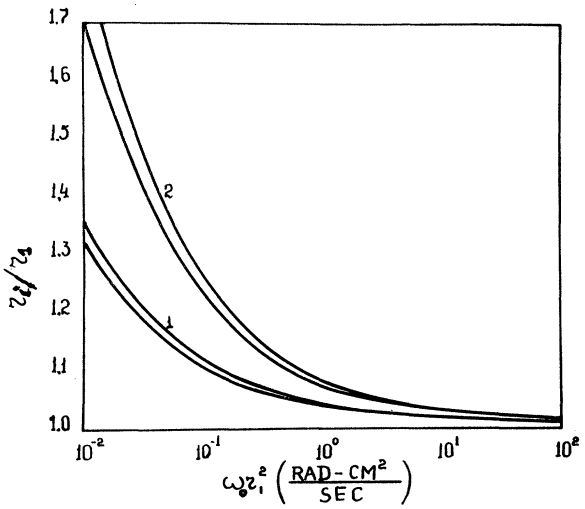

FIG. 3.13. The results of Bendt and Oliphant's calculations (1961). r_i is the radius of the irrotational region, r_1 is the radius of the inside cylinder. Band 1 corresponds to the calculation made on the assumption of continuity of the averaged velocity on the boundary between the irrotational region and the region occupied by vortex lines; band 2 corresponds to the calculation made without this limitation. Band use instead of curves is connected with a weak dependence of ln (b/a_0) on ω_0; b is the effective radius of a vortex line (outside the irrotational region).

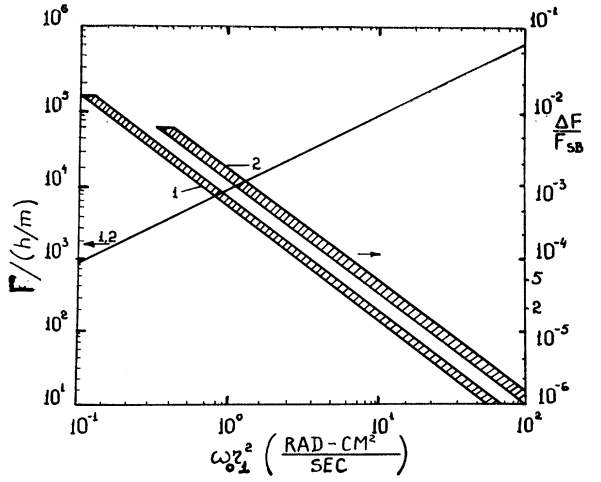

FIG. 3.14. The results of calculations of Bendt and Oliphant (1961). Γ is the velocity circulation around the inside cylinder (in the irrotational region). F is the free energy of rotating helium in the presence of the irrotational region; F_{sb} is the free energy of the solid-body rotation simulated by the presence of uniformly distributed vortex lines, $\Delta F = F - F_{sb}$ ($\Delta F < 0$, $F_{sb} < 0$). The sense of the notations 1 and 2 and the reason for the use of bands instead of lines are explained in the caption to Fig. 3.13.

cylinder was discussed in the paper of Kemoklidze and Khalatnikov as well (1964).

If the existence of an inside irrotational region is favorable thermodynamically, then it is natural to ask whether its creation is possible when there is no inner cylinder, in which case the liquid could have formed a hollow cylindrical core. Kemoklidze and Mamaladze (1964a) have shown that it is impossible for two reasons: the radius of such a core corresponding to the minimum free energy should have a value less than interatomic distances, and the circulation under such conditions is not quantized and is equal to $\sim 1.5\ \Gamma_0$. However, the existence of an irrotational region was found to be favorable thermodynamically when there is an ordinary Feynman's vortex line of unit circulation. The radius of this region is about three times as large as the vortex separation at their usual density (see Table I).

An irrotational region surrounding the central cylinder was found experimentally by Tsakadze (1964b). He used a cylindrical vessel with a rod placed along its axis. Another vessel was put onto the rod, so that there was a narrow gap between the bottoms of the two cylinders. The superfluid had to leak through a slit from the inner cylinder not glued to the rod due to the difference of levels. Flowing into the gap between the bottoms, it was moving in the horizontal direction. If there are vortex lines in the gap between the bottoms then the velocity of the liquid flow out should depend, due to mutual friction (see Sec. 7), on the angular velocity of rotation. And if, with a decrease of the angular velocity of rotation followed by an increase of the irrotational region radius, vortex lines leave the gap between the bottoms, the rate of the leakage becomes constant. Tsakadze sucked the liquid into the inside vessel by means of the thermomechanical effect and then measured the time of its leakage as a function of the angular velocity of rotation (Fig. 3.15).

TABLE I.

ω_0 sec^{-1}	$10^2 r_i$ cm	$r_i/b[b=(\hbar/m\omega_0)^{\frac{1}{2}}]$
0.01	82	6.6
0.1	25	6.4
1	7.8	6.2
5	3.4	6.0
10	2.4	6.0
20	1.7	5.9
30	1.4	5.9

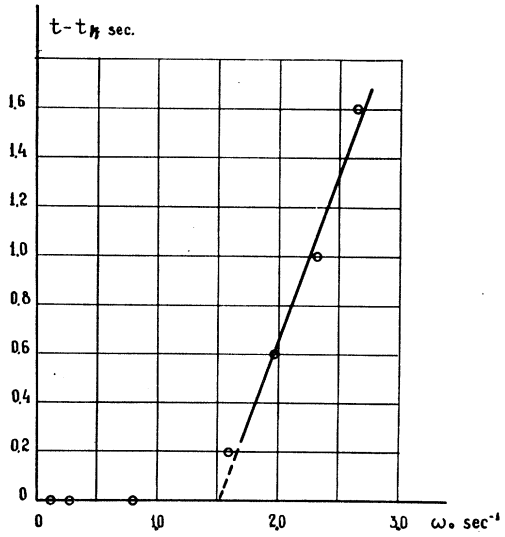

FIG. 3.15. (a) Velocity dependence of the time of helium II outflow in the experiment of Tsakadze (1964b) in the presence of an axial rod. t and t_n are the periods of time of the outflow in the rotating vessel and in the vessel at rest, respectively. $T = 1.75$°K. (b) Results of the same experiment (Tsakadze, 1964b) at $T = 1.46$°K.

A break on the curve observed in such a way means that, when $\omega_0=1.5$ sec^{-1}, the radius of the irrotational region r_i becomes equal to the outside radius of the inside vessel, equal to 0.8 cm. The radius of the rod is $r_i=0.5$ cm. Under such conditions the ratio $r_i/r_1=1.6$. Meanwhile, according to Bendt and Oliphant (Fig. 3.13), such a value should be obtained when $\omega_0\sim 2\times 10^{-2}$ sec^{-1} in an obvious contradiction with the data of the experiment. The discrepancy increases at a decrease of temperature, though the theoretical calculation concerns the case $T=0$°K.

A similar, but rather smaller discrepancy was found between the observations and calculations of Kemoklidze and Khalatnikov, according to which one should have $r_i-r_1=0.055$ cm, when $\omega_0=1.5$ sec^{-1} and $r_i-r_1=0.022$ cm, when $\omega_0=10$ sec^{-1}. This disagreement of theoretical calculations with the experimentally found values $r_i-r_1=0.3$ cm could be explained, at least partially,

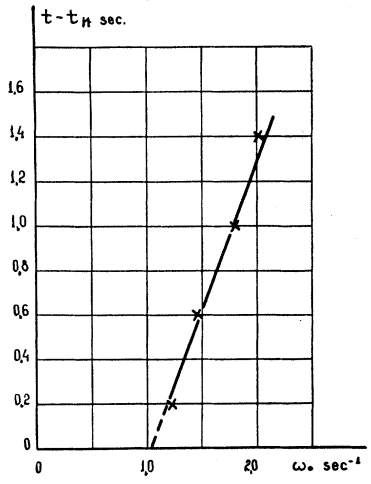

FIG. 3.16. Dependence of the time of helium II outflow through a capillary in the absence of an axial rod. $T=1.38$°K. (Tsakadze, 1964b.)

by the conditions under which the experiment was performed. In Tsakadze's device the narrow gap between the bottoms was transformed into a volume limited from the top by the free surface at a higher level than the bottom of the inside vessel. Meanwhile, the calculations of Bendt and Oliphant and of Kemoklidze and Khalatnikov were made for the case when the liquid flew between two parallel planes.

A similar technique was used by Tsakadze to find an irrotational region without the inside cylinder. With this aim he chose a version of the just now described device. He has removed the axial rod and made the liquid leak from a capillary placed on the rotation axis. Flowing out of the capillary, it passed through the gap between the lower edge of the capillary (it had a flat section) and the bottom of the vessel. The results are shown in Fig. 3.16. The radius of the irrotational region was equal to $r_i=0.1$ cm, when $\omega_0=1$ sec^{-1}. Calculations of Kemoklidze and Mamaladze gave under such conditions $r_i=0.08$ cm (the experiment was made at $T=1.38$°K).

3.6. Distribution of Vortex Lines when There Is a Free Surface

A free surface of the liquid can also be a peculiar reason of nonuniform distribution of vortex lines. A vortex line in equilibrium should be perpendicular to the free surface, so that the tangential component of tension would not make it drift. But in this case it will not be parallel to the rotation axis as the surface has the shape of a nonflat meniscus near which vortices should bend. In this connection Kemoklidze and Mamaladze (1946b) considered solutions of hydrodynamical equations (4.2.1), (4.2.2), (4.2.3) of rotating helium II. These solutions were considered under the usual boundary conditions on solid surfaces and under the condition on the free surface (using the tensor of momentum flux, see, for instance, Landau and Lifshitz, 1953), which should be self-consistent with the solution of the equations mentioned above.

The authors did not manage to solve this problem completely because of great difficulties of calculations. But they have shown that the solution $v_s=\omega_0 r$ and $|\operatorname{curl}\mathbf{v}_s|=\omega_z=2\omega_0=$ const (the constancy of the density of vortex lines) is not compatible with the parabolic meniscus. Small deviations from this solution show the tendency to an increase of curl $\mathbf{v}_s$ (increase of vortex line density) at the approach to the rotation axis and to the deepening of the meniscus near this axis, in the immediate vicinity of which deviations become large. Evidently, a conic pit on the meniscus observed by Andronikashvili (Andronikashvili and Kaverkin, 1955) is the result of these circumstances. One would rather assume that, in the vicinity of the rotation axis, the region of closely spaced vortex lines is replaced by an irrotational region [where Eqs. (4.2.1), (4.2.2), (4.2.3) are already not applicable] and a unit vortex line is situated on the very axis. As the confirmation of such an assumption can be used the results of the mentioned above (3.5) Kemoklidze and Mamaladze paper (1964a). Though they concerned the case of the liquid confined by flat planes, they should remain valid at distances deep under the meniscus of the liquid as well.

3.7. Direct Observations of Vortex Lines in a Uniformly Rotating Helium II

We begin this paragraph from the paper in which rather clear indications were obtained concerning the existence of vortex lines arranged in a definite geometrical order, in spite of the fact that they were not observed directly. That was Chase's experiment (1960a). He rotated round the vertical axis a horizontally placed tube with the diameter 2.62 mm packed with 70 thin wires with the diameter 0.25 mm. These wires produced a large number of narrow parallel channels of irregular cross section. A heat current was switched on along these channels filled with helium II. The critical value of this current w_c should depend according to Vinen

(1957a, b, c, 1958b) on the presence of vortex lines. Measuring w_c as a function of the square root of the angular velocity of rotation, Chase has obtained that this dependence has a step shape, and the first step is characterized by an appreciable hysteresis which is absent at high angular velocities (see Fig. 3.17). The points were taken under the conditions of an accelerated rotation (open circles) and its slowing down as well (solid circles). There are no vortex lines at the first step. Their sudden appearance corresponds to creation of the stable configuration of vortex lines with the separation $(\pi\hbar/m\omega_0)^{\frac{1}{2}}$ equal to 0.34 mm. This value is compatible with the wire size. Separation of vortex lines equal to 0.17 and 0.11 mm corresponds to transitions to the next steps, i.e., the separation of vortex lines for different steps gives the ratio $1:\frac{1}{2}:\frac{1}{3}$. Such a situation could take place only if there exists some discrete succession of stable configurations of vortex arrays.

Unfortunately, Chase has not obtained such clear results for channels of another shape and larger size (Fig. 3.18, Chase, 1960b). Maybe the vortex lines formed in such channels are "blown away" by a heat current or the conditions of their fastening are sharply different from those existing between the thin wires of the first of capillaries used by him.

A direct observation of vortex lines in rotating helium II was realized by Steyert, Taylor, and Kitchens (1965). For this purpose they observed (and took photos as well) the motion of tiny particles of solidified hydrogen–deuterium mixture. Most of such particles moved in rotating helium II along smooth circular trajectories with the center on the rotation axis. But a part of them made small closed loops from time to time. That meant undoubtedly that a particle was in the vicinity of a vortex line. It was easy to calculate the vortex line circulation if to know the loop diameter and the period of revolution. The results of the similar calculations given in the mentioned paper show that together with vortex lines with the circulation close to unit one (Γ_0), there are vortex lines with $\Gamma=2\Gamma_0$, $3\Gamma_0$, etc. Their

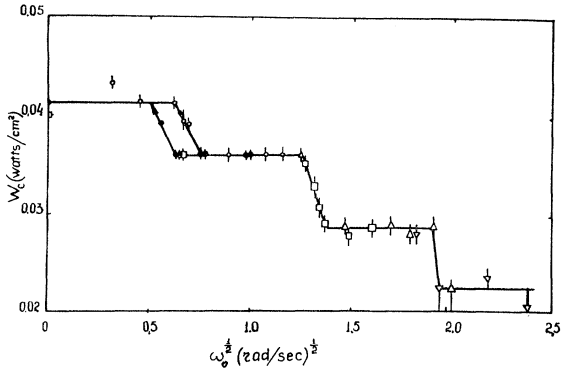

FIG. 3.17. Dependence of the critical thermal flux W_c on the velocity of rotation in the experiment of Chase (1960a).

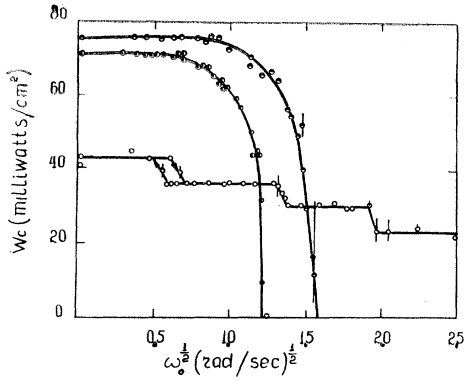

FIG. 3.18. Dependence of the critical thermal flux W_c on the velocity of rotation in the experiment of Chase (1960b). The upper curve is obtained with 9 rectangular canals 0.102×0.051 cm (the long axis is in the plane of rotation). The middle curve is obtained with the same canals, but with the long axis perpendicular to the plane of rotation. The lower curve reproduces the result of the previous paper of Chase (1960a) with a tube of diameter 2.62 mm, filled with 70 wires of diameter 0.252 mm.

number decreases with an increase of Γ/Γ_0. It should be also noted that according to their data there are allowed not multiple circulations $\Gamma=0.8\Gamma_0$, $1.5\Gamma_0$, etc. The maximum circulation observed in this study was $10.5\Gamma_0$. (*Note added in proof.* We think it is possible that these results are caused by a difference in velocities of the particles and the superfluid component.)

4. HYDRODYNAMICS OF ROTATING HELIUM II

4.1. Averaged Hydrodynamics of Rotating Helium II

Considerations of 2.4 formed the basis for the representation of rotating helium II hydrodynamics in terms of velocities, pressures, and other physical magnitudes averaged over the volume containing many vortex lines. Such an averaging is desirable, because at solution of hydrodynamical problems, associated with the existence of many vortex lines, it would be necessary to give boundary conditions on each of them, which would take into account such "local" forces as tension, Magnus force,[4] and forces caused by interaction of vortices with thermal excitations. The offered averaging does not only simplify the complex picture of velocity distribution (Fig. 2.2), but ascribes to local forces a character of space ones. Thus the necessity of taking into account numerous boundary conditions is excluded. But the new space forces which have appeared in such a manner should be included into hydrodynamical equations. Due to this fact the latter become more complicated than usual Landau equations of two component hydrodynamics.

[4] If the velocity $\mathbf{v}_s$ of the superfluid component in the points through which the vortex line passes is different from the velocity $\mathbf{v}_L$ of the vortex line itself, then the following force (reduced to unit length) acts on a vortex line with the circulation $\boldsymbol{\Gamma}$:

$$\mathbf{f}=\rho_s[\mathbf{v}_s-\mathbf{v}_L, \boldsymbol{\Gamma}].$$

4.2. The Equations of Hydrodynamics of Rotating Helium II

The averaged hydrodynamics of rotating helium II was formulated in succession at first in Hall's papers (1957a, 1960), then by Mamaladze and Matinyan (1960a) (see, also Andronikashvili, Mamaladze, Matinyan, and Tsakadze, 1961) and at last by Bekarevich and Khalatnikov (1961). If to take only the case of low (in comparison with the velocity of second sound) relative velocities of the superfluid and the normal components and small temperature gradients, then the complete set of equations of hydrodynamics of helium II will be

$$(\partial \mathbf{v}_s/\partial t)+(\mathbf{v}_s, \nabla)\mathbf{v}_s+\nu_s[\boldsymbol{\omega}, \text{curl}\,(\boldsymbol{\omega}/\omega)] = -\rho^{-1}\nabla(\rho+\eta_s\omega)+s\nabla T+\mathbf{F}_{sn}, \quad (4.2.1)$$

$$(\partial \mathbf{v}_n/\partial t)+(\mathbf{v}_n, \nabla)\mathbf{v}_n-\nu_n\Delta\mathbf{v}_n = -\rho^{-1}\nabla(P+\eta_s\omega)-(\rho_s/\rho_n)s\nabla T-(\rho_s/\rho_n)\mathbf{F}_{sn}, \quad (4.2.2)$$

$$\text{div}\,\mathbf{v}_s=\text{div}\,\mathbf{v}_n=0, \quad (4.2.3)$$

where $\nu_s=\epsilon/\rho_s\Gamma_0=\eta_s/\rho_s$, $\boldsymbol{\omega}=\text{curl}\,\mathbf{v}_s$ is the curl of the mean velocity of the superfluid component (symbols of averaging are omitted everywhere for simplicity), P is the pressure, s is the entropy of unit mass, $\nu_n=\eta_n/\rho_n$ is the kinematic viscosity of the normal component, and $\mathbf{F}_{sn}$ is the force of mutual friction acting on unit mass of the superfluid component [see formulas (7.2.1) and (7.3.4)].

The first of these equations is the equation of motion of the superfluid component; it is an analog of Euler's equation for the ide ıl liquid, more complicated because of taking into account the thermomechanical effect (the term $s\nabla T$) and the existence of vortex lines (terms containing ω and the force of mutual friction). The second equation is the equation of motion of the normal component, similar to the Navier–Stokes equation for a viscous liquid and also containing some additional terms taking into account the same effects. In the equations of continuity (4.2.3), both components appear as incompressible liquids, and it is natural, in the cases when motions with high velocities or nonstationary processes of mutual transformations of the components are not considered. In the latter cases the equation,

$$(\partial\rho/\partial t)+\text{div}\,(\rho_s\mathbf{v}_s+\rho_n\mathbf{v}_n)=0, \quad (4.2.3a)$$

should be used instead of (4.2.3).

The terms, containing $\boldsymbol{\omega}$ and the magnitude $\mathbf{F}_{sn}$ provide taking into account vortex singularities to such an extent as is necessary after averaging as well. In particular, the term $\eta_s\omega$ added to the pressure P is associated with the additional pressure caused by the tension of vortex lines ($m\omega_0\epsilon/\pi\hbar=\eta_s\omega$). Further a special role of the term $\nu_s[\boldsymbol{\omega}, \text{curl}\,(\boldsymbol{\omega}/\omega)]$ should be emphasized more than once. Therefore, it is necessary to explain its origin. It describes elastic properties of vortex lines, due to which straightening forces are created preventing distortion of vortex lines (Fig. 4.1). The straightening force (reduced to unit length) for one vortex line, the tension of which is $\boldsymbol{\varepsilon}=\epsilon\boldsymbol{\omega}/\omega$, is equal to $\epsilon/R_c=\epsilon(\boldsymbol{\omega}/\omega, \nabla)\boldsymbol{\omega}/\omega$, where R_c is the radius of curvature. Let us recollect now that the density of vortex lines is ω/Γ_0 and $\nu_s=\epsilon/\rho_s\Gamma_0$; then calculate the mean straightening force reduced to unit mass of the superfluid component:

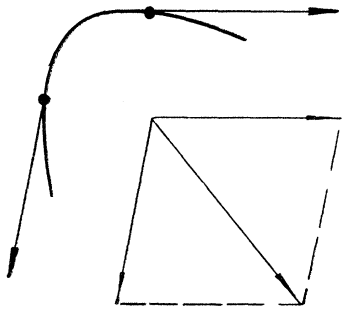

FIG. 4.1. The sum of tension forces, acting on an element of a distorted vortex line, constitutes a straightening effort.

$$\left(\frac{1}{\rho_s}\right)\left\{\epsilon\left(\frac{\boldsymbol{\omega}}{\omega}, \nabla\right)\frac{\boldsymbol{\omega}}{\omega}\right\}\left(\frac{\omega}{\Gamma_0}\right)=\nu_s(\boldsymbol{\omega}, \nabla)\frac{\boldsymbol{\omega}}{\omega}=-\nu_s\left[\boldsymbol{\omega}, \text{curl}\frac{\boldsymbol{\omega}}{\omega}\right].$$

The existence of the second derivatives of velocity over the coordinates in this expression makes two equations similar by their mathematical structure: the equation of the superfluid liquid and that of the normal liquid containing the viscous term $\nu_n\Delta\mathbf{v}_n$. It is shown in Sec. (5.5) that the presence of terms with second derivatives of velocities causes peculiar processes of energy dissipation (though, as it has just been shown, the term $\nu_s[\boldsymbol{\omega}, \text{curl}\,\boldsymbol{\omega}/\omega]$ is a purely elastic one by its physical meaning) and that the constant ν_s acts as a peculiar "kinematic viscosity of the superfluid component." One can emphasize that its dimension coincides with the dimension of ν_n. The numerical values of ν_n ν_s are of the same order of magnitude, rather close to each other, at least in the range of temperatures in which the experiments discussed in this review were made.

4.3. Additional Boundary Conditions

The necessity of additional boundary conditions is also a consequence of the existence of the velocity second derivatives. In addition to the evident condition for the velocity component of the superfluid liquid perpendicular to the wall (the liquid does not flow into the wall and does not flow out of it at the constant temperature), we have to look for conditions for the tangential component as well. Such conditions are given indirectly. At first the conditions of vortex fastening to the surface crossing them are written down, and then the relation between the velocity of vortex lines $\mathbf{v}_L$ and the velocity of the superfluid component $\mathbf{v}_s$ is used to transform the boundary conditions for $\mathbf{v}_L$ into the boundary conditions for $\mathbf{v}_s$. This program is realized by the following equations.

The condition of vortex line fastening to a solid surface, the velocity of which is $\mathbf{v}_\sigma$ has the form

$$(\mathbf{v}_L-\mathbf{v}_\sigma)_t=a\{\mathbf{N},[\mathbf{N},(\boldsymbol{\omega}/\omega)]\}-a'[\mathbf{N},(\boldsymbol{\omega}/\omega)], \quad (4.3.1)$$

where the index t denotes the tangent component to the surface; $\mathbf{N}$ is a unit normal to the surface. a and a' are coefficients of sliding. Here the first term describes sliding of a vortex line along the surface due to tension of a vortex line inclined to it ($\mathbf{v}_L-\mathbf{v}_\sigma\sim\epsilon\boldsymbol{\omega}/\omega$). The second term, perpendicular to the first one, is caused by Magnus effect "drifting away" the sliding vortex line. Let us note that two terms of formula (4.3.1) correspond to two terms of expression (7.2.1) for the force $\mathbf{F}_{sn}$. Really the first term describes the direct action of some force, and the other one describes a secondary effect directed perpendicularly to the "drag" force. Therefore, it is natural that Bekarevich and Khalatnikov (1961) predicted the following proportionality of the coefficients a and a' on the one hand and B, B' on the other hand (we remind that $B'<0$):

$$a/a'=-B/B'. \quad (4.3.2)$$

In the absence of sliding, $a=a'=0$. When there is a complete sliding, $a=a'=\infty$. Roughness of a solid surface, made, for instance, of grains of sand attached to it, prevents sliding of vortex lines, as stretched vortices tending to have the minimum length are fastened to the grains. Accordingly, Bekarevich and Khalatnikov (1961) obtained the following estimate:

$$a\sim(\hbar/m\delta)B(\rho_n/\rho), \quad (4.3.3)$$

where δ is the height of a grain.

If vortex lines are parallel to the rotation axis, then curl $\boldsymbol{\omega}/\omega=0$; there is no term with ν_s in Eq. (4.2.1), and the necessity in additional boundary conditions disappears.

The relationship between $\mathbf{v}_L$ and $\mathbf{v}_s$ is realized by means of formula

$$[\boldsymbol{\omega},\mathbf{v}_s-\mathbf{v}_L]+\nu_s[\boldsymbol{\omega},\text{curl }\boldsymbol{\omega}/\omega]+\mathbf{F}_{sn}=0 \quad (4.3.4)$$

or formula

$$(\partial\mathbf{v}_s/\partial t)-[\mathbf{v}_L,\boldsymbol{\omega}]=-\rho^{-1}\nabla(P+\eta_s\omega)+s\nabla T-\tfrac{1}{2}\nabla v_s^2. \quad (4.3.5)$$

Equation (4.3.4) is the condition of equilibrium of Magnus force, straightening force, and force of mutual friction which act on vortex lines. When such a condition is maintained (and not when one of these forces is equal to zero), vortex lines are free.

We note, in the association with Eq. (4.3.5), that an equality of the type $(\partial\mathbf{v}_s/\partial t)-[\mathbf{v}_L,\boldsymbol{\omega}]=\nabla G$, where G is an arbitrary function, gives $(\partial\boldsymbol{\omega}/\partial t)-\text{curl }[\mathbf{v}_L,\boldsymbol{\omega}]=0$ and describes the transport of the magnitude $\boldsymbol{\omega}$ with the velocity $\mathbf{v}_L$.

5. OSCILLATIONS OF SOLID BODIES WITH AXIAL SYMMETRY IN ROTATING HELIUM II AND ANISOTROPY OF ITS ELASTIC-VISCOUS PROPERTIES

5.1. Anisotropy of Elastic-Viscous Properties of Rotating Helium II

Experiments, in which small oscillations of solids immersed in rotating helium II were studied, have given abundant information on properties of vortex lines. In these experiments, solid bodies of axial symmetrical shape performed rotation together with helium II and small oscillations superimposed on their rotational motion.

Though chronologically we should begin from the experiments in which dampling of an oscillating disk was determined (Andronikashvili and Tsakadze, 1959b), let us start the description of such investigations from the simplest one made by Tsakadze (1962a). Tsakadze measured the logarithmic decrement of damping of an upside-down hollow cylinder, performing two motions simultaneously: rotation together with helium II and oscillation upwards and downwards, so that the side of the cylinder moved along vortex lines. As a result of the measurements, it was found that damping in rotating helium II is indistinguishable from that taking place in helium II at rest. It does not depend on the angular velocity of rotation ω_0, i.e., it does not depend on the number of vortex lines. In such an experiment, helium II behaves as a classical liquid.

In another experiment (Tsakadze and Chkheidze, 1960), a cylinder, turned upside down and suspended on an elastic thread, performed in addition to rotation with helium II axial oscillations around the rotation axis. In the case of a classical liquid, damping of such oscillations does not depend on the velocity of rotation. But, in rotating helium II, a layer of the normal component, adjacent to the wall of the cylinder at the distance of the order of the penetration depth, dragged, due to mutual friction (Sec. 7), all those vortex lines which pierced this layer into its motion. Therefore the damping of the cylinder was different from that in a liquid at rest and increased proportionally to the angular velocity in accordance with the increase of the density of vortex lines according to formula (2.5.1). The data of the experiment made by Tsakadze and Chkheidze are shown in Fig. 5.1, where solid lines show the results of calculations made according to the formula obtained by Mamaladze and Matinyan (1960b).

The common feature for these two experiments is that both the shape of the oscillating surface and the direction of its motion do not cause immediate contact of vortex lines with the moving body.

This situation is changed when axial oscillations of the surfaces of a disk or a pile of disks suspended on an elastic thread crossing the array of Onsager–Feynman vortex lines are considered. Vortex lines fastened to these oscillating surfaces are distorted during the disk motion,

and waves propagate along them. Thus the changes of the character of oscillations of a solid body carry information on elastic properties of vortex lines. Propagation of elastic waves is a common phenomenon for all the experiments of such a type, because, due to mutual friction between the components, the waves on vortex lines are excited even in the complete absence of direct contact between them and the solid surface (sliding).

First of all, one should expect some manifestation of vortex elasticity with an increase in frequency of the disk oscillations, the fact observed in the experiment made by Andronikashvili and Tsakadze (1962). The data of these measurements with a sufficiently light disk, "feeling" the elasticity of vortex lines, are given in Fig. 5.2. At small angular velocities, the frequency

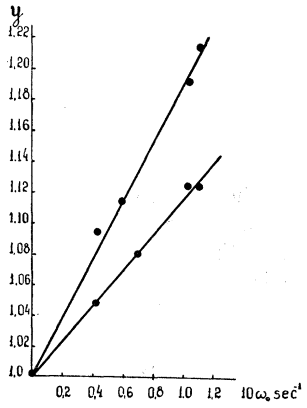

FIG. 5.1. Dependence of damping of the cylinder axial oscillations on the velocity of rotation. $y=A(\delta_2-\delta_1)/(l_2-l_1)$, where δ_2 and δ_1 are the logarithmic decrements of damping of the cylinder oscillations at its immersion to the depths l_2 and l_1, respectively; $A=(I/2\pi^2R^3)(\Omega/2\eta_n\rho_n)^{\frac{1}{2}}$; I is the moment of inertia of the oscillating system; R is the radius of the cylinder; Ω is the frequency of oscillations; η_n and ρ_n are the viscosity and the density of the normal component, respectively. The points are the experimental data of Tsakadze and Chkheidze (1960). The straight lines are plotted according to formula (7.3.1) (Mamaladze and Matinyan, 1960b). The upper straight line represents the case when $T=1.48$°K, the lower one when $T=1.75$°K.

of oscillations increases in accordance with the increase of the number of vortex lines. But when $2\omega_0/\Omega\sim0.2$, where Ω is the frequency of oscillations, the rate of frequency increase slows down sharply and the experimental curve begins to show the tendency to saturation. This phenomenon is caused by collectivization of vortex oscillations, which takes place at such a ratio of frequencies. The collectivization of vortices is discussed in more detail in Sec. 6.3. The experiment of Andronikashvili and Tsakadze clearly establishes the fact of existence of the modulus of rigidity in rotating helium II, manifested in elastic counteraction to the torsion deformation of this liquid with respect to the axis of its rotation.

As noted in 4.2 {at the consideration of the physical sense of the term $\nu_s[\boldsymbol{\omega}, \text{curl}\,(\boldsymbol{\omega}/\omega)]$ in the equation of motion of the superfluid component}, the elastic prop-

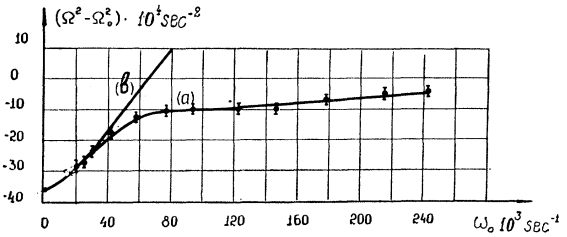

FIG. 5.2. Dependence of the frequency of axial oscillations of a "light" disk on the velocity of rotation. Curve (a) shows the experimental data of Andronikashvili and Tsakadze (1962); curve (b) is plotted according to formula (5.2.1) (when the edge corrections are taken into account).

erties of vortex lines can be also seen in a very "inelastic manner," being the cause of dissipative processes. The first indication of such a possibility was the experiment of Andronikashvili and Tsakadze (1959b) in which the damping of a disk suspended on an elastic thread, rotating with helium II, and performing simultaneous axial oscillations around the axis of rotation was measured. First of all, a disk with a rough surface, with grains of sand ($\sim$50 μ) glued to it, and a smooth disk show different dependencies of damping on the angular velocity of rotation (Figs. 5.3, 5.4). It is connected with conditions (4.3.1) of fastening vortex lines to the surface (Andronikashvili, Tsakadze, and Mesoed, 1961). Indeed, as mentioned in 4.3, a grain of sand on the disk fastens a vortex line. Actually, a vortex line having slid off the grain has to become longer, i.e., to increase its energy. Therefore, the tension of a vortex line sliding from the grain tends to return it.

Increasing the period of the disk oscillations, we apparently improve the conditions of vortex line fastening to its surface. That is why a smooth disk begins to behave quite similarly to a rough one (Fig. 5.4). But in any case and at any temperature, the dependence of damping on the angular velocity had a maximum at

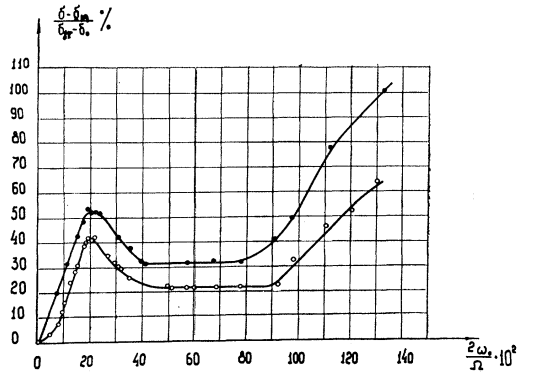

FIG. 5.3. Dependence of the damping of axial oscillations of a rough disk on the velocity of rotation according to the data of Andronikashvili and Tsakadze (1959b). The upper curve is obtained at the frequency of oscillations $\Omega=0.361$ sec^{-1}, the lower one at $\Omega=0.581$ sec^{-1}, δ_n is the logarithmic decrement of damping of the disk in the liquid at rest. δ_0 is that in the vacuum. The disks are "heavy" ($\Omega\approx\Omega_0$). $T=1.78$°K.

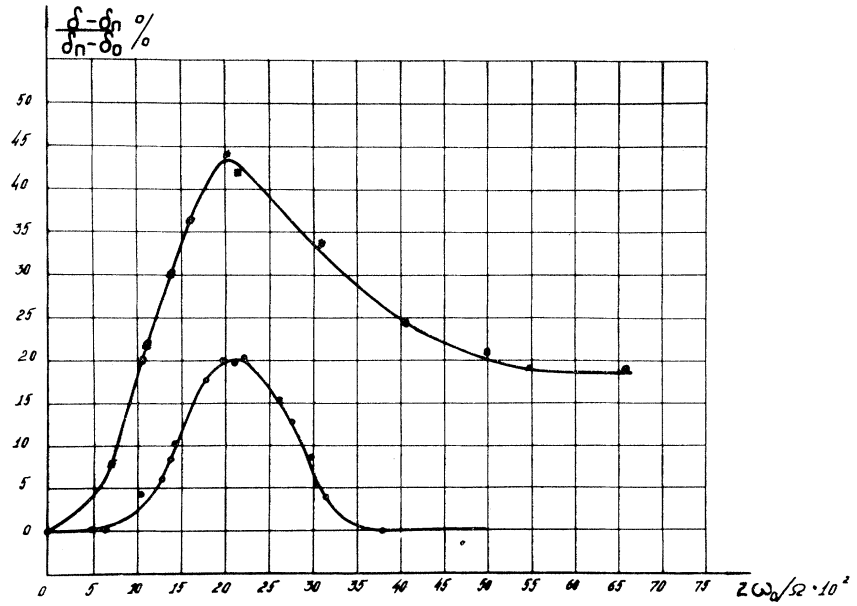

FIG. 5.4. Dependence of the oscillation damping of a smooth disk on the velocity of rotation (Andronikashvili, Tsakadze, and Mesoed, 1961). The symbols are explained in the caption to Fig. 5.3. The upper curve is for $\Omega=0.368$ sec^{-1}, the lower one for $\Omega=0.551$ sec^{-1}. The disks are "heavy" ($\Omega\approx\Omega_0$). $T=1.78$°K.

$2\omega_0/\Omega\sim0.2$, i.e., at the value at which the increase of the frequency of a light disk shows the tendency to saturation.

The dependence obtained for rotating helium II does not resemble the dependence obtained for a classical liquid, which shows a deep minimum of the logarithmic decrement of damping when $2\omega_0/\Omega\sim1$. The results of measurements of the velocity dependence for damping of oscillations of the disk rotating in water (Mesoed and Tsakadze, 1961; also, see Tsakadze and Shultz 1960) are given in Fig. 5.5, as well as the theoretical curve of Mamaladze and Matinyan (1960c). The similar results are obtained at oscillations of a disk in helium I.

Elastic waves, excited by an oscillating disk and propagating along vortex lines of rotating helium II,

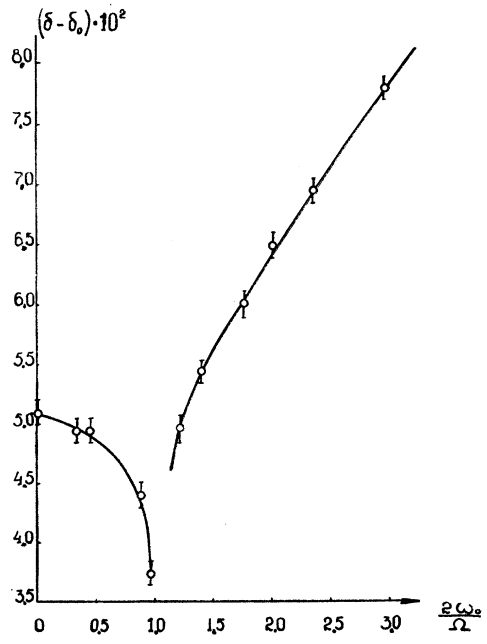

FIG. 5.5. Dependence of the damping of the disk oscillations on the velocity of rotation in the case of the classical liquid. The experimental data were obtained by Mesoed and Tsakadze (1961) in rotating water. The solid curves represent the theoretical results (Mamaladze and Matinyan, 1960c).

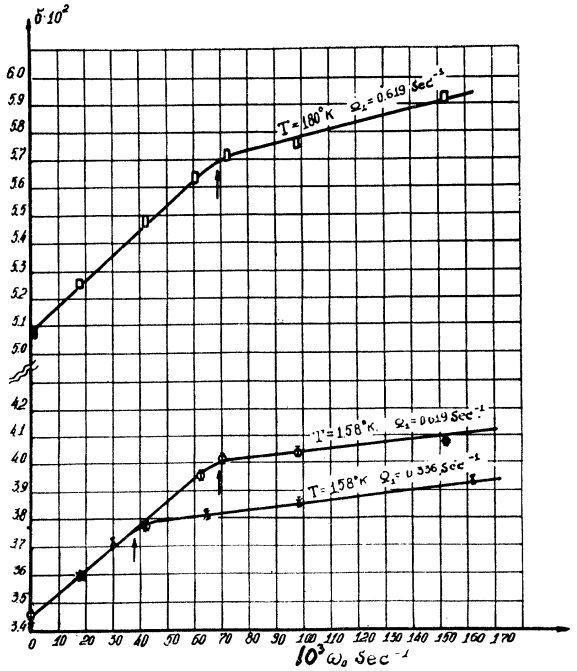

FIG. 5.6. Dependence of damping of the vertical oscillations of the cylinder on the velocity of rotation when there is a disk, below the cylinder, oscillating with the frequency Ω_1 (Tsakadze, 1963d). Arrows show the angular velocities $\tilde{\omega}_0=0.11\Omega_1$ (6.3.4) from which the collectivization of vortex oscillations starts.

change the character of its interaction with a vertically oscillating cylinder as well. Placing an oscillating disk under this cylinder (Tsakadze, 1962b, 1963a,d), damping of the cylinder shows the linear dependence on the velocity of rotation (i.e., on the number of vortex lines). As is shown in Fig. 5.6, the velocity of rotation at which $2\omega_0/\Omega_1 \sim 0.2$ (Ω_1 is the frequency of disk oscillations and not that of the cylinder) is connected in this case as well with the existence of a certain peculiarity leading to a break on the experimental curves.

Figure 5.7 gives a summary of the results described in this paragraph concerning the velocity dependence of damping in rotating helium II for bodies of different shape. It gives a clear picture of anisotropy of elastic–viscous properties of rotating helium II. Detailed analysis of the peculiarities of the observed curves is given in the next paragraphs, but we note here the complete agreement of this picture with the conceptions on vortex lines arranged along the rotation axis. In the two latter cases, it is essential that vortex lines are deformed by transversal motion of their ends fastened to the surface of oscillating disks.

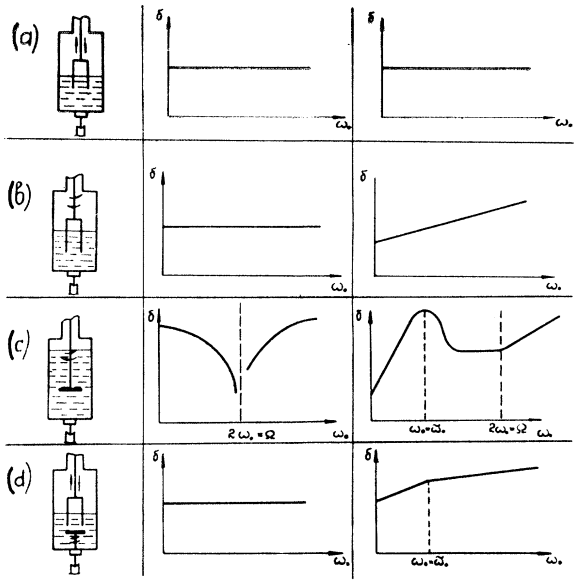

FIG. 5.7. Summary of the data on the dependence of oscillation damping upon the velocity of rotation. The schematic representation of the oscillating body and the direction of its oscillations are given in the first column; the velocity dependencies of damping of the corresponding bodies in the classical liquid are given in the second column (in arbitrary units); the same dependencies in helium II are given in column three.

5.2. Hydrodynamics of Small Oscillations of Bodies with Axial Symmetry in Rotating Helium II

All the described experiments are united by a common idea: properties of vortex lines and properties of the stationary state of rotating helium II are studied by the method of superimposing small perturbations on this state. Quasi-stationarity of these perturbations, which have the character of harmonic oscillations and smallness of their amplitude, simplifies the hydrodynamical analysis of the corresponding problems, as Eqs. (4.2.1) and (4.2.2) as well as condition (4.3.1) and equalities (4.3.4) and (4.3.5) are linearized in such a situation and exponential factors containing time (and the amplitude) cancel. But even linearized equations do not have simple solutions at all boundary conditions.

Problems of motion of cylinders oscillating in a vertical direction (Mamaladze, 1960a) or in an axial one (Mamaladze and Matinyan, 1960b) are solved rather easily. Solutions of the set (4.2.1), (4.2.2), (4.3.3) in such cases are radially propagating transverse waves of the normal component. They drag or do not drag the superfluid component as well, depending on the orientation of vortex lines and on the direction of oscillations in these viscous waves coinciding with the direction of oscillations of the cylinder. The study of such phenomena gives the information on orientation and density of vortex lines, we mentioned in the previous paragraph, and on the character of interaction of vortex lines with the normal component.

In the case of disk oscillations, the solution of the set of equations of rotating helium II hydrodynamics is much more complicated (Mamaladze and Matinyan, 1961; also, see Andronikashvili, Mamaladze, Matinyan, and Tsakadze, 1961). Formulas describing the frequency Ω and dampling δ of the disk oscillations are so cumbersome that, with the aim of physical interpretation of the obtained data, we limit ourselves with a very rough approximation associated with neglection of phenomena of sliding ($a=a'=0$) and mutual friction. Then

$$\Omega^2-\Omega_0^2=(\pi R^4\Omega/2I)\left[-(\eta_n\rho_n/2)^{\frac{1}{2}}\left[(\Omega+2\omega_0)^{\frac{1}{2}}+(\Omega-2\omega_0)^{\frac{1}{2}}\right]+(\nu_s)^{\frac{1}{2}}\rho_s(2\omega_0/\Omega)\,(\Omega+2\omega_0)^{\frac{1}{2}}\right],$$

when $2\omega_0<\Omega$; (5.2.1)

$$\Omega^2-\Omega_0^2=(\pi R^4\Omega/2I)\left\{-(\eta_n\rho_n/2)^{\frac{1}{2}}\left[(\Omega+2\omega_0)^{\frac{1}{2}}-(2\omega_0-\Omega)^{\frac{1}{2}}\right]+(\nu_s)^{\frac{1}{2}}\rho_s(2\omega_0/\Omega)\left[(\Omega+2\omega_0)^{\frac{1}{2}}+(2\omega_0-\Omega)^{\frac{1}{2}}\right]\right\},$$

when $2\omega_0>\Omega$; (5.2.1a)

$$\delta-(\Omega_0/\Omega)\,\delta_0=(2\pi^2R^4/I\Omega)\left\{(\eta_n\rho_n/2)^{\frac{1}{2}}\left[(\Omega+2\omega_0)^{\frac{1}{2}}+(\Omega-2\omega_0)^{\frac{1}{2}}\right]+(\nu_s)^{\frac{1}{2}}\rho_s(2\omega_0/\Omega)\,(\Omega-2\omega_0)^{\frac{1}{2}}\right\},$$ when $2\omega_0<\Omega$; (5.2.2)

$$\delta-(\Omega_0/\Omega)\,\delta_0=(2\pi^2R^4/I\Omega)\,(\eta_n\rho_n/2)^{\frac{1}{2}}\left[(2\omega_0+\Omega)^{\frac{1}{2}}+(2\omega_0-\Omega)^{\frac{1}{2}}\right],$$ when $2\omega_0>\Omega$; (5.2.2a)

where Ω_0 and δ_0 are the values of the magnitudes Ω and δ at oscillations in the vacuum, R and I are the radius of the disk and the moment of inertia of the device, respectively, and η_n is a dynamical viscosity of the normal component.

Though these formulas cannot be considered quantitatively accurate, they are quite sufficient as an initial point for the qualitative analysis. Curves which could be plotted according to these formulas are by their main features similar to graphs in Figs. 5.3 and 5.4. It is necessary to describe processes taking place in rotating helium II at the disk oscillations in detail to understand the physical nature of the main peculiarities of the observed dependencies and those of Eqs. (5.2.1), (5.2.1a), (5.2.2), and (5.2.2a). That will give an explanation of the physical causes of discrepancies between them.

5.3. Transverse Waves

A disk generates transverse oscillations propagating parallel to the axis of rotation and consisting of four waves. The relative amplitudes of these waves are different in the superfluid and normal components; therefore, they can be called s^+, s^-, n^+, and n^-, because if there had been no mutual friction, the waves $s^\pm$ would have propagated only in the superfluid component and $n^\pm$ only in the normal one. The sign "+" is used for the wave numbers of these waves described by the term $\Omega+2\omega_0$, and the sign "−" for those described by the term $\Omega-2\omega_0$ [see formulas (5.3.1) and 5.3.2)]. "Plus" and "minus" waves have opposite circular polarization.

In the approximation $\mathbf{F}_{sn}=0$[5] the waves called $S^\pm$ are elastic waves, their complex wave numbers[6] are determined in the following way:

$$k_{s0}^{(\pm)2}=\mp\,(\Omega\pm2\omega_0)/\nu_s, \qquad \mathrm{Im}\,k_{s0}^{(\pm)}>0 \quad (5.3.1)$$

(the index 0 means a zero approximation over the mutual friction).

In the same approximation the waves called $n^\pm$ are viscous waves with the wave numbers

$$k_{n0}^{(\pm)2}=-i\,(\Omega\pm2\omega_0)/\nu_n, \qquad \mathrm{Im}\,k_{n0}^{(\pm)}>0. \quad (5.3.2)$$

Let us note once more the similarity of formulas (5.3.1) and (5.3.2) that recalls the analogous role of the elastic constant ν_s and viscous constant ν_n, but let us still emphasize a very different character of the waves, described by them.

The wave $k_{n0}^{(+)}$ has a usual character of a viscous wave. The same may be said about the wave $k_{n0}^{(-)}$ if Ω is not very close to $2\omega_0$.[7] Their penetration depth is rather small in comparison with the wavelength and the conception "wave" is somewhat conventional (Fig. 5.8). It would be better to speak about oscillations of a layer with the effective thickness $\frac{1}{2}\lambda$ adjacent to the disk (Landau and Lifshitz, 1953). The reason for these circumstances is the equality of the real and imaginary parts of $k_{n0}^{(\pm)}$ (see footnote 6) and in this connection the following relationship is obtained:

$$L_{n0}^{(\pm)}=2\pi\lambda_{n0}^{(\pm)}$$

$$\lambda_{n0}^{(\pm)}=(1/2\pi)\,L_{n0}^{(\pm)}=(2\nu_n/|\,\Omega\pm2\omega_0\,|)^{\frac{1}{2}}. \quad (5.3.3)$$

Under the conditions of the experiments of Andronikashvili, Tsakadze, and Chkheidze (the usual conditions of such experiments), the values of $\lambda_n^{(\pm)}$ are usually of the order of fractions of a millimeter and do not exceed a few millimeters. If there are solid

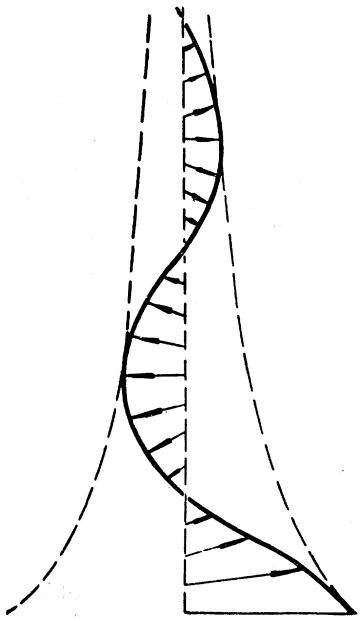

FIG. 5.8. Hodograph of velocities of the liquid motion in the viscous waves with circular polarization. To make the drawing simpler the scale is distorted. In reality, at the distance from the disk surface equal to one-half wavelength the velocity is exp $(-\pi)\approx0.043$ times less than that on this surface, and at the distance equal to the wavelength exp $(-2\pi)=0.0019$ times. Only the first half turn of the hodograph, shown in this figure, exists effectively.

[5] Having solved the equation of motion of the superfluid liquid (4.2.1) in this approximation Hall (1958) has found expressions of the wave numbers $k_{s0}^{(\pm)}$ (5.3.1) and used them to determine ν_s. The following expressions (5.3.2) for $k_{n0}^{(\pm)}$ are characteristic of the classical viscous liquid (Mamaladze and Matinyan, 1960c). The complete expressions of the wave numbers $k_s^{(\pm)}$, $k_n^{(\pm)}$ taking into account the mutual friction between the components are found by Mamaladze and Matinyan (1960a, more accurate formulae are published in the paper of Mamaladze and Matinyan 1961 and in the paper of Andronikashvili, Mamaladze, Matinyan, and Tsakadze, 1961).

[6] A complex wave number $k\equiv\sigma+i\tau$ determines the wavelength L and the depth of the wave penetration λ: $L=2\pi/|\,\sigma\,|$, $\lambda=1/\tau$ (it is implied that $\tau>0$).

[7] We imply everywhere that the case $\Omega-2\omega_0\gg\gamma$ is considered, where γ is the coefficient of damping ($\gamma=\Omega\delta/2\pi$), δ is the logarithmic decrement of damping). That excludes some interval of angular velocities of rotation from consideration. Phenomena taking part in this interval are not sufficiently studied and are not described in this paper. Deep penetrating viscous waves are observed in a classical liquid in this interval (Mamaladze, Mesoed, and Tsakadze, 1964, Mamaladze, 1964).

surfaces at intervals of the order of a few centimeters from the disk, we can consider that the disk is immersed in an infinite liquid.

The wave number $k_{s0}^{(+)}$ is always obtained as a purely imaginary one. The same is true for the number $k_{s0}^{(-)}$, when $2\omega_0>\Omega$. Hence, the corresponding wavelengths are infinite and the penetration depths are equal to

$$\lambda_{s0}^{(+)}=(\nu_s/\Omega+2\omega_0)^{\frac{1}{2}} \tag{5.3.4}$$

$$\lambda_{s0}^{(-)}=(\nu_s/2\omega_0-\Omega)^{\frac{1}{2}}, \quad \text{when} \quad 2\omega_0/\Omega>1. \tag{5.3.5}$$

They are of small magnitudes of the same order as $\lambda_{n0}^{(\pm)}$. There are even fewer reasons here to use the conception "wave." In addition to the fact that the hodograph of velocities again has the shape shown in Fig. 5.8, the oscillations of the liquid in this case occur everywhere in the same phase (Fig. 5.9), i.e., there is no wave in general. Nevertheless we shall use the term s^- "waves", when $2\omega_0>\Omega$ and s^+ "waves," meaning that under real conditions the mutual friction makes these wavelengths finite and thus makes them like $n^\pm$ waves.

Only the wave s^-, when $2\omega_0<\Omega$ has the character completely corresponding to the ideas associated with the conception of an "elastic wave." The wave number $k_{s0}^{(-)}$, when $2\omega_0<\Omega$ is purely real. The penetration depth $\lambda_{s0}^{(-)}$ in this case is infinite. The velocity amplitude does not depend on the distance from the oscillating disk and an instantaneous profile of velocities as well as an instantaneous photo of a vortex line have the shape shown in Fig. 5.10. The wavelength is expressed by the formula

$$L_{s0}^{(-)}=(\nu_s/\Omega-2\omega_0)^{\frac{1}{2}}, \quad \text{when} \quad 2\omega_0<\Omega. \tag{5.3.6}$$

It is natural that the mutual friction does not leave the penetration depth of this wave equal to infinity. However, even when the dissipation of energy due to mutual friction is taken into account, the penetration depth $\lambda_s^{(-)}$, when $2\omega_0<\Omega$ is (under usual conditions) larger than the other three ($\lambda_s^{(+)}$, $\lambda_n^{(\pm)}$) and larger than the wavelength $L_s^{(-)}$. But $\lambda_s^{(-)}$ is smaller than the distances of the order of ten centimeters or in some cases even smaller than one centimeter [formula (7.3.3)]. Therefore it is not difficult to create such conditions when the disk is oscillating in an "infinite" liquid.

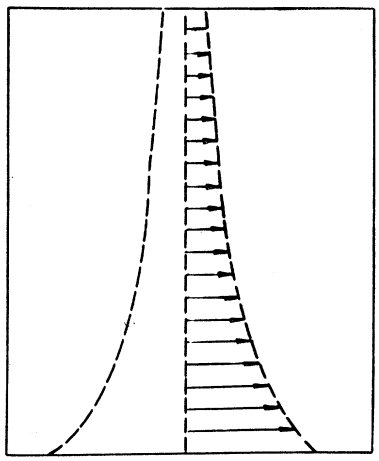

FIG. 5.9. Hodograph of velocities in the s^+ wave in the absence of mutual friction ($L_{s0}^{(+)}=\infty$). The value of the velocity decreases at the removal from the disk along the z axis, according to the exponential law $\exp(-z/\lambda_{s0}^{(+)})$. A similar situation exists for the s^- wave when $2\omega_0>\Omega$.

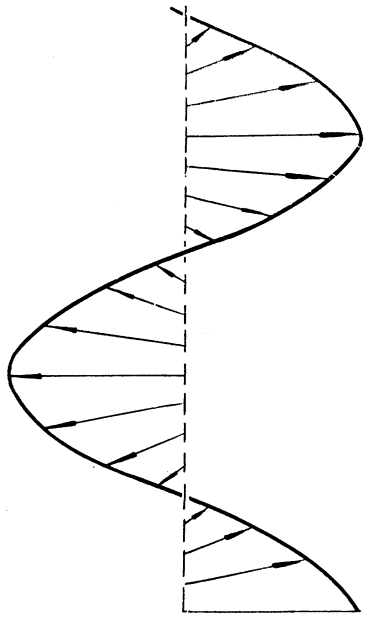

FIG. 5.10. Hodograph of velocities in the s^- wave when $2\omega_0<\Omega$ in the absence of mutual friction ($\lambda_{s0}^{(-)}=\infty$).

5.4. The Mechanism of Interaction of an Oscillating Disk with a Rotating Viscous Liquid

Now we can return to the interpretation of formulas (5.2.1), (5.2.1a), (5.2.2), and (5.2.2a). They describe the summarized effects of action of the normal and the superfluid components on the disk. The normal component interacts with the disk by means of viscous forces, which are proportional to the coefficient of viscosity η_n and to the gradient of velocity, i.e., inversely proportional to the penetration depth λ (see Fig. 5.8). Therefore the contribution of $n^\pm$ waves into the change of frequency and damping of oscillations, described by formulas (5.2.1), (5.2.1a), (5.2.2), (5.2.2a) contain terms proportional [according to (5.3.3)] to $(\eta_n\rho_n)^{\frac{1}{2}}\times(|\Omega\pm2\omega_0|)^{\frac{1}{2}}$. The same expressions describe the frequency and damping of the axial disk oscillations in a rotating classical liquid (Mamaladze and Matinyan, 1960c). When $2\omega_0<\Omega$ they give a decrease of oscillation damping at an increase of the velocity of rotation (negligible, when $2\omega_0/\Omega\lesssim0.5$). When $2\omega_0>\Omega$, this decrease is replaced by an increase of damping. This fact is associated with the change of the sequence of terms in the difference $|\Omega-2\omega_0|$. Thus expressions (5.3.3) for the penetration depths of viscous waves explain the existence of the minimum in Fig. 5.5.

5.5. The Mechanism of Interaction of an Oscillating Disk with a Rotating Superfluid Liquid

In contrast to the normal component, the superfluid component of rotating helium II interacts with the disk

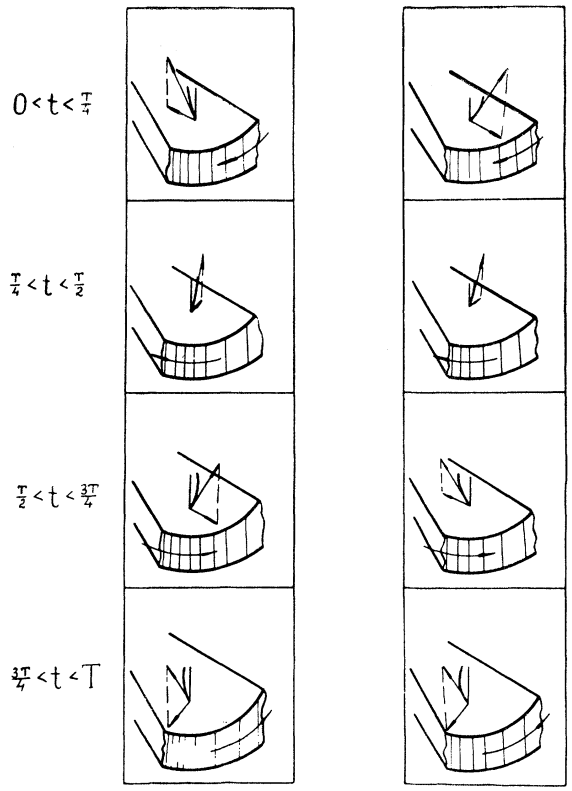

FIG. 5.11. Schematic representation in time of the change of the mutual orientation of the vortex line tension (and its projection on the disk surface) and the direction of the disk oscillations. The action of the s^+ wave is shown in the first column. Similarly the s^- wave acts when $2\omega_0>\Omega$; only the direction of the circular polarization changes. The action of the s^- wave when $2\omega_0<\Omega$ is shown in the second column.

by means of tension in vortex lines curved by the waves. The corresponding tangent forces are proportional to the density of vortex lines and to their tension and inversely proportional to the wavelength of s^-, when $2\omega_0<\Omega$ (Fig. 5.10). When $2\omega_0>\Omega$, then the tangent forces are inversely proportional to the penetration depth of the same s^- wave, and in all the cases to the penetration depth of the wave s^+ (Fig. 5.9). Therefore the contributions of these waves are proportional to $(\omega_0/\Gamma)\epsilon/L_{s0}^{(-)}$ or $(\omega_0/\Gamma)\epsilon/\lambda_{s0}^{(\pm)}$, respectively, i.e., to $\omega_0(\nu_s)^{\frac{1}{2}}\rho_s(|\Omega\pm2\omega_0|)^{\frac{1}{2}}$.

Considering formulas (5.2.1), (5.2.1a), (5.2.2), and (5.2.2a) from this point of view, we should pay attention to the fact that when $2\omega_0<\Omega$, the s^+ wave contributes only to the change of oscillation frequency and the s^- wave only to damping. When $2\omega_0>\Omega$ both $s^\pm$ waves contribute only to the frequency. Damping in this case is completely determined by $n^\pm$ waves.

The cause of such a separation of functions between the components of a complex wave could be explained if you make a more detailed analysis of solutions of hydrodynamical equations (Mamaladze, 1960b). Its results are schematically shown in Fig. 5.11. It is seen that the s^+ wave distorts a vortex line so that every quarter of the period it sometimes accelerates an approach of the disk to the position of the equilibrium, sometimes slows down its removal from this position. It is clear that such an interaction can change only the oscillation frequency, but does not cause their damping. When $2\omega_0>\Omega$, the s^- wave has the opposite direction of the circular polarization, nevertheless it acts on the disk in the same way as the s^+ wave. But when $2\omega_0<\Omega$, the difference between the s^- and s^+ waves is connected not only with the different signs of polarization, but with the existence of a difference of the initial phases as well. As a result of this the s^- wave distorts a vortex line so that it continuously slows down the disk motion. This fact causes damping of oscillations.

So the nature of the disk vortex damping is similar to the physical nature of radiation damping of electric charge oscillations. The dissipation of the energy of the disk oscillating axially in rotating helium II is caused (in addition to the action of viscous forces) by leakage of energy along oscillating vortex lines in the form of the energy flux of s^- waves.

An idealized picture drawn here, neglecting vortex line sliding and the mutual friction, in reality could have led to disk oscillation damping only in a truly infinite liquid. In the opposite case the energy transferred to vortex lines would return to the disk by waves reflected from the boundaries of the liquid. Under real conditions sliding of vortex lines should be taken into account. It decreases the intensity of the waves running from a given surface, both from a generating surface and a reflecting one. The mutual friction also should be taken into account, as it has been already mentioned, it gives a finite value $\lambda_s^{(-)}$ (instead of $\lambda_{s0}^{(-)}=\infty$) to the penetration depth of an s^- wave. If the distance between the disk and the reflecting surface is sufficiently large in comparison with $\lambda_s^{(-)}$ (not necessarily much larger than $\lambda_s^{(-)}$) then the reflected waves are really absent. Then the dissipation of the disk energy carried away by means of waves along vortex lines, is realized by mutual friction. But the mechanism of energy transfer is still, under the most real conditions of the experiment, caused by elastic properties of quantized vortex lines. Thus formulas (5.2.1), (5.2.1a), (5.2.2), and (5.2.2a) need only small corrections, taking into account mutual friction forces. The exception is the region $2\omega_0\approx\Omega$ where the parameters of the s^- (and n^-) wave are determined rather by mutual friction, and the region $T\approx T_\lambda$, where the tension of vortex lines, proportional to ρ_s, is very small, but the mutual friction is significant (Pitaevski, 1958b). Let us note, by the way, that below $T\sim2$°K dampling, apparently, changes roughly as ρ_s (Fig. 5.12). The increase of the role of mutual friction near the λ-point can explain the slowing down of the drop of vortex line damping with an increase of temperature above 2°K.

In contrast to mutual friction, sliding of vortex lines along the disk surface has, under all real conditions, a

very important role in the determination of the character of vortex oscillation influence on the disk motion (though sliding does not influence the expressions for the wave numbers of the $s^{\pm}$, $n^{\pm}$ waves). Let us nevertheless note that even without taking sliding into account, formula (5.2.2) gives the possibility to understand the main peculiarity of the graphs in Figs. 5.3 and 5.4 distinguishing them from the graph in Fig. 5.5, i.e., instead of a minimum at oscillations in classical liquids including helium I, there is a maximum of damping at oscillations in helium II.

Damping in the rotating normal component (similarly to that in a classical liquid) decreases with an increase of the velocity of rotation almost till $2\omega_0 \sim \Omega$ and damping in helium II is always greater than in a liquid at rest. This means that the main term in formula (5.2.2) is the vortex term (containing $\rho_s \nu_s^{\frac{1}{2}}$). But there is a product $\omega_0(\Omega-2\omega_0)^{\frac{1}{2}}$ in this term that gives a maximum, when $2\omega_0/\Omega=\frac{2}{3}$. The origin of this maximum is easy to understand if you recall that the factor ω_0 characterizes the density of vortex lines and $(\Omega-2\omega_0)^{\frac{1}{2}}$ determines the value of the projection of the vortex line tension on the disk surface. The number of vortex lines increases with an increase of ω_0, but the action of each of them on the disk oscillations is weakened, because of a decrease of the inclination of a vortex line to the disk surface, caused by an increase of the wavelength $L_{s0}^{(-)}$. The struggle of such opposite tendencies leads just to the maximum of δ when $2\omega_0/\Omega=\frac{2}{3}$. But this magnitude is about three times as large as the experimental one. The cause of this discrepancy cannot be understood without consideration of vortex sliding, which is considered in the next section.

5.6. Resonance Phenomena

The waves $n^{\pm}$, $s^{\pm}$, being generated by an oscillating disk and reflected from the top or the bottom of the vessel, from the free surface of the liquid, or from the surface of another oscillating disk, could interfere in a different way in dependence on the passed distance. The maximum and the minimum intensities would then be achieved at different distances between the surfaces, multiple to the half-wavelength or a quarter wavelength, in dependence on the character of the surface and its motion. The surface may be free or solid. In the latter case it may be at rest or oscillate.

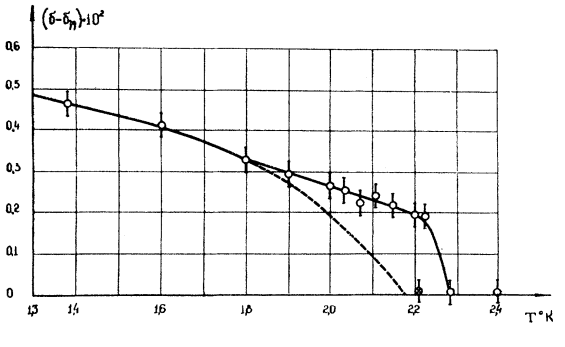

FIG. 5.12. Temperature dependence of the disk axial oscillation damping at $2\omega_0/\Omega=0.21$ (corresponding to the maximum in Fig. 5.3). The dashed line shows the law $\delta-\delta_n \sim \rho_s$; δ_n is the decrement of damping in helium II at rest. The experimental data shown by open circles (Andronikashvili, Mesoed, and Tsakadze, 1964) are stable when $T<T\lambda$, but when $T>T_\lambda$ they are obtained only at the transition from helium II into helium I in the state of rotation (11.2). The stable value obtained by rotation at $T>T_\lambda$ is given by a circle with a cross.

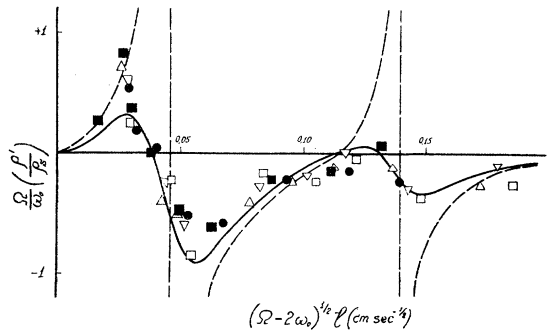

FIG. 5.13. Change of the oscillation frequency of the pile of disks at the change of disk separation $2l$, according to Hall's data (1958a, 1960). ρ' is the effective density of the superfluid component dragged into the pile oscillations, determined by the formula

$$\rho'/\rho_s=[(T_\omega^2-T_0^2)/(T_2^2-T_1^2)][(I_2-I_1)/I_s],$$

where $T\omega$ and T_0 are the periods of oscillation of a disk in the rotating helium II and in helium II at rest. T_2 and T_1 are the periods of oscillation at room temperature; the corresponding moments of inertia are I_2 and I_1; I_2-I_1 is the known moment of inertia; I_s is the moment of inertia of the superfluid component in the pile. The dashed line was calculated by Hall not taking into account vortex sliding. The solid line is obtained when sliding is taken into account (6.1). Different symbols for the experimental points correspond to different conditions of the experiment. In all cases, $2\omega_0<\Omega$.

Therefore it is clear that waves, the penetration depths of which are small in comparison with the wavelengths ($n^{\pm}$, s^{+}, and s^{-} when $2\omega_0>\Omega$) could not manifest themselves appreciably in resonance phenomena. Only a s^{-} wave has such an ability, when $2\omega_0<\Omega$.

In actuality, having studied the velocity dependence of the oscillation frequency of a pile of disks in rotating helium II, Hall (1958a) found resonance phenomena disappearing when $2\omega_0>\Omega$. It was found that, when $2\omega_0<\Omega$, the frequency of oscillations Ω sometimes decreases, sometimes increases with an increase of the velocity of rotation in such a way that some function of Ω (see Fig. 5.13) depends almost sinusoidally on the combination $(2\omega_0-\Omega)^{\frac{1}{2}}l$ (where l is the half of the disk separation). Let us recall that Hall's pile of disks had variable separation between the disks. The magnitude $(2\omega_0-\Omega)^{\frac{1}{2}}l$ is proportional to the ratio of $2l$ to the length of the S^{-} wave. Hall has determined the parameter ν_s entering formula (5.3.6) for $L_{s0}^{(-)}$ for the known distance between two nearest maxima (minima) on the curve in Fig. 5.13. He has obtained for ν_s the value $\nu_s=(8.5\pm1.5)10^{-4}$ cm^2 sec^{-1}. In addition he made an estimation of the radius of the core of a vortex line

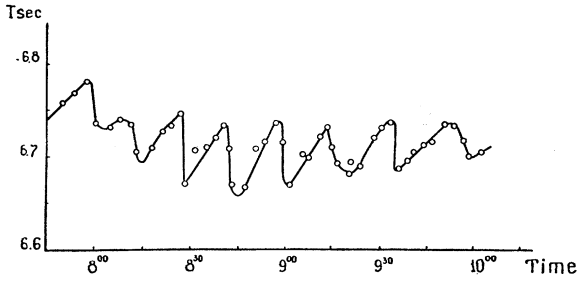

FIG. 5.14. Change of the period of the disk oscillations in time at the removal of the free surface from it (Hall, 1958b, 1960). $T=1.3°K$, $2\omega_0<\Omega$.

(entering the expression for ν_s). According to his estimation $a_0\approx 7$ Å, but Gopal (1964), having recalculated data of Hall's experiment, has shown that they correspond to the value $a_0\approx 4$ Å.

The described investigation made by Hall and the similar results published by Andronikashvili and Tsakadze (1958),[8] in which oscillations of a pile of disks were studied, were the first ones in the series of the following studies of solid body motion in rotating helium II. Many of these studies have already been described in the previous paragraphs. Just the experiment with a pile of disks was the basis of the statement of Andronikashvili and Tsakadze on the existence of the modulus of rigidity in rotating helium II with respect to the rotation axis. However, Hall who was the first to determine the parameters of elastic waves $s^{\pm}$, nevertheless has interpreted the results of his experiments in terms of "effective density of the superfluid component dragged into oscillations of the pile of disks." In particular, he considered the observed increase of the frequency as an indication of the effective decrease of the moment of inertia. Therefore he explained it by the superfluid motion in the antiphase to the motion of disks of the pile. However, it would be more natural to consider the observed phenomena as a result of the torque increase as it was made by Andronikashvili and Tsakadze.[9] In this connection we should mention the

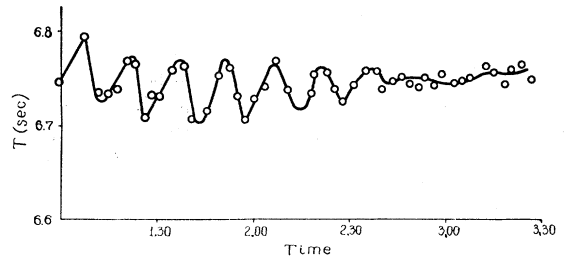

FIG. 5.15. Same as in Fig. 5.14, but at the temperature $T=1.6°K$ (Hall, 1958b, 1960). Comparison of Figs. 5.14 and 5.15 shows how the penetration depth of the s^- wave decreases at an increase of mutual friction, when the wavelength practically does not change [compare formulae (5.3.6), (7.3.3), and (7.3.5)].

[8] The results of both experiments were reported simultaneously by both groups of authors at the Fourth All-Union Conference on Low Temperature Physics, Moscow, 1957.

results of a detailed analysis of hydrodynamical equations. This analysis shows that when vortex lines are completely fastened onto the surface of the disk, the superfluid component oscillates in the radial direction, i.e., not in the phase or antiphase with the disks, but perpendicular to the direction of their oscillations. Certainly, this phenomenon is connected with the Magnus effect. In general, one should always remember that the superfluid component does not interact directly with a solid body, just vortex lines existing in it do that.

Resonance phenomena were also observed at oscillations of a single disk under the free surface of rotating helium II. Hall (1958b, 1960) has measured the period of the disk oscillations as a function of the distance from it to the free surface changed as a result of helium inflow along the film (Figs. 5.14 and 5.15). Andronikashvili and Tsakadze (1959a) have measured the damping of

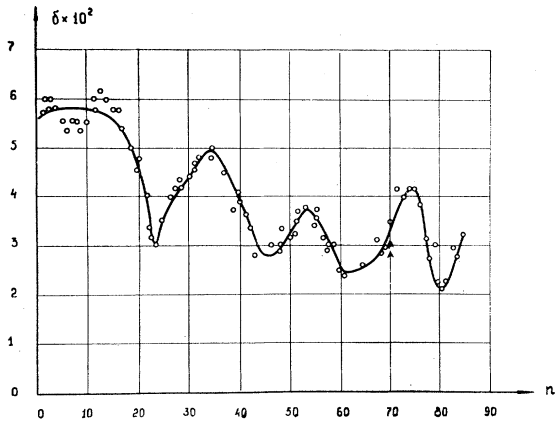

FIG. 5.16. Change of the disk oscillation damping in time at an approach of the free surface to the disk (Andronikashvili and Tsakadze, 1959a). Here n is the number of half-periods of oscillations. $2\omega_0<\Omega$.

oscillations at the change of the distance from the disk to the liquid surface because of its evaporation (Fig. 5.16). The calculation of ν_s according to the results of these experiments gives $\nu_s=9.7\times10^{-4}$ cm^2 sec^{-1} and $\nu_s\approx 8\times10^{-4}$ cm^2 sec^{-1}, respectively.

Finally, Hall (1960) observed resonance phenomena between two disks performing measurements similar to those shown in Fig. 5.13.

The comparison of Figs. 5.14 and 5.15 shows how the penetration depth $\lambda_s^{(-)}$ of the s^- wave decreases at an increase of temperature and hence at an increase of the role of mutual friction. This decrease takes place practically at its constant length $L_s^{(-)}$ and at the maintenance of the unequality $\lambda_s^{(-)}\gg L_s^{(-)}\approx L_{s0}^{(-)}$. The weakness of the dependence of $L_s^{(-)}$ on temperature

[9] More detail is given on the difference between Hall's conception and that of the Tbilissi group as well as on the more accurate interpretation of Hall's experiments in the paper of Andronikashvili, Mamaladze, Matinyan, and Tsakadze (1961).

was also found as a result of Hall's experiment with the disks.

6. OSCILLATIONS OF SOLID BODIES WITH AXIAL SYMMETRY IN ROTATING HELIUM II (CONTINUATION). SLIDING OF VORTEX LINES AND COLLECTIVIZATION OF VORTEX OSCILLATIONS

6.1. Sliding of Vortex Lines

The coefficients a and a' first mentioned in Sec. 4.3, in the boundary conditions of Bekarevich, Khalatnikov (4.3.1) being practically always not equal to zero, describe sliding of vortex lines along the disk surface. Their values depend on many conditions. According to formulas (4.3.2), (4.3.3) the coefficient a depends on the scale of roughness of the considered surface and the coefficient a' can be very small in comparison with the coefficient a. In the temperature interval $T>1°K$, it does not exceed $\sim 0.3a$. [*Note added in proof.* According to a new estimation of the coefficient B', made by Iordanski (Sec. 12.8), even the ratio $a'/a\sim 0.3$ should be considered as too large.] Thus we can take into account only the coefficient a in the interpretation of many experimental data.

In addition to the size of protuberances the following factors may influence the values of the coefficients of sliding: the number of protuberances on the surface and the velocity of rotation determining the ratio between the number of protuberances and the number of vortex lines; the frequency of oscillations of the surface, determining together with the velocity of rotation the values of forces dragging the vortex line along the surface; the amplitude of oscillation determining the change of vortex energy as a result of which it either becomes longer at the removal from the position of equilibrium or it slides off the proturberance of a given size, and finally it is also reduced to the value of the drag force, etc.

Hall, who has introduced the coefficient a into consideration for the first time, analyzing his results, which have been described in 5.6 (Hall, 1958a, 1960), has determined the following empirical values for a: $a=0.5\Omega/k_{s0}^{(-)}$, when $2\omega_0<\Omega$ and $a=0.5\Omega(2\omega_0/\nu_s)^{-\frac{1}{2}}$, when $2\omega_0\gg\Omega$. Under the conditions of the experiments that corresponded to the values

$$a\sim(1.5\div 2.3)\times 10^{-2}\ \text{cm sec}^{-1}$$

when

$$2\omega_0/\Omega\sim 0.13\div 0.26$$

and

$$a\sim(2.3\div 3)\times 10^{-1}\ \text{cm sec}^{-1}$$

when

$$2\omega_0/\Omega\sim 6\div 8.$$

The necessity to obtain at least an approximate estimation of the coefficient of sliding was connected with the fact that the magnitude plotted along the ordinate in Fig. 5.13, has, in the theory neglecting sliding, infinite jumps between its experimental maxima and minima (i.e., near the second, fourth, and the following even zeros).

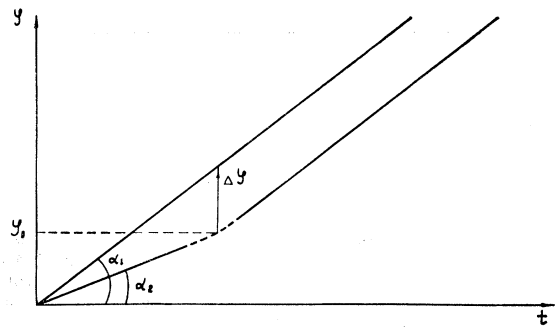

FIG. 6.1. Change in time of the deflection angle of the suspension head with respect to the rotating vessel takes place according to the law $\varphi=\omega_0' t(\omega_0'=tg\alpha_1)$. The deflection angle of the disk changes in time by the law

$$\varphi=\begin{cases} t\cdot tg\alpha_2 & \text{at } \varphi<\varphi_0 \\ \omega_0' t-\Delta\varphi & \text{at } \varphi>\varphi_0 \end{cases}$$

(Gamtsemlidze, Japaridze, Salukvadze, and Turkadze, 1966). The constancy in time of the disk delay from the suspension head, taking place at $\varphi=\varphi_0$, means that vortex sliding prevents their further distortion.

The direct measurement of a was made by Gamtsemlidze, Japaridze, Salukvadze, and Turkadze (1966) in an experiment, the idea of which arose from the following circumstances. Osborne (1961) made an attempt to measure the force with which vortex lines are fastened to a solid surface. For this purpose he deflected for some angle a disk suspended on an elastic thread near the bottom of the rotating vessel and taking part in the rotation. The experiment failed, because vortex lines, sliding along the surface of the disk or the bottom, became parallel again to the rotation axis. After that they could not already create the torque acting on the disk. Therefore Gamtsemlidze *et al.* decided to use a disk performing continuous motion with respect to the vessel bottom. They constructed a device in which the vessel with helium II and the disk rotated together. An additional rotation of the disk suspension head was superimposed on this rotation. Depending on the forces acting on it, the disk could either rotate with the same velocity as its suspension head, or rotate with some delay with respect to it. At the start of an extra rotation the disk was at first behind the suspension head, being slowed down due to inclined vortex lines (Fig. 6.1). But with an increase of delay the torque of the suspension head increased gradually, while an increase of slowing down action of the inclined vortex lines was limited by their sliding. If we neglect the coefficient a' then the boundary condition (4.3.1) gives in this case $\omega_0' r\approx a\sin\alpha\approx ar\phi_0/d$ (Fig. 6.2) or $a=\omega_0' d/\phi_0$, where ϕ_0 is the angle of torsion at which the disk delay reaches some constant value,

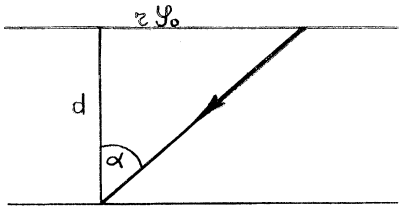

FIG. 6.2. The point of the vortex line fastening to the disk is shifted with respect to its point of fastening to the bottom of the vessel at the distance $r\varphi_0$. Here r is the distance from the rotation axis, φ_0 is the angle the physical sense of which is explained by Fig. 6.1, and d is the distance from the disk to the vessel bottom. The arrow shows the tension of the vortex line after deflection.

d is the distance from the disk to the bottom, and ω_0' is the angular velocity of the additional rotation.[10]

The estimation obtained in such a way gave $a=0.1$ cm sec^{-1}, when $\omega_0=0.038$ sec^{-1} (and $\omega_0'=0.0035$ sec^{-1}). Within an order of magnitude it agrees rather well both with Hall's data (1960) and with the estimation (4.3.3) as the size of sand grains glued to the disk was $\delta\sim 50\ \mu$.

6.2. The Role of Sliding in an Interaction of an Oscillating Disk with Rotating Helium II

Let us return now to the problem of axial oscillations of a disk in helium II. If sliding is taken into account formulas (5.2.1), (5.2.1a), (5.2.2), and (5.2.2a) became much more complex. We shall not write the corresponding cumbersome expressions, but we shall note (Mamaladze, 1965) that sliding changes the relation of phases of the s^+ and s^- waves and each of them begins to contribute both to damping and to oscillation frequency. In addition, as it was already noted, sliding influences the value of the tangent component of the vortex line tension. Let us take into account all these factors, without taking the mutual friction into account explicitly, though it enters all these phenomena not explicitly, since it is possible to neglect the reflected waves. Then the calculation of vortex damping at different coefficients of sliding leads to the results given in Fig. 6.3. An increase of the coefficient a leads at first to an increase of damping and then to its drop. The coefficient a' has a comparatively insignificant role.

The curves in Fig. 6.3 are very much like the experimental curves in Figs. 5.3 and 5.4. The only essential difference between them is the position of the maximum, which, as it was before sliding was taken into account, is on the calculated curves at the value of $2\omega_0/\Omega$ much greater than in reality.

Comparing Fig. 6.3 with Figs. 5.3 and 5.4, we can note that experimental curves hardly correspond to some constant values of the coefficients of sliding. That should not be expected, if we take into account their probable dependence on the velocity of rotation. The first portions of the experimental curves (especially in the case of a smooth disk) have a small slope indicating that the sliding coefficient a has large values. Relatively high maxima, on the contrary, show that a is rather small. It becomes clear that the experimental maximum is associated with the minimum of sliding and the shapes of the experimental curves are due to its smooth change.

Numerical calculations made by a computer have shown (Fig. 6.4) that the experimental data agree completely with the theory, when both sliding and mutual friction are taken into account. Here it was suggested that the coefficient of sliding is a function of the velocity of rotation as it is shown in Fig. 6.5 (Andronikashvili, Mamaladze, Matinyan, and Tsakadze, 1961). The order of magnitude of a according to these data also agrees with the data of other authors.

6.3. Collectivization of Vortex Line Oscillations

The maximum on the curves of the disk damping dependence on the velocity of rotation is always found at $2\omega_0/\Omega\approx 0.2$ and its position does not depend either on temperature or on the extent of roughness of the disk surface. The minimum of the sliding coefficient is always located at this point and the reason for this fact does not depend directly on the peculiarities of the phenomenon of sliding itself. Here the properties of vortex lines and of waves running along them are displayed and lead, when $2\omega_0/\Omega\approx 0.2$, to the phenomenon of collectivization of vortex oscillations [Mamaladze, see, for instance, Andronikashvili and Tsakadze (1959b) and Andronikashvili, Mamaladze, Matinyan,

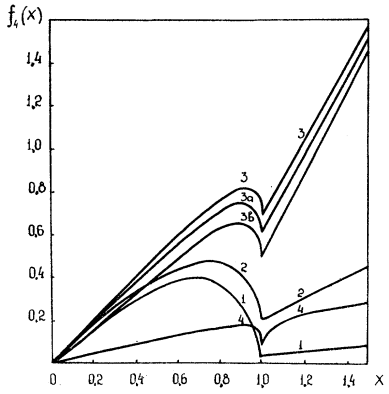

FIG. 6.3. Dependence of axial oscillation damping of the disk on the velocity of rotation of the superfluid at different values of coefficients of sliding according to calculations of Mamaladze (1965). The symbols are $x=2\omega_0/\Omega$,

$$f_4(x)=\frac{2I\Omega^{\frac{3}{2}}(\delta-\Omega_0\delta_0/\Omega)}{\pi^2R^4\rho_s(\nu_s)^{\frac{1}{2}}}.$$

The coefficient b equal to $b=a/(\Omega\nu_s)^{\frac{1}{2}}$ takes the following values on the curves 1, 2, 3, and 4, where the coefficient $a'=0$: (1) $b=10^{-2}$; (2) $b=10^{-1}$; (3) $b=1$; (4) $b=10$. On curves 3a and 3b as well as on curve 3, $b=1$, and the coefficient b' equal to $b'=a'/(\Omega\nu_s)^{\frac{1}{2}}$ takes the values: (3a) $b'=10^{-1}$; (3b) $b'=3\times 10^{-1}$.

[10] Apparently, the absolute sense should not be attributed to Fig. 6.2. In reality vortex lines slide off the grains and try to straighten, but fasten themselves to new grains and become inclined again, etc. Figure 6.2 can be considered as a result of the averaging of this process in time.

and Tsakadze (1961)]. Let us begin the description of this phenomenon.

When a wave runs along a vortex line, the superfluid liquid both rotates around the vortex line and oscillates with it as well. The distances from a vortex line at which the liquid takes an effective part in rotation around one of the vortex lines can differ significantly from distances at which it participates in vortex oscillations. The participation of the superfluid component in vortex oscillations is characterized by the additional energy ϵ' (Pitaevski, 1958b).

$$\epsilon' = \pi\rho_s(\hbar^2/m^2)\tfrac{1}{2}(q^2\sigma^2)\ \ln\ (\sigma a)^{-1}, \qquad (6.3.1)$$

where q is the amplitude of oscillations and σ is the real wave number. Comparing this expression with formula (2.3.1) for the energy of the liquid rotation in a vortex, we obtain the following estimation for the effective radius b_1 of the region where the liquid oscillates together with a vortex line

$$b_1 \approx 1/\sigma. \qquad (6.3.2)$$

This estimate agrees with the Kelvin formula (1880) according to which $b_1 = 1.046/\sigma$.

As noted in Sec. 5.3, when $2\omega_0 < \Omega$, the s^- waves are the main ones running along vortex lines. To estimate the value of b_1 for these waves, the wave number $k_{s0}^{(-)}$ should be substituted into formula (6.3.2). Neglecting the mutual friction, we obtain

$$b_1 = [\nu_s/(\Omega - 2\omega_0)]^{\frac{1}{2}}. \qquad (6.3.3)$$

At sufficiently small velocities of rotation, the vortex line separation $(\pi\hbar/m\omega_0)^{\frac{1}{2}}$ is large and exceeds the effective radius of oscillations b_1. Under such conditions,

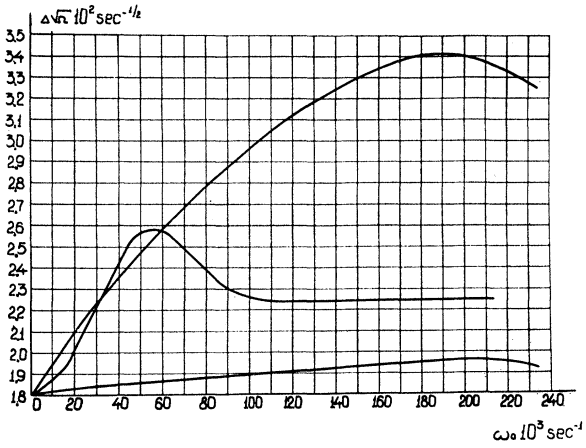

FIG. 6.4. Dependence of the disk oscillation damping, calculated according to the formula which takes into account completely both sliding and mutual friction (Andronikashvili, Mamaladze, Matinyan, and Tsakadze, 1961). The parameters of the device and the temperature correspond to the conditions of the experiment described by the lower curve in Fig. 5.3. Δ denotes $\delta - \Omega_0\delta_0/\Omega$. The upper curve is calculated when $a=0$, the lower one when $a=\infty$. The middle curve reproduces the experimental data and is obtained using a variable a, the velocity dependence of which is shown in Fig. 6.5.

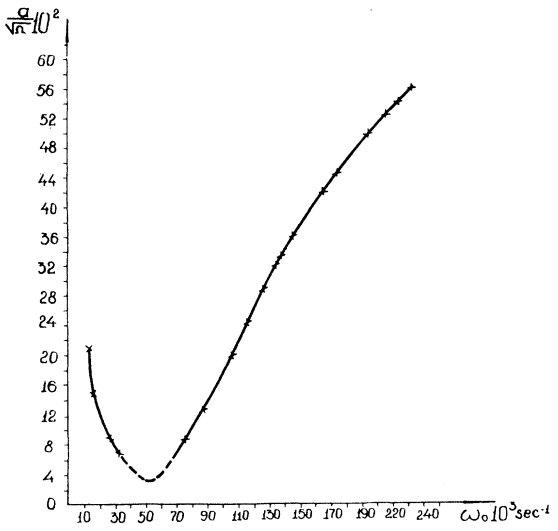

FIG. 6.5. Empirically established dependence of the coefficient of sliding a on the angular velocity of rotation under the conditions of the experiment described by the lower curve in Fig. 5.3. (Andronikashvili, Mamaladze, Matinyan, and Tsakadze, 1961).

the whole superfluid liquid moved by vortex lines does not participate in oscillations, but only some part of it, directly adjacent to them. Oscillations of separate vortex lines are independent. But when the velocity of rotation is increased, the distance between vortex lines decreases while the effective radius of oscillations b_1 increases. At the velocity, which we shall denote as $\tilde{\omega}_0$, the effective radius b_1 becomes equal to half of the vortex separation

$$[\nu_s/(\Omega - 2\tilde{\omega}_0)]^{\frac{1}{2}} = \tfrac{1}{2}(\pi\hbar/m\tilde{\omega}_0)^{\frac{1}{2}},$$

hence,

$$2\tilde{\omega}_0/\Omega = (2m\nu_s/\pi\hbar + 1)^{-1}. \qquad (6.3.4)$$

Beginning from the velocity $\tilde{\omega}_0$ and when $\omega_0 > \tilde{\omega}_0$ the effective radii of vortex oscillations overlap and their mutual interaction occurs. Under such conditions, oscillations of a vortex line are transferred to its neighbors and, on the contrary, the existence of nonoscillating neighbors prevents vortex line oscillations.

If we substitute numerical values for the parameters which are in the right-hand side of formula (6.3.4), then $2\tilde{\omega}_0/\Omega$ is of the order of 0.2. This value coincides with the point of maximum on the experimental curves of damping dependence on the velocity of rotation (Figs. 5.3, 5.4) and with the point of the minimum on the curve of the sliding coefficient a dependence on the velocity of rotation (Fig. 6.5). Proceeding from the idea of collectivization of vortex oscillations the character of the latter curve can be understood in the following way.

At small velocities of rotation when there are few vortex lines, the coefficient of sliding depends mainly on the roughness of the surface. We should take into account that even in the presence of artificial roughness

(glued sand grains) the sliding of vortex lines can be rather strong since not every vortex line can be fastened to a grain. When the velocity of rotation and the number of vortex lines are increased, a still greater number of vortex lines fastens to the rough surface of the disk. At the same time a decrease of the tangent component of the vortex line tension $[\sim(\Omega-2\omega_0)^{\frac{1}{2}}]$ contributes to a decrease of the probability of a vortex line tearing off from the protuberance of the disk. All these circumstances lead to a decrease of the coefficient of sliding, providing that it was not too small from the very beginning, because of an extremely rough surface.

The picture is changed when the collectivization of vortex oscillations takes place. Beginning from $\omega_0\approx\tilde{\omega}_0$ and at higher velocities, vortex lines not fastened to the surface (i.e., vortex lines without grains of sand near them or vortex lines out of the disk periphery) influence oscillations of fastened vortex lines. Thus they increase the averaged coefficient of sliding a. This increase of sliding leads just to the maximum of damping (Figs. 5.3, 5.4). As noted before (Fig. 6.3) even stronger damping of disk oscillations corresponds to smaller coefficients of sliding than in the case $a=0$. Such a phenomenon is connected with the fact that when there is sliding, the s^+ wave, in addition to the change of frequency of disk oscillations (5.5), begins to participate in the increase of damping. In its turn large coefficients a correspond to weak damping, as the projection of vortex tension does not sufficiently slow down the disk oscillations.

Now it is possible to understand another phenomenon in which the special role of the point $2\tilde{\omega}_0/\Omega\approx0.2$ is seen. It is a sharp slowing down of the frequency increase

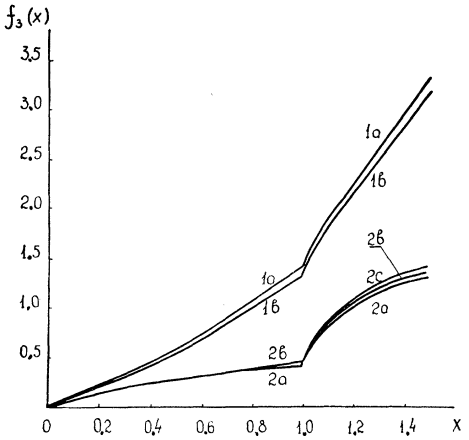

FIG. 6.6. The influence of sliding on the velocity dependence of the disk oscillation frequency in the rotating superfluid. It was calculated when mutual friction was not taken into account (Mamaladze 1965). The symbols used are: $x=2\omega_0/\Omega$,

$$f_3(x)=2I(\Omega^2-\Omega_0^2)/\pi R^4\rho_s(\nu_s\Omega)^{\frac{1}{2}}.$$

The symbols b and b' are the same as in Fig. 6.3. Their values on different curves: (1a) $b=10^{-1}$, $b'=0$; (1b) $b=10^{-1}$, $b'=3\times10^{-2}$; (2a) $b=1$, $b'=0$; (2b) $b=1$, $b'=10^{-1}$; (2c) $b=1$, $b'=3\times10^{-1}$.

of light disk oscillations, depending on the velocity of rotation. In the beginning of the curve in Fig. 5.2, the experimental data agree rather well with formula (5.2.1), which does not take sliding into account. But when $2\omega_0/\Omega>0.2$ an increase of sliding leads to a decrease of vortex line contribution to the torsion momentum acting on the disk. Then the increase of frequency is slowed down (Fig. 6.6).

The third fact confirming the validity of the considerations on the role of collectivization is the break of the curves in Fig. 5.6. When $2\omega_0/\Omega_1>0.2$ vortex lines begin to slide along the disk surface, which is a generator of waves. The intensity of s^- waves, running along them, decreases as well as the damping of the cylinder performing vertical oscillations.

The hydrodynamics of rotating helium II by its very nature cannot take into account completely the phenomenon of collectivization of vortex line oscillations. It deals with magnitudes averaged over the volume containing many vortex lines and therefore the parameters b_1 or $\tilde{\omega}_0$ do not appear naturally in the equations of hydrodynamics or in their solutions. The considerations used to determine these parameters were beyond the frames of an averaged hydrodynamical treatment and the phenomena associated with the collectivization of oscillations were described, in the language of hydrodynamics of rotating helium II, as changes of the averaged coefficient a. Thus it is an arbitrary parameter, selected to achieve an agreement between the theory and experiment (Figs. 6.4 and 6.5).

Gopal (1964a,b) approached this problem in another way, without averaging, while solving the problem of single vortex line oscillations in a cylindrical vessel (1963). Then he imagined that each vortex line, appearing in rotating helium II, is in a cylinder the radius of which is determined by vortex line separation. Such a consideration, not quite precise, but more detailed than in the case of averaging, allowed him to obtain the expression for the wave number $k_{s0}^{(-)}$. This expression, when $k_{s0}^{(-)}b\ll1$ (i.e., when $\omega_0<\tilde{\omega}_0$) coincides with expression (5.3.1) and when $k_{s0}^{(-)}b\sim1$, (i.e., when $\omega_0\sim\tilde{\omega}_0$) begins to deviate essentially from it. Unfortunately, Gopal's calculations were made for a purely superfluid liquid. The generalization of such a consideration for the real conditions of the experiment, i.e., when the existence of the normal component, mutual friction, and sliding are taken into account would have given the possibility of making more precise calculations, similar to those illustrated in Figs. 6.4 and 6.5. Then the coefficient a would acquire more direct sense.

7. MUTUAL FRICTION BETWEEN THE SUPERFLUID AND NORMAL COMPONENTS

7.1. The Conception of Mutual Friction in Rotating Helium II

Preliminary data on mutual friction between the superfluid and normal components of rotating helium II

were given in the paper of Hall and Vinen (1955). The anisotropic character of such an interaction was also emphasized there. Feynman's point of view on the nature of critical phenomena in helium II explains completely both the causes of the creation of mutual friction and its anisotropic character. The mutual friction is due to scattering of thermal excitations on singularities, which are vortex lines. In rotating helium II where vortex lines are aligned along the rotation axis, the transfer of the thermal excitation momentum to a vortex line (i.e., of the normal component momentum to the superfluid liquid) should be essentially different in radial and axial directions.

7.2. The First Experimental Confirmation of Feynman's Theory

In the investigations which gave the first experimental confirmation of Feynman's theory, the force of mutual friction reduced to unit mass of the superfluid component was expressed by Hall and Vinen (1955, 1956a, b) in the following way:

$$\mathbf{F}_{sn}=-\tfrac{1}{2}(\rho_n/\rho)B[(\boldsymbol{\omega}/\omega),[\boldsymbol{\omega},\mathbf{v}_n-\mathbf{v}_s]]$$
$$-\tfrac{1}{2}(\rho_n/\rho)B'[\boldsymbol{\omega},\mathbf{v}_n-\mathbf{v}_s]. \quad (7.2.1)$$

In this formula the both terms are proportional to the values of two vectors, to the relative velocity $\mathbf{v}_n-\mathbf{v}_s$ and to $\boldsymbol{\omega}=$ curl $\mathbf{v}_s$ (because of the linear dependence of the number of vortex lines on the velocity of rotation). The first term with the coefficient B has the direction of the relative velocity projection $\mathbf{v}_n-\mathbf{v}_s$ on the plane perpendicular to the rotation axis. It is just the direction which one could imagine at an elementary consideration of the action of the normal component flow on vortex lines existing in the superfluid component. But in the expression for $\mathbf{F}_{sn}$ there is a second term, with the coefficient B' also directed perpendicularly to vortex lines and at the same time perpendicular to $\mathbf{v}_n-\mathbf{v}_s$. Its existence is connected with the Magnus effect.

Hall and Vinen used second-sound resonators of two different types: a radial mode resonator, in which emission, reflection, and reception of thermal waves were realized by means of two coaxial cylinders with side surfaces facing each other and an axial mode resonator in which the bottom and the top of a hollow cylinder were used with the same aim.

The results of the Hall and Vinen study were the following: (a) detection of second-sound attenuation due to mutual friction in the radial mode resonator and its absence in the axial mode resonator, (b) confirmation of formula (2.5.1) by the linear increase of mutual friction with an increase of velocity of rotation, (c) a theoretical analysis of scattering of thermal excitations on vortex lines and comparison of the calculated values of the mutual friction coefficients B with its experimental dependence on temperature, (d) confirmation of circulation quantization (Fig. 7.1). Hall and Vinen did not manage to measure the coefficient B'.

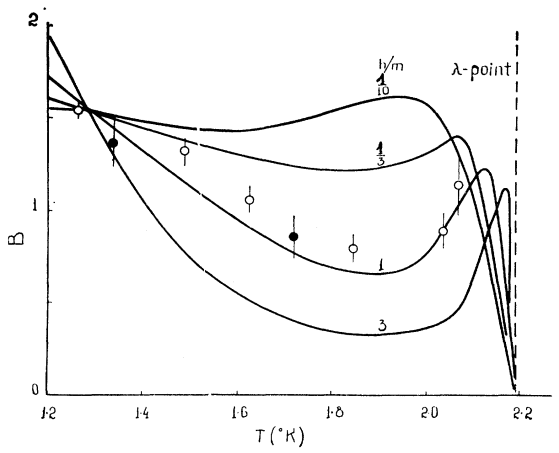

FIG. 7.1. Dependence of the coefficient of mutual friction B on temperature studied experimentally by Hall and Vinen, and calculated by them at different values of the vortex circulation, which are given (in units of h/m) above each curve (Hall and Vinen, 1956a, b).

7.3. Further Investigations

Lifshitz and Pitaevski (1957) have critically considered the calculations of Hall and Vinen and showed the necessity of replacing Born's approximation, used by them at the consideration of scattering of thermal excitations on vortex lines, by a quasi-classical one. That did not lead to sufficient results. To achieve agreement of the theory with the experiments of Hall and Vinen on measurements of B, it was necessary to introduce such a mechanism of roton scattering, at which a roton passes an intermediate stage of its capture to a stationary orbit by a vortex line. Having selected the effective radius of this capture $\sim$10 Å, Lifshitz and Pitaevski have brought their calculations to agreement with the experimental values of B and obtained the theoretical dependence of B' on temperature shown in Fig. 7.2.

Dependence of B and B' on temperature in the vicinity of the λ-point is studied in comparatively less detail. Pitaevski (1958b) has shown that here one should not expect a gradual approach of B and B' to zero and large values of both coefficients are possible.

The data of Tsakadze and Chkheidze (1960, see Fig. 5.1) also give a possibility to measure B. According to Mamaladze and Matinyan (1960b), the results of their experiments should be described by the formula

$$\frac{\delta_2-\delta_1}{l_2-l_1}=\frac{2\pi^2R^3}{I}\left(\frac{2\eta_n\rho_n}{\Omega}\right)^{\frac{1}{2}}\left(1+\frac{\omega_0}{\Omega}\frac{\rho_s}{2\rho}B\right). \quad (7.3.1)$$

(Symbols used are the same as in caption to Fig. 5.1.) The agreement of the theory and the experiment shown in Fig. 5.1 confirms the calculations made by Lifshitz and Pitaevski (1957), as the values obtained by them for B were used while plotting the theoretical straight lines.

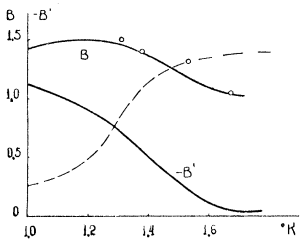

FIG. 7.2. Results of the calculations of Lifshitz and Pitaevski (1957). The solid lines give: the upper one B, the lower one B'. The experimental points are obtained by Hall and Vinen (Fig. 7.1). The dashed line shows the wrong dependence $B=B(T)$ obtained at the quasiclassical approximation without taking into account the temporary capture of rotons to the stationary orbits.

Formula (7.3.1) is valid at relatively small velocities satisfying the unequality $\omega_0\rho_s B/\rho\Omega\ll 1$ (depending also on temperature). In the opposite limiting case the dependence (7.3.1) should be replaced by the formula of Mamaladze:

$$\frac{\delta_2-\delta_1}{l_2-l_1}=\frac{2\pi^2R^3}{I}\left(\frac{2\eta_n\rho}{\Omega}\right)^{\frac{1}{2}}. \tag{7.3.2}$$

Equation (7.3.2) does not give the dependence of damping on the velocity of rotation. It is especially interesting that it contains the total density ρ instead of ρ_n. Thus the formula has such a form as if oscillations take place in a liquid at rest with the density ρ, but viscosity η_n.

In the method of an oscillating cylinder edge effects are excluded by subtraction of damping measured at different depth of immersion. Because of this the described method is very convenient for measurements of viscosity of different liquids (Tsakadze and Mesoed, 1962). Formula (7.3.2) should be used for classical liquids (η_n is replaced by η).

The coefficient B' is not sufficiently well studied experimentally so far. It was not determined in the experiments of Hall and Vinen (1956a, b), because of a lack of accuracy in the measurements. The accuracy of measurements of this magnitude was also insufficient in Hall's experiment with two disks. In that experiment, as mentioned earlier, the length $L_s^{(-)}$ of an s^- wave was determined. After making a correction in formula (5.3.6) for mutual friction, $L_s^{(-)}$ can be expressed in the following way (when $2\omega_0\ll\Omega$, $\rho_n B'/4\rho\ll 1$):

$$L_s^{(-)}=2\pi\left(\frac{\nu_s}{\Omega-2\omega_0}\right)^{\frac{1}{2}}\left(1-\frac{\rho_n}{4\rho}\frac{\Omega}{\Omega-2\omega_0}B'\right). \tag{7.3.3}$$

According to Sneider's preliminary data (1963) (he used a cubic mode resonator of second sound), $B'\ll 1$ at $T<2$°K. The coefficient B' increases at a temperature rise. Lifshitz and Pitaevski (1957) predicted its increase at temperatures below 1.4°K as well. However such a phenomenon was not found in Sneider's experiment.[11] The data on the final results of this study are not known to us.

[11] These results are in complete agreement with the theoretical calculation of Iordanski (1965b), whose paper we read when this chapter was already written (see 12,8).

At the consideration of the phenomena, in which vortex lines are parallel to the rotation axis, it is quite sufficient to use the expression for the force of mutual friction. But when transverse waves run along vortex lines, a more complete formula should be used (Bekarevich and Khalatnikov, 1961; also, see, Hall, 1960):

$$\mathbf{F}_{sn}=\frac{\rho_n}{2\rho}B\left[\frac{\boldsymbol{\omega}}{\omega},\left[\mathbf{v}_n-\mathbf{v}_s-\nu_s\,\mathrm{curl}\,\frac{\boldsymbol{\omega}}{\omega},\,\boldsymbol{\omega}\right]\right]$$
$$+\frac{\rho_n}{2\rho}B'\left[\mathbf{v}_n-\mathbf{v}_s-\nu_s\,\mathrm{curl}\,\frac{\boldsymbol{\omega}}{\omega},\,\boldsymbol{\omega}\right]$$
$$+\frac{\rho_n}{2\rho}B''\left(\frac{\boldsymbol{\omega}}{\omega},\,\mathbf{v}_n-\mathbf{v}_s-\nu_s\,\mathrm{curl}\,\frac{\boldsymbol{\omega}}{\omega}\right). \tag{7.3.4}$$

This formula is a result of decomposition of the force $\mathbf{F}_{sn}$ into three vectors with mutually perpendicular directions. Each of these three components of the force of mutual friction is proportional to the density of vortex lines, represented by the curl of the mean velocity of the superfluid component, and to the velocity of the normal component with respect to a vortex line. This velocity is represented by the vector

$$\mathbf{v}_n-\mathbf{v}_s-\nu_s\,\mathrm{curl}\,(\boldsymbol{\omega}/\omega).$$

In calculations the results of which are given in Figs. 6.4 and 6.5 just this formula was used in which B'' is put equal to zero and the values of B and B' correspond to those of Lifshitz and Pitaevski (1957). Earlier calculations made by Mamaladze and Matinyan (1960a) were performed using formula (7.2.1); i.e., without taking into account the term with $\nu_s\,\mathrm{curl}\,(\boldsymbol{\omega}/\omega)$. The comparison of the results shows that this term has no special role in the calculation of the disk oscillation damping. But it influences the expression of the penetration depth of the s^- wave essentially. This penetration depth, when $2\omega_0\ll\Omega$, at the first approximation over the mutual friction is determined by formula

$$\lambda_s^{(-)}\approx 4\rho\left[(\Omega-2\omega_0)\nu_s\right]^{\frac{1}{2}}/\rho_n\Omega B. \tag{7.3.5}$$

The assumption $B''=0$ encountered in papers of many authors is associated both with experimental facts and the theoretical considerations on the impossibility of mutual friction existence along vortex lines. Hall and Vinen (1956a, b) have not found any additional damping in an axial mode resonator. Mamaladze (1960a) suggested to use, with the aim of verification of equation $B''=0$ (or for measurements of B'' if it is different from zero), vertical oscillations of a cylinder, for which, similarly to (7.3.1), we obtain

$$\frac{\delta_2-\delta_1}{l_2-l_1}\sim 1+\frac{\omega_0}{\Omega}\frac{\rho_s}{2\rho}B''. \tag{7.3.6}$$

The results of Tsakadze's experiment (1962a), in which the independence of δ on ω_0 was shown (see Sec. 5.1), mean that $B''=0$. If we take into account the

errors of the experiment we must write down more precisely that $B''=0\pm0.025$ (when $B\sim1$ at $T=1.86°K$).

In the paper of Sneider (1963) already mentioned, the author did not manage to obtain reproducible values of B''. In 30% of events $B''=0$. In the other cases B'' was always much less than B in a wide range of temperatures from 1.34° to 2.17°K, while the ratio B''/B varied between 0.25 and 0.01. At the highest temperatures it even reached 0.002. Unfortunately, the errors of these data are not given. It is also difficult to say whether the values of B'' different from zero correspond to the equilibrium configurations of vortex lines.

The results of another experiment by Tsakadze (1962b, 1963a) with vertical oscillations of a cylinder above an axially oscillating disk (5.1) show that vortex line oscillations lead to the creation of mutual friction along the rotation axis (as this axis is not parallel to vortex lines). But it means that a rather small effective value of B'' can arise even without artificial generation of vortex oscillation as well, because vortex lines always experience zero and thermal oscillations.

The difference between the coefficients B, B', and B'' determining the intensity of mutual friction in three mutually perpendicular directions once more speaks in favor of anisotropy of elastic-viscous properties of rotating helium II.

8. PERSISTENT CURRENTS OF THE SUPERFLUID LIQUID

8.1. Observations of Persistent Currents

The best illustration of the complete absence of viscosity of the superfluid component is the existence of circular currents which, once formed, exist for an arbitrary long time.

The first attempt to find such currents of the superfluid component was made by Andronikashvili (1952). For this purpose, he used a pile of strictly parallel light disks spaced 0.2 mm apart and surrounded by a thin walled aluminium shell. The pile suspended on an elastic thread was carefully protected from light, which could cause some mechanical effects due to its thermal action. The pile was brought into a uniform rotation at temperatures close to that of the transition point. Then under the conditions of a continuous rotation of the pile, the helium bath was cooled to 1.5°K and after that the suspended system was smoothly (aperiodically) slowed down. This process was realized by electromagnetic forces acting on a special metal ring placed much higher than the pile. After a certain period of time, the pile was heated during $\frac{1}{4}$ of the period of the suspended system oscillation to a temperature of 1.65°K. That led to the transition of $\sim$10% of the superfluid component into the normal state. Heating was realized by eddy currents, which were induced in the cylindrical case of the pile by a high-frequency generator with a frequency of 2000 cps. Thus an absolute symmetry of the thermal flow was reached with respect to the rotation axis.

No deviation of the device was found, though it had to appear if the superfluid component, continuing to rotate around the axis of the stopped device, would have given its angular momentum to the walls and disks of the pile after its transition into the normal component.

In the published paper of Andronikashvili (1952) there was an error in calculations, but even without it the statement remains valid that the measured random angles of the pile deviation at the moment of heating were much less than the calculated one, which highly exceeded the experimental errors.

At present the negative results of this experiment should be ascribed to critical velocities, but in 1952 nothing was known about their values for rotating systems.

The first indication of the existence of the persistent current was presented in Hall's investigation (1957). It was shown that a rather slowly rotating vessel with a pile of disks [similar to Andronikashvili's device (1952)] does not give away, at its slowing down, the whole angular momentum obtained at its acceleration. It was found that there is conserved some angular momentum in the stopped vessel at least for about 25 min.

8.2. Persistent Current with an Elementary Circulation

Vinen (1958a, 1961a, b) has observed the existence of circulation (not exceeding two quanta of this magnitude) during a long time in the stopped device. The aim of his experiment was not the study of the persistent current, but the direct observation of a unit quantum circulation. It was found that it is more convenient to make such measurements after the stop of the vessel's rotation. That is why we discuss Vinen's experiments in this chapter. The idea of the experiment was the following. Oscillations of a stretched string are doubly degenerate, as they can be decomposed into two mutually perpendicular linearly polarized oscillations. Each of these oscillations will be quite equivalent to the second one. The same statement is valid at the decomposition into two oscillations with mutually opposite circular polarization. The situation changes when the string is run around by the circulation motion of the liquid. Then degeneration disappears and the oscillations with the circular polarization (the direction of rotation of one of which coincides with the imposed circulation, while the other one is opposite to it) acquire different frequencies. Indeed, depending on the mutual direction of the rotation of some elementary portion of the wire and the rotation of the fluid around it, the Magnus force is either added to the elastic straightening force or is subtracted from it. The vector sum of these two forces determines the value of the centrifugal

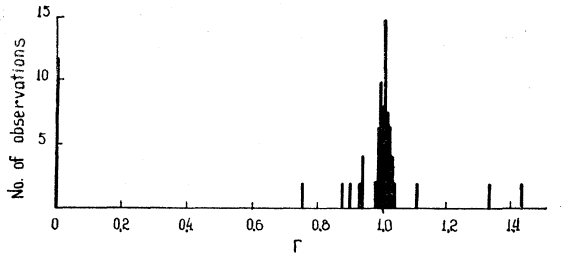

FIG. 8.1. The histogram confirming quantization of circulation (Vinen, 1961a, b).

force and hence the frequency of the wire's rotation. In Vinen's experiment a thin wire with a diameter of 2.5×10 cm^{-3} was stretched along the rotation axis of a narrow cylinder with a diameter of 0.5 cm, filled with helium II. The wire was placed in an external magnetic field and its oscillations excited by a short current pulse as a result of a capacity discharge. The registration of oscillations was made by observation of the current induced by a magnetic field in this wire. The difference of frequencies of the main modes of oscillations led to the generation of beats and that allowed the rather accurate measurement of the circulation of the liquid velocity determining the difference between frequences of oscillations with the opposite circular polarization.

At the above-mentioned value of the diameter of the rotating vessel there could arise from one to three vortex lines in the range of velocities used by Vinen $\omega_0\simeq2\times10^{-3}\div2\times10^{-2}$ sec^{-1}. Directly measured values of circulations were not always integers in units of h/m. The fact is that vortex lines could only partially cover the wire, fastening by one of the ends or by both of them to any point of the device. Shaking of the device had to give a more stable configuration to a vortex line and really, because of shaking the value of the measured circulation changed. The results are shown in Fig. 8.1 and leave no doubts as to the existence of vortex lines with unit circulation. They are obtained as a result of starting the device rotation above the λ-point, its cooling lower than this temperature and shaking more than once to obtain the stable circulation.

Vinen's conclusion that the data of his experiment correspond to the value of the vortex core $a_0\sim10^{-4}$ cm agrees poorly with the theory of Onsager and Feynman. However, Griffiths (1964) doubted the validity of Vinen's analysis (1961a, b), which had led to a such conclusions. According to Griffiths' estimation the core of Vinen's vortex lines had a radius not larger than 3×10^{-6} cm and probably much smaller.

Recently, Whitmore and Zimmermann (1965) have repeated Vinen's experiment. They have noticed an increase of stable circulation around the wire while increasing the diameter of the wire and the velocity of rotation. Their data, obviously, have something in common with the calculations of Bendt and Oliphant (1961), according to which (see Sec. 3.5) an increase of $\omega_0 r_1^2$ causes an increase of Γ.

8.3. An Irrotational Region and a Persistent Current

It was assumed by Bendt and Oliphant (1961) that an irrotational motion of the superfluid in an annulus can be conserved as a metastable state after the stop of the device as well.

The corresponding measurements were made by Bendt (1961, 1962) to find the persistent current in the annulus formed by two cylindrical surfaces rotating together until the stop; he immersed in helium II wings suspended on an elastic thread or a foil strip used as a peculiar Rayleigh disk. The most interesting results were obtained with the second version of the device. At an immersion of the strip to a definite depth (0.3 cm), the existence of a persistent current was registered. But at the repeated immersion of the foil the persistent current was not found. The disappearance of the current indicated firstly that the state with the persistent current in the stopped device is metastable and secondly the coherence of such a kind of flow, since at the repeated immersion of the foil the absence of the current was established until the depth of 1.3 cm (0.3 cm is about $\frac{1}{5}$ of the annulus depth).

8.4. Dependence of a Persistent Current on Temperature

Depatie, Reppy, and Lane (1962) have observed persistent currents in a device similar to that of Andronikashvili (1952) with the only difference that heating of the liquid, needed for the transition of the superfluid component into the normal one, was realized by a light beam. In addition, the vessel with a pile of disks was suspended not on an elastic thread, but by means of a magnetic suspension. This allowed the vessel to rotate practically without friction. When the initially uniformly rotated vessel was slowed down, then freed and heated, the velocity of its rotation increased and this indicated the existence of a persistent current in the slowed down vessel (Fig. 8.2). This effect occurred in the liquid which could be placed both in

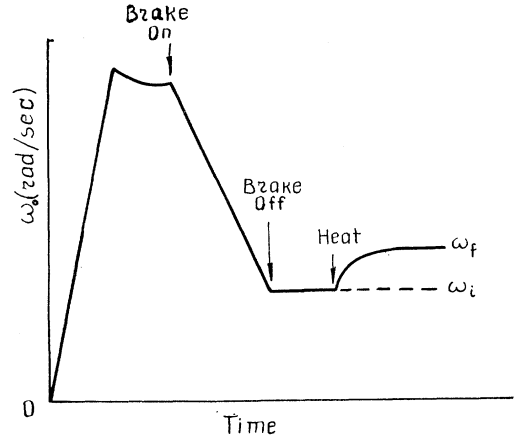

FIG. 8.2. Observations of a persistent current in the experiment of Depatie, Reppy, and Lane (1962).

the devices with doubly connected and with simply connected regions. In the first case the disk spacers were placed in the center of the vessel and in the second one they were at the periphery.

Reppy and Depatie (1964) used this technique to study the temperature dependence of the persistent current angular momentum. It was found that it is proportional to ρ_s, but not the value of ρ_s at the start or slowing down of the rotation, which leads to the formation of a persistent current. On the contrary the angular momentum is proportional to the value of ρ_s at the temperature from which the freed vessel is heated with the aim to show the conserved angular momentum (Fig. 8.3). Thus in a slowed down vessel the angular momentum changes as ρ_s during variation of temperature. That is explained by *conservation of the*

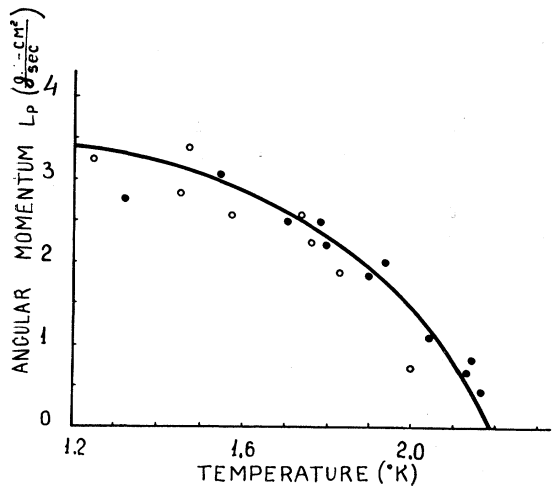

FIG. 8.3. Temperature dependence of the angular momentum of a persistent current according to the data of Reppy and Depatie (1964). The solid line corresponds to the law $L_P \sim \rho_s$; solid circles represent the data obtained at constant temperature; open circles show data obtained by lowering the temperature after a persistent current was formed until it was found.

velocity circulation, i.e., of an integral over the contour of $\mathbf{v}_s$, which represents a part of the integral of $\rho_s[\mathbf{r}, \mathbf{v}_s]$ over the volume which is equal to the angular momentum.

8.5. A Superfluid Gyroscope

Later Reppy (1965), having used the gyroscopic method of observation of a persistent current, developed by Clow, Depatie, Weaver, and Reppy (1965), had investigated the dependence of the angular momentum of a persistent current on temperature. The temperature range studied earlier was extended to the λ-point, to 10^{-5} °K. The superfluid current was formed in an annular container filled with fibrous foam to increase the critical velocity. This system constituted a superfluid gyroscope the angular momentum of which L_P was directed in the horizontal plane. One could judge the

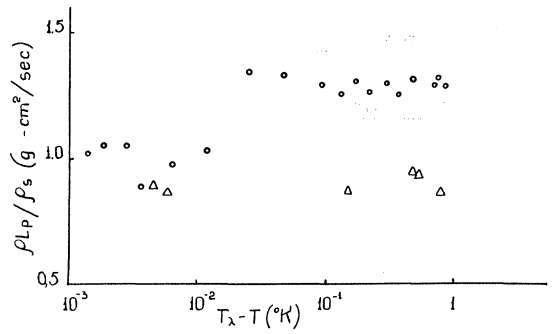

FIG. 8.4. The transition of a persistent current into a more stable state by liquid heating (Reppy, 1965). Circles give the data when the current was formed at $T_\lambda - T > 2\times10^{-2}$°K. Triangles show the data when the current was formed at $T_\lambda - T < 2\times10^{-2}$°K.

existence of a superfluid current, perpendicular to the L_P horizontal torque, required for excitation of gyroscope rotation around the vertical axis. The magnitude of $\rho(L_P/\rho_s)$ was determined, that excluded the dependence of L_w on temperature associated with the conservation of the circulation. Figure 8.4 shows that, when $T_\lambda - T \sim 2\times10^{-2}$ °K, persistent currents formed at lower temperatures display a tendency to transfer to a more stable state. This state, in the case when the current is formed near the λ-point and a smooth cooling followed, was not changed in time. In the vicinity of the λ-point the magnitude $\rho(L_P/\rho_s)$ characterizing in reality the flow rate, changes suddenly from the value larger than zero in helium II to zero in helium I. as shown in Fig. 8.5. This phenomenon takes place in the temperature range, which differs from T_λ by $\pm10^{-5}$ °K. The magnitude $\rho(L_P/\rho_s)$ has a tendency to a decrease at $\Delta T = T_\lambda - T \to 0$. This tendency is displayed when $T_\lambda - T$ drops from 4×10^{-5} °K to 0.5×10^{-5} °K. But this decrease of $\rho(L_P/\rho_s)$ does not exceed explicitly the errors of measurements.

Gyroscopic observations of a persistent current were also made by Mehl and Zimmerman (1965). They used a spherical vessel, filled with a porous substance,

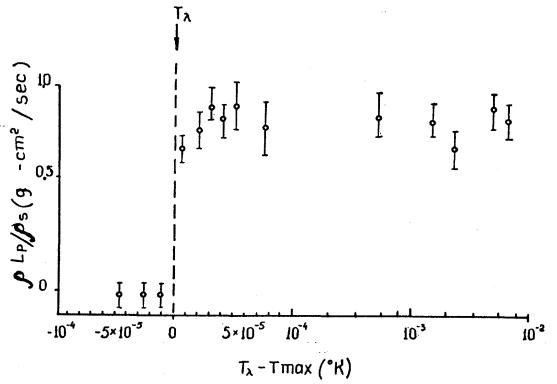

FIG. 8.5. A sharp disappearance of the persistent current at $T = T_\lambda$ (Reppy, 1965).

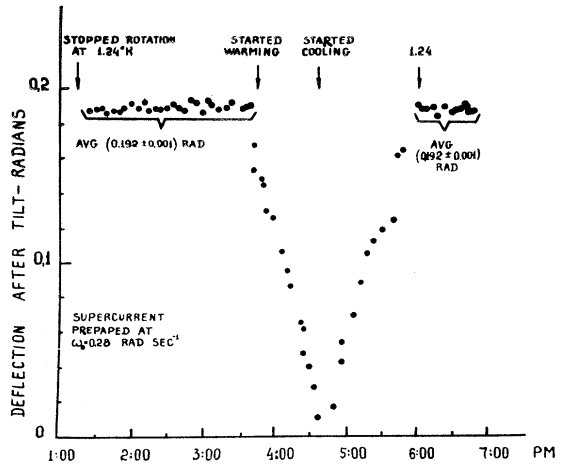

FIG. 8.6. Reversible change of the angular momentum of a persistent current on heating from 1.24°K to $T \lesssim T_\lambda$ and cooling till 1.24°K (Mehl and Zimmerman, 1965).

hanging freely on an elastic thread. During the measurements, after the rotation was stopped, this vessel was turned by a magnetic field for ~90°. As a result the persistent current angular momentum, which was directed vertically, changed its orientation into a horizontal one. The change was compensated by a deflection of the suspended system with respect to the vertical axis, permitting one to judge the existence of a persistent current, and the value of its angular momentum. Heating and cooling of the system have confirmed the conservation of circulation and the dependence $L_P \sim \rho_s$ in this case as well, as shown in Figs. 8.6 and 8.7.

8.6. The Critical Velocities

The uniform rotation of the superfluid component, taking place with an averaged velocity $v_s = \omega_0 r$ and accompanying the uniform rotation of the normal component, is realized by means of an array of Onsager–Feynman vortex lines. However, after the stop of the vessel, vortex lines existing outside the irrotational region, begin to inhibit the superfluid motion, creating mutual friction between it and the normal component in the process of its slowing down. This means that the persistent current is practically unable to conserve the whole angular momentum of the superfluid component. This angular momentum is lost due to mutual friction only if we do not deal with completely irrotational motion between two cylinders.

Presently, there are no definite data on the values of the critical velocities at which persistent currents appear and disappear. The picture becomes more complicated because of the peculiarities of the twisting and slowing down of helium II. These phenomena are discussed in more detail in Sec. 10. Both dragging of the superfluid component into rotation and the disappearance of vortex lines after the vessel is stopped take rather a long time. At low velocities of vessel rotation ($\omega_0 \sim 0.1$ sec^{-1}), the superfluid liquid can even remain stopped for a rather long time ($\tau \sim 10^3$ sec) before an interaction with the rotating container will take place. This phenomenon is especially clearly pronounced if before rotation helium was at rest for a long time, being in the state of helium I. At high velocities of rotation ($\omega_0 \gtrsim 0.2$ sec^{-1}), the interaction of the vessel with the superfluid begins practically at once and is over after a time of the order of $10^3 \div 10^2$ sec. After the rotated vessel is stopped, the vortex lines decay according to the exponential law with the period of half-decay of the order of 30 sec.

Let us assume that a slowly rotating vessel was stopped and we have not found any persistent current. Does that mean that at such angular velocities this annular current cannot be realized in general? Taking into account everything mentioned above about the time of dragging the superfluid component into the vessel rotation, we can suppose that it simply had no time to interact with the rotating vessel or the normal component. Similarly the absence of a persistent current in the vessel stopped after a rapid rotation does not mean that some absolute critical velocity, i.e., the upper limit of the persistent current existence, was exceeded. Simply the angular momentum of the superfluid was dissipated before the completion of the process of vortex line disappearance. Thus a persistent current is created practically at such velocities of rotation at which an irrotational region is formed occupying the whole volume of the liquid. In any case one can say that these are the velocities at which the number of vortex lines in the vessel is relatively small. It is possible that there is no exact upper limit of the vessel velocity, it depends on the sensitivity of the device, on the possibility of finding a much weakened persistent current.

Considerations just described explain the failure of Andronikashvili's experiment (1952) in which $\omega_0 \approx 3$ sec^{-1}. The same consideration concerns Hall's experiment (1957), in which he had not observed any retention of the angular momentum by the superfluid component at slowing down of the container which rotated

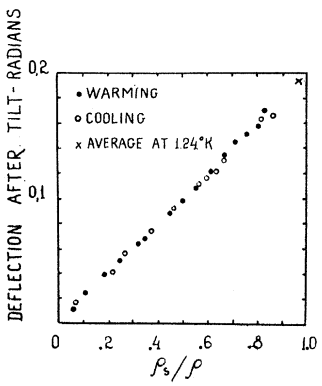

FIG. 8.7. The data of Fig. 8.6 confirm the law $L_P \sim \rho_s$ (Mehl and Zimmerman, 1965).

with high velocity. Only at small velocities was the momentum lost by slowing down helium II smaller than the momentum L_c obtained by the liquid at twisting. Similarly in the Walmsley and Lane experiments (1958) the angular momentum obtained from slowing down helium II was smaller than L_c, but it tended to this value at an increase of the velocity of rotation and of temperature rise.

According to Bendt (1962), who made experiments with the annular channel between cylindrical surfaces with the radii $R_1=8.72$ cm and $R_2=8.94$ cm and the height 0.18 cm, the critical velocity had the value varying in the interval $1.75\div1.19$ rpm depending on the initial state of the liquid, which could be either rotated before the experiment or be at rest. Bendt determined critical velocities of rotation below which the appearance of a persistent current was not observed. He noticed quite reasonably that there were no grounds to think that a persistent current rotates with the same velocity as the vessel before its stop.

In the case when the device was filled with a porous substance the vortex formation became more difficult and the critical velocity increased. At sufficiently small dimensions of the pores of the used substance, such conditions could be created when the critical velocity limiting the value of the persistent current is the velocity of the breakdown of superfluidity (in Landau's sense) and not the velocity of vortex formation. Using the results of the paper of Mamaladze and Cheishvili (1965)[12] for rough estimation of this velocity, it is described by the equation

$$v_c=(\hbar/\sqrt{3}ma_0)[1-(\delta_c^2a_0^2/\delta^2)]^{\frac{1}{2}}, \qquad (8.6.1)$$

where $a_0=4.3\times10^{-8}(T_\lambda-T)^{-\frac{1}{3}}$ cm is a characteristic dimension of the phenomenological quantum theory of superfluidity near the λ-point (see Sec. 12.1), δ is the size of pores, $\delta_c\sim3\div5$ (dimensionless critical size of pores). When $\delta\gg a_0$ and $T\approx T_\lambda$ this formula gives a very large value ($\sim$30 m/sec) close by the order of the magnitude of Landau's critical velocity of the breakdown of superfluidity. However, according to (8.6.1), when T approaches T_λ, $v_c\to0$. It is interesting in this connection to discuss Reppy's results described in the previous paragraph (Fig. 8.5). Reppy did not find that v_c tends to zero, when $T\to T_\lambda$, and concluded that the critical velocity experiences a jump at $T=T_\lambda$. That would distinguish the superfluid persistent current from a superconducting persistent current. The critical velocity of the latter tends smoothly to zero as the temperature of the point of the phase transition is approached.

Meanwhile there is no principal difference here. An essential difference, but not a principal one is only that the parameter in the phenomenological theory of superfluidity a_0 is much smaller than the similar parameter in the theory of superconductivity, i.e., than the length of coherence. An increase of a_0 and the corresponding decrease of v_c take place in a very narrow interval of temperatures near T_λ.

In Reppy's experiment, apparently, δ is always much larger than a_0, as $a_0\leq1.9\times10^{-5}$ cm, when $T_\lambda-T\geq5\times10^{-6}$ °K (the value of δ in the paper of Reppy is not given). Then $v_c\approx\hbar/\sqrt{3}ma_0$, i.e., v_c decreases from the value -30 m/sec at low temperatures to ~5 cm/sec. Such a value corresponds to the maximum approach to the λ-point which in Reppy's experiment reached 5×10^{-6} °K. On the other hand, the velocity of the persistent current in Reppy's device was about 0.2 cm/sec. Hence when the λ-point is approached down to 5×10^{-6} °K, that decreases the value of the critical velocity to 5 cm/sec, it is not sufficient to find a smooth drop of the critical velocity to zero. The persistent current all the time has a velocity much less than the critical one.

9. STABILITY OF HELIUM II MOTION BETWEEN TWO CYLINDERS ROTATING WITH DIFFERENT ANGULAR VELOCITIES

9.1. The First Experiments

As early as 1941 Kapitza noticed that rotation of a thin rod set into a capillary with helium II sharply changes the character of heat transfer along the circular slit formed by them (Kapitza, 1941). Then Wheeler, Blackwood, and Lane (1955) measured damping of second sound in rotating helium II. In contrast to the experiments made by Hall and Vinen (1955, 1056a, b) about the same time, they found a considerable increase of scattering of thermal waves as a result of rotation, though the direction of propagation of these waves was parallel to the axis of rotation. In the device constructed by Wheeler, Blackwood, and Lane, helium II was between the two cylinders, the inside cylinder was rotating and the outside one was at rest. Therefore their results should be considered as an indication of an instability of such a kind of motion under the conditions of these experiments. The same can be said about Kapitza's experiments.

9.2. Distribution of Velocities in a Liquid Rotating Between Two Cylinders

Let us give a brief survey of the state of theories of stability of such motions. Both in viscous and in ideal fluids, which are between two cylinders with the radii R_1 (inside) and R_2 (outside) and rotating with the angular velocities ω_{01} and ω_{02} the following distribution of velocities is established:

$$v_r=v_z=0, \qquad v_\phi=\frac{\omega_{02}R_2^2-\omega_{01}R_1^2}{R_2^2-R_1^2}r+\frac{(\omega_{01}-\omega_{02})R_1^2R_2^2}{R_2^2-R_1^2}\frac{1}{r}. \qquad (9.2.1)$$

Equations (9.2.1) represent the only solution of the Navier–Stokes equation, corresponding to the con-

[12] Mamaladze and Cheishvili (1965) have considered strictly speaking not a rotational, but a translational motion.

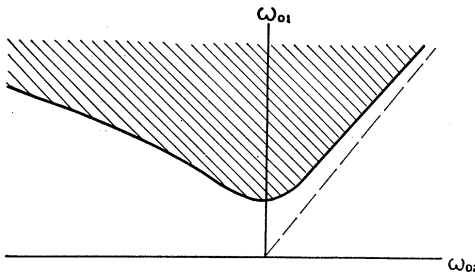

FIG. 9.1. The dashed line corresponds to the equation $\omega_{02}^2 R_2^2 = \omega_{01} R_1^2$. The region of stability of a classical ideal liquid is situated between this dashed line and the line $\omega_{01}=0$. The region of stability of a real (viscous) classical liquid is wider and extends to the hatched region. (The figure is taken from the book of Landau and Lifshitz, 1953.)

sidered boundary conditions. They do not contain viscosity and therefore are valid for an ideal liquid as well. However, the Euler equations allow other solutions. As to the equations of hydrodynamics of rotating helium II, the distribution (9.2.1) is also the only possible solution for them. It is required by the normal component, and the mean velocities of both components under the stationary conditions reach the same values due to mutual friction.

9.3. Stability of Rotation of an Ideal Liquid

The problem of stability for a laminar motion (9.2.1) for an ideal liquid was studied by Rayleigh (1916). He showed that at rotation of cylinders in the opposite directions the motion is unstable, while at the same direction of rotation the condition of stability has the form

$$\omega_{02}R_2^2-\omega_{01}R_1^2>0. \qquad (9.3.1)$$

In particular, this means instability in case of the rotation of the inside cylinder, when the outside one is at rest ($\omega_{02}=0$).

For the further representation of the material it is essential to note that the sense of the Rayleigh condition is connected with the following considerations. Let an element of the liquid M occasionally leave the orbit of its rotation, i.e., a circumference with the radius $_p$, and let it be displaced for some distance. Before this fluctuation occurred the centrifugal force $Mv_\phi^2/r=L^2/Mr^3$ (here L is the angular momentum) P and the force caused by the gradient of pressure $(M/\rho)\partial P/\partial r$ balance each other ($\partial P/\partial r=\rho v_\phi^2/r$). As a result of fluctuation the element considered is in the region with another value of the pressure gradient. But the magnitude L is conserved and the stability or instability of the motion depends on the ratio of two forces having opposite directions: which of them will be larger? Will the element be returned to its orbit? As shown in the book of Landau and Lifshitz (1953) the solution of this problem leads to the Rayleigh condition (9.3.1).

9.4. Stability of a Viscous Liquid Rotation

In Fig. 9.1 is shown how the Rayleigh condition is modified if, according to Taylor (1923), the role of viscosity is taken into account. For this one studies the Navier–Stokes equation (instead of the Euler equation) to determine the stability of its solution (9.2.1) with respect to relatively small perturbations.

9.5. Stability of Helium II Rotation

A similar thing for helium II was studied by Chandrasekhar and Donnelly (1957). They concluded that there are two conditions of stability for this liquid. One of them, when there is no mutual friction, leads to condition (9.3.1), the other one to that shown in Fig. 9.1. That means, for instance, that if there is an outside cylinder at rest and the angular velocity of the inside cylinder is increased (that was done in Donnelly's experiment (1959)], then one will find the existence of two critical points: one of them corresponds to the appearance of the Rayleigh's instability of the superfluid component rotation, the other to Taylor's instability of the normal component rotation.

Donnelly's device was a viscometer, the inside cylinder of which was rotating causing deflection of the outside cylinder suspended on an elastic thread. At small velocities (large periods θ) the deflection of the outside cylinder did not depend on θ, but with the decrease of this magnitude two critical points were observed (Fig. 9.2), θ_s and θ_n, marking the appearance

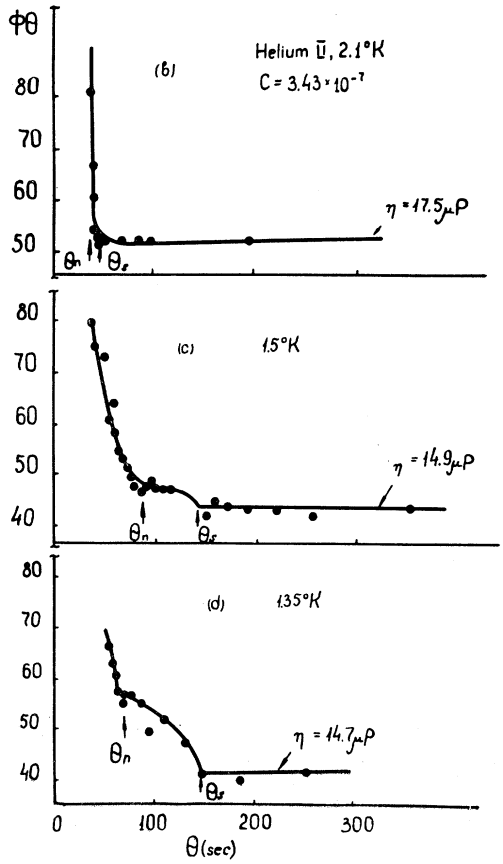

FIG. 9.2. The angle of deflection of the outside cylinder φ in dependence on the period of the inside cylinder rotation θ according to the data of Donnelly (1959).

of instability of motion of the corresponding components predicted by the theory of Chandrasekhar and Donnelly. However, quantitative data of this experiment did not agree with the theory.

The reason for this discrepancy was explained by Mamaladze and Matinyan (1963), who paid attention to the fact that the existence of vortex lines in rotating helium II is not completely taken into account in the equations used by Chandrasekhar and Donnelly. The mutual friction is included, but the term $\nu_s[\boldsymbol{\omega}, \text{curl } \boldsymbol{\omega}/\omega]$ is absent and this term, as we know, describes the elastic properties of vortex lines. As shown in Fig. 9.3, the role of elastic effects can be very essential for the solution of the problem of stability. To verify this assumption Mamaladze and Matinyan studied Eq. (4.2.1) with $F_{sn}=0$ and div $v_s=0$ for the stability of solution (9.2.1) with respect to small perturbations. As one should expect in the condition of equilibrium obtained in such a way

$$\omega_{02}^2 R_2^2 - \omega_{01}^2 R_1^2 > -\tfrac{1}{2}\pi^2 \nu_s [(R_2+R_1)/(R_2-R_1)], \quad (9.5.1)$$

the stabilizing action of vortex lines is clearly expressed indeed. It shifts the boundary of stability in comparison with condition (9.3.1). Though condition (9.5.1) is valid strictly speaking only when $T=0$°K, nevertheless it can be compared with the data of Donnelly, as they are reduced to the temperature 1.35°K and at such a temperature the relative density of the normal component is only about 7%. Therefore one can consider that, when $T=1.35$°K the role of the mutual friction is not very essential and the critical point $\theta_s \sim 140$ sec in Fig. 9.2 should agree with condition (9.5.1). And indeed, using the values of ν_s obtained in different experiments (see Sec. 5.6), we get, according to (9.5.1), $\theta_s = 120 \div 150$ sec.

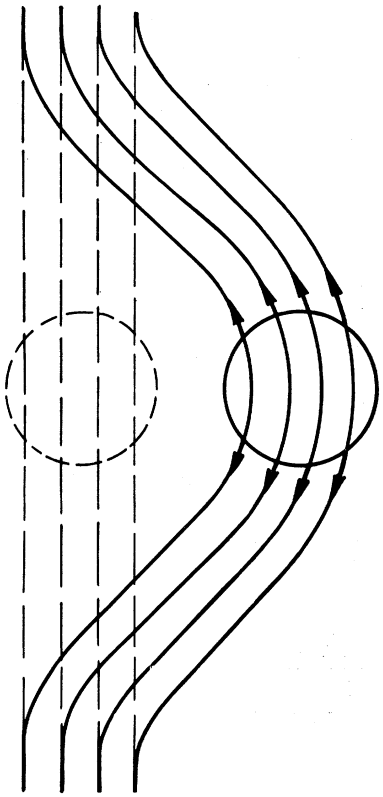

FIG. 9.3. Tension of the distorted vortex lines (solid lines) promotes the return of an occasionally shifted element of the liquid (a circle) to its initial position (dashed lines).

Hollis–Hallett (1953) in contrast to Donnelly (1959) has used a viscosimeter with rotating outside cylinder, while the inside cylinder, suspended by means of an elastic thread was at rest. According to (9.5.1) in this case ($\omega_{01}=0$) the motion of the superfluid component should be stable. However, such an assumption cannot be considered sufficiently rigorous. Indeed, condition (9.5.1) does not take into account actions both of viscous forces and mutual friction force. Besides, condition (9.5.1) determines instability with respect to infinitesimal perturbations, but there can exist instability with respect to finite perturbations, realized in a classical liquid even in the unhatched region in Fig. 9.1. That suggests an idea that instability of motion should appear in the case of helium II as well, even when $\omega_{01}=0$. The results of the calculations of Chandrasekhar and Donnelly (1957) as well as those of Donnelly's experiment (Fig. 9.2) allow one to expect that when the Hollis-Hallett viscosimeter is used there should be manifested two critical velocities v_{cn} and v_{cs}.

Meanwhile, Heikkila and Hollis–Hallett (1955), while measuring the viscosity of the normal component of helium II, decreased the velocity of rotation of Hollis–Hallett's viscosimeter only a little lower than the critical velocity v_c found by them. (They measured the effective viscosity defined by the formula of the classical hydrodynamics. The dependence of this effective viscosity on the velocity of rotation disappears just at this velocity v_c, when $v \leq v_c$.) Woods and Hollis–Hallett (1958) have shown that the velocity v_c has a classical nature, as it is manifested in the experiments with classical liquids as well. They have shown that between this experiment and the helium experiment there is maintained similarity according to Reynolds number, calculated in the latter case with the use of the viscosity of the normal component. Thus the velocity v_e is a critical velocity v_{cn} and there are all the grounds to assume that at lower velocities the second critical point v_{cs} may appear (compare Fig. 9.2, where $\theta_s > \theta_n$).

The viscosity of helium II measured by a rotating viscosimeter is somewhat different from the viscosity measured by means of an oscillating disk (Andronikashvili, 1948c). (The results of many other authors who used this method later confirm the data of his paper.) Such a difference between "rotating" and "oscillating" viscosities of helium II is undoubtedly connected with insufficient analysis of one of the procedures of measurement (or even of both of them). We think that the attempt to find the second critical point v_{cs} in the experiments with the rotating viscosimeter could elucidate this problem as the viscosity measured when $v < v_{cs}$ could coincide with the "oscillating" one.

Another possible source of misunderstanding in the

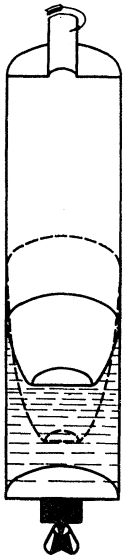

FIG. 10.1. Schematic representation of the gradual development of the meniscus at the dragging of helium II into rotation.

analysis of the results obtained with the rotating viscosimeter can be insufficient clarity of the picture of vortex line arrangement in such a device. At present we do not even know if there are vortex lines in it when $v<v_c$. Indeed, nobody has made calculations similar to those made by Bendt and Oliphant (1961) for cylinders rotating with different velocities. If the superfluid in a rotation viscosimeter does not move at all when $v<v_c$, then there are no grounds for appearance of the critical velocity v_{is} smaller than v_c. If it moves then, in addition to the possibility of v_{cs} appearance, there is another possibility of the existence of complications which were not taken into account so far. It is not excluded that at low temperatures vortex separation or the distance between vortices and the wall can be comparable with the free path length of thermal excitations and thus the law of the momentum transfer from the moving cylinder to the cylinder at rest can be changed.

We think that the question about the difference of viscosities measured by the two methods deserves great attention and its solution can form a source of interesting information on properties of helium II.

10. FORMATION AND DECAY OF VORTEX LINES IN HELIUM II

10.1. Dragging of Helium II into Rotation by a Moving Wall of a Container

The first data on kinetics of helium II dragged into rotation were published by Andronikashvili and Kaverkin (1955). The experiment was made with a transparent cylindrical container, which was rapidly brought from the state of rest into the state of uniform rotation.

Every normal liquid under such conditions would rather soon form a parabolic meniscus, the depth of which would gradually increase in time. Such behavior, for instance, is established for water and helium I. But the behavior of helium II is quite different as compared with that of usual liquids. In particular, at first only its peripheral layers are dragged into rotation, while the central part of the meniscus remains flat.

Gradually the radius of the flat part of the meniscus becomes narrower (see Fig. 10.1) and at last a parabola is formed the usual shape of which is indistinguishable at low and moderate velocities of rotation from the parabolic meniscus of viscous liquids. But already at an angular velocity about 30 sec^{-1} a characteristic conic pit appears on the lower part of the parabola. This fact was mentioned at the beginning of this paper (Fig. 10.2).

At angular velocities of the order of 30 sec^{-1} the equilibrium shape of the meniscus is formed during 120 sec, that corresponds to the velocity of the vortex front propagation of the order of 0.1 mm/sec.

The process of helium II dragging into rotation was studied by Eselson, Lazarev, Sinelnikov, and Shvetz (1956), who brought into rotation, during the period of the order of some seconds a pile of narrow disks with the separation equal to 0.15 mm and surrounded by a thin metal case. The device was hung by means of a magnetic suspension and rotated with velocities of several revolutions per second. The authors reported that the bulk of helium was dragged into the device rotation during not more than 2 sec. The vortex front traveled in this case with the velocity more than 0.04 mm/sec, if the direction of the front propagation coincided with that of the rotation axis.

Nearly the same method was used by Reppy, Depatie, and Lane (1960), who gave a rotational pulse to a cylindrical container without the pile of disks, filled with liquid helium and hung on the magnetic suspension. The duration of the pulse was 0.5 sec. The

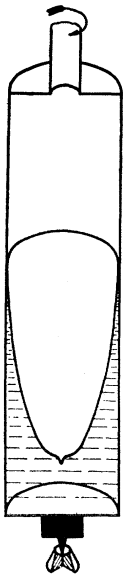

FIG. 10.2. Schematic representation of the equilibrium meniscus of rotating helium II at high velocities of rotation.

authors reached the velocity of rotation of ~ 0.2 sec^{-1}. Under such conditions, in contrast to the results of Eselson *et al.*, they observed the subsequent slowing down of the container due to redistribution of the angular momentum between it and the liquid. Reppy *et al.* found that the laws of helium II dragging into rotation and those of helium I are quite different (see Fig. 10.3).

Reppy and Depatie (1961) used a similar technique, but at still lower velocities of vessel rotation and found some additional details of the process of the superfluid liquid twisting, as mentioned in Sec. 8.6. It was found that rather slow twisting of helium II observed at the initial portions of curves similar to that shown in Fig. 10.3, when $\omega_0 \sim 0.2$ sec^{-1}, was replaced by a long delay of the beginning of twisting at smaller values of ω_0. When $\omega_0 \approx 0.1$ sec^{-1} and $T = 1.2$°K $(\rho_n/\rho = 3\%)$, the superfluid can remain at rest during some thousands of seconds even when the vessel gets additional pulses of rotation acceleration. However, it concerns only the cases when helium II was at rest during a sufficiently long time, and, if it rotated previously not for a long time, then during the start of its repeated twisting there was not any appreciable relaxation. When $\omega_0 \approx 0.065$ sec^{-1}, the twisting of the superfluid component was not observed till the end of the experiment (during 10^4 sec). In their recent paper Reppy and Lane (1965) have shown that these delays disappear completely if there is an artificial protuberance on the inner side surface. Dragging of the liquid into rotation begins without any delay even at the minimum velocity $\omega_0 = 0.05$ sec^{-1}, used in this experiment. The dragging is always completed by the liquid aquiring the classical angular momentum L_c.

There is some information on the process of helium II twisting in Pellam's paper (1960) as well. It was mentioned in Sec. 3.5 that the results of his investigation were connected with the influence of a light beam on the Rayleigh disk deflection. But on the other hand, according to Tsakadze and Shanshiashvili (1965), such an influence was observed only in rotating helium II (in the liquid at rest the effect of illumination was

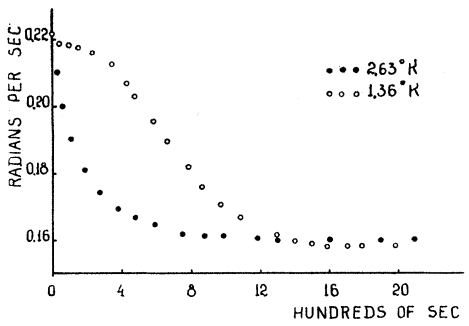

FIG. 10.3. Dragging into rotation of helium I (solid circles) and helium II (open circles) according to the data of Reppy, Depatie, and Lane (1960).

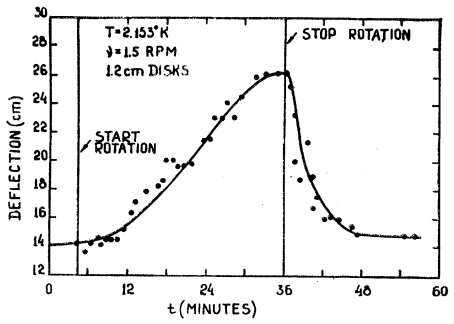

FIG. 10.4. Change of the angle of the torsional balance deflection in time in the experiment of Craig (1961).

much smaller). Therefore Pellam's data on some increase of the delay of the Rayleigh disk at its removal from the wall of the rotating vessel indicate the propagation of the rotation front from the periphery to the axis of the container. At the rotation velocity 2 rpm and $T = 2$°K the velocity of the front was of the order of 2 mm/min.

A similar method was used by Craig (1961) for the study of helium II dragging into rotation. He suspended a beam of a torsional balance with two wings immersed into liquid helium above the cylindrical vessel and studied the moment of forces acting on the device. The angle of torsion of an elastic suspension to which the beam of the balance was fastened (the balance was at rest in the laboratory system of coordinates) was the measure of dragging the liquid into rotation. Craig's results are given in Fig. 10.4, where it is seen that he has also observed a delay at the beginning of twisting, and that at the angular velocity 1.5 rpm the complete dragging of helium II into rotation takes about 30 min.

It is seen that the mechanism of dragging of helium II into rotation is quite different from that valid for classical liquids. The process of dragging of classical and quantum liquids into rotation of a container was studied in particular detail by Tsakadze (1964c) and by Tsakadze and Cheremisina (1966).

First of all it was shown by precise measurements of the meniscus depth z on stills of a film taken by a cinematographic camera, which was switched on every 3 sec by an electronic circuit, that the character of the meniscus deepening is quite different for helium I and helium II. Figure 10.5 shows that $\log \Delta z$(He I) is a straight line breaking after some time, which depends linearly on the angular velocity of rotation.

At the point of the phase transition the character of the meniscus development is changed in a jump and $\log \Delta z$ in He II gives a curve without any breaks, immediately after the temperature is reduced below $T = 2.17$°K.

The time of helium I twisting was less than that of helium II in the studied cases. An increase of the container radius caused the linear increment of the velocity of the meniscus deepening for helium I, while for helium

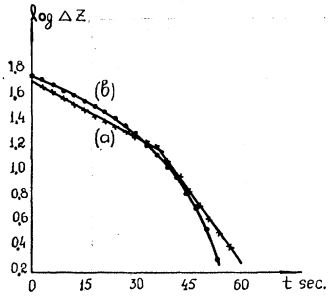

FIG. 10.5. Time dependence of the meniscus depth of helium I (curve a) and helium II (curve b) brought into rotation, according to the data of Tsakadze and Cheremisina (1966). The temperatures are $T=2.186°K$ and $T=2.164°K$, respectively.

II it dropped in the initial portion of the curve according to the law close to a hyperbola. The dependence of the time of helium II dragging into rotation on the angular velocity ω_0 was the same in character. The dependence of the time of acceleration on ω_0 for helium I is a straight line with a negative slope. The same time for helium II decreases slowly with an increase of temperature and only in the interval 2.0–2.17°K this dependence becomes sharper (Figs. 10.6, 10.7, 10.8, 10.9).

At the beginning of the analysis of the results of this paper, all the experiments were made at high Reynolds numbers ($\mathrm{Re}\sim 5\times10^5\div 2\times10^7$). That excluded the possibility of laminar regimes of helium I dragging into rotation or that of the normal component of helium II. Therefore the observed durations of the liquid acceleration obtained were much shorter than those expected for a laminar regime, i.e., $R^2/\nu\sim10^6$ sec.

The turbulent character of the motion makes the treatment of the results, obtained in this case, more difficult for the classical liquid. But it simplifies, and that sounds paradoxical, the understanding of the processes of helium II dragging into rotation.

First of all as seen from the shape of the meniscus of helium II in the process of its acceleration and from the figures given in this paragraph, the quantum turbulence in a certain sense depresses the classical one as soon as in all the cases dragging into motion of the normal component of helium II takes place slower than that of helium I.

The authors of the paper give reliable considerations that help us to understand the character of the experimental data obtained by them, proceeding from an assumption that quantized vortex lines are generated

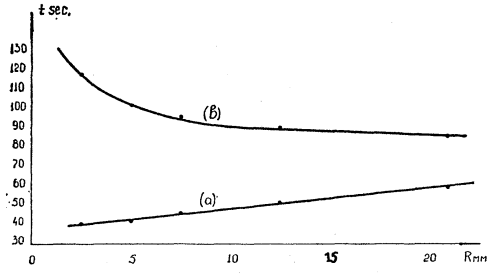

FIG. 10.6. Dependence of the time required to drag helium I (a) and helium II (b) into rotation on the radius of the vessel (Tsakadze and Cheremisina, 1966).

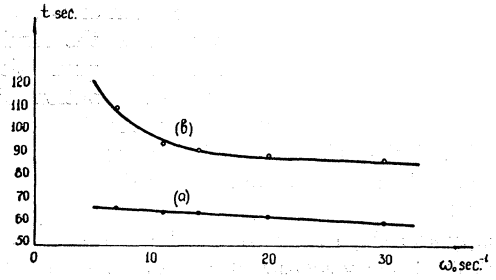

FIG. 10.7. Dependence of the time required to drag helium I (a) and helium II (b) into rotation on the angular velocity of rotation (Tsakadze and Cheremisina, 1966).

at the periphery and propagate to the rotation axis. According to (2.5.1) the total number of vortex lines, formed by the end of the process of acceleration, is proportional to the cross section of the vessel and to the angular velocity: $N_0\sim R^2\omega_0$. In addition, let the number of vortex lines n generated in unit time per unit of the vessel periphery depend on the difference of mean velocities of the normal and the superfluid liquids v according to the law $n\sim v^\alpha$. This magnitude varies from the value $\omega_0 R$ at the beginning of the process till zero by its end. It is natural to assume that a stationary regime of rotation will be established at formation of an equilibrium number of quantized vortex lines in the container. Then

$$t\sim(N_0/Rn)\sim(\omega_0 R)^{1-\alpha}.$$

Hence at any law of the form $n\sim v^\alpha$ there appears an universal dependence of the time of dragging into rotation t on the velocity. Just such a conclusion is given by the experiment (Fig. 10.8).

The observed decrease of t with an increase of ω_0, R and v requires $\alpha>1$. The numerical estimation shows, that the experimental curve shown in Fig. 10.6 corresponds to an averaged value $\alpha\approx1.3$. Let us note for comparison that in Vinen's paper (1957c), devoted to the study of the quantized turbulence in the thermal flux, the dependence of the type $n\sim v^2$ is obtained, i.e., $\alpha=2$.

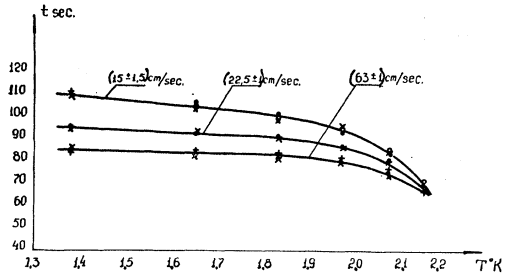

FIG. 10.8. Temperature dependence of time of helium II dragging into rotation at different linear velocities on the periphery of the vessel (Tsakadze and Cheremisina, 1966). The different signs used for experimental points correspond to different values of ω_0 and R, the products of which are shown in each curve (Tsakadze and Cheremisina, 1966).

10.2. Decay of Vortex Lines at the Stop of Rotation

The first information on rotating helium II slowing down was given in the paper of Andronikashvili and Kaverkin (1955). In a suddenly stopped cylindrical container an initially parabolic meniscus begins to straighten at the walls and only a conic crater is left in the center, disappearing in 30 sec. Thus the time of slowing down is one fourth as long as the time of dragging into rotation.

Pellam (1960) has also noted that slowing down proceeds much quicker than acceleration and that the beginning of slowing down of the liquid in the vessel takes place immediately after its stop.

Craig (1961) described the action of forces applied to the torsional balance wings immersed into helium II. Confirming Andronikashvili's observations (Andronikashvili and Kaverkin, 1955), he has noticed that a sharp decrease of the drag force at slowing down occurs

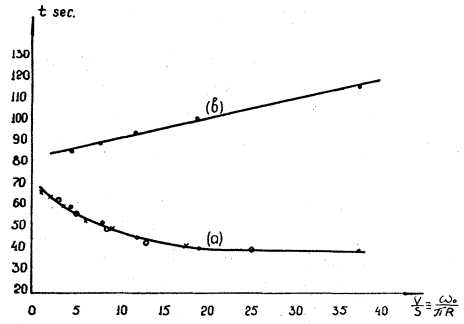

FIG. 10.9. The time of helium I dragging into rotation at different ω_0 and R is an universal function of ω_0/R (compare Fig. 10.8). This situation is illustrated by curve (a) on which points for different ω_0 and R are denoted in a different way. The time of helium II dragging into rotation is shown by curve (b). Here the dependence of t on ω_0/R is linear, but not universal (Tsakadze and Cheremisina, 1966).

three or four times as fast as its increase at acceleration. An essential difference in the absolute values of time measured in Andronikashvili's experiment on the one hand and that of Craig on the other hand is explained by the fact that angular velocities of rotation were many times different from each other.

Hall and Vinen (1956a, b) also observed relaxation effects at the stop and at the beginning of motion, when they studied attenuation of second sound in rotating resonators. However, such a great difference in the time of establishment of the stationary rotation regime of helium II and of its slowing down was not observed.

Similar data were obtained in the investigation of Careri, McCormick, and Scaramuzzi (1962) described in Sec. 3.3. It is shown in Fig. 10.10 that an equilibrium value of the current (after switching on of rotation) is reached in ~2 min (when $T=1.27$°K). Approximately the same time is required for the current to reach almost its initial value after the stop of rotation.

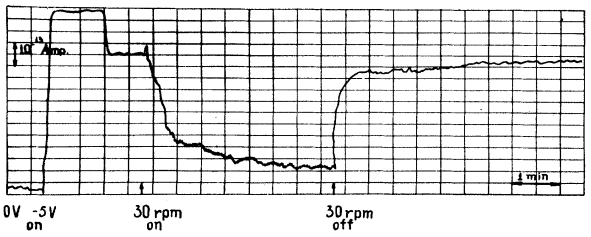

FIG. 10.10. Changes of the currents of negative ions in helium II: at voltage application, start of rotation and stop of rotation (Careri, McCormick, and Scaramuzzi, 1962).

However, a complete recovery of the current takes much longer time. At $T=0.9$°K it is about an hour and near the λ-point it is several minutes.

Further, the same authors (1963) reported that the period of half-decay of vortex lines τ after the stop of rotation was inversely proportional to the total number of thermal excitations, determined in the paper of Bendt, Cohwan, and Yarnell (1959). This conclusion is confirmed by Table II. There are the data obtained at a velocity of 10 rpm and at a voltage of 4 V. Careri *et al.* think that this result shows the participation of all the thermal excitations in the process of vortex line decay.

Interesting experiments for the study of the process of decay of vortex lines were made by Gamtsemlidze, Japaridze, and Turkadze (1965), who observed attenuation of the torsional pendulum (a flat disk) suspended inside of a uniformly rotating cylindrical container. The idea of the experiment was the following: The existence of vortex lines causes an additional attenuation of a torsional pendulum (5.1, 6.5). By watching the decrease of this additional attenuation after the stop of the container, it is possible to determine the time dependence of the number of vortex lines. An extra attenuation α was determined as the difference of two attenuations $\alpha=\delta_t-\delta_\infty$, where δ_∞ is the attenuation of the disk in helium II at rest and δ_t is the attenuation at some moment of time after the container stops.

As seen from the curves of Fig. 10.11, the extra attenuation can be described by an exponential law

$$\alpha=\alpha_0 \exp\left[-(\ln 2\tau/)t\right], \qquad (10.2.1)$$

where $\ln 2/\tau$ is the angle of the slope of the curves $\ln 2$ (t), τ is the period of half-decay. Curve A corre-

TABLE II.

T°K	τ sec	$10^{-19}N$ cm^{-3}	$10^{-22}\tau N$ cm^{-3} sec
0.87	510	1.56	0.8
1.12	192	5.43	1.0
1.27	105	11.4	1.2
1.40	96	20.4	2.0
1.54	48	37.0	1.8
1.93	12	154	1.8
2.05	6	233	1.4
2.12	3	313	0.9

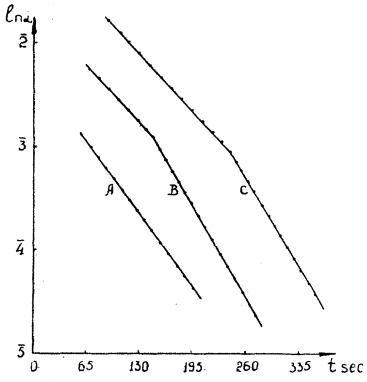

FIG. 10.11. Time dependence of the damping of a disk oscillating round its axis in the rotated and stopped vessel (Gamtsemlidze, Japaridze, and Turkadze, 1966).

sponded to a decay at the velocity of rotation $\omega_0=(0.10\pm0.02)$ sec^{-1}, measured before the stop of the device. This velocity was closer to that $\tilde{\omega}_0$ at which collectivization of vortex lines takes places (6.3). Under the conditions of this experiment $\tilde{\omega}_0=0.11$ sec^{-1}.

But at the velocities $\omega_0>\tilde{\omega}_0$ there is a sharp break on Curves B ($\omega_0=0.24$ sec^{-1}) and C ($\omega_0=0.48$ sec^{-1}). At small velocities the period of half-decay of vortex lines τ is equal to (55 ± 5) sec and at higher velocities the decay takes place with another half-period τ_1, for instance, for curve B $-\tau_1=(70\pm5)$ sec. It is rather evident that an increase of the period of half-decay is caused by the process of collectivization. Actually, the estimation according to the formula $\omega_1=\omega_0\exp(-t_1\ln 2/\tau_1)$, (where t_1 is the time from the moment of the rotation stop until the moment of the break of curves in Fig. 10.11) leads in each case to the value $\omega_1\approx\tilde{\omega}_0$.

The decay of vortex lines was studied by the method of second sound by Bablidze (1965). He has established that the slowing down of rotating helium II is characterized by the period of half-decay $\tau=30$ sec.

The conditions of this experiment differ essentially from those of Gamtzemlidze *et al.* (1966). Therefore it is, so far, difficult to indicate definitely the cause of some difference in their results ($\tau=30$ sec should be compared with $\tau=55$ sec).

10.3. Formation of Vortex Lines in Rotating Helium II at the Passage through the Point of the Phase Transition

The study of formation of Onsager–Feynman's vortex lines at cooling of uniformly rotating helium I lower than the temperature of the phase transition was undertaken in detail by Andronikashvili, Bablidze, and Tsakadze (Andronikashvili, Bablidze, Gujabidze, and Tsakadze, 1964a,b; Andronikashvili, Bablidze, and Tsakadze, 1965, 1966; Bablidze, 1965).

With this aim a radial mode resonator was constructed in which the waves of second sound generated on the surface of the inside cylinder were reflected on the inner surface of the outside cylinder and then received by a detector, wound on the inside cylinder.

The resonator was tuned to some temperature, then liquid helium was heated till $T=2.21$°K at which it rotated about 30 min. After that, without a stop of the container rotation, it was cooled to the temperature at which second sound was tuned for resonance.

By means of this device it was established by attenuation of second-sound waves that vortex lines in rotating helium II appear at the passage through the point of the phase transition with a considerable delay. At the velocity of the liquid rotation $\omega_0=1.76$ sec^{-1} the resonance amplitude reaches its equilibrium value ($T=2.168$°K) only after 300 sec (see Fig. 10.12).

Depending on the rate of cooling the relaxation phenomena accompany the process of rotation till 2.12°K. Below this temperature nonequilibrium phenomena were not observed at any velocity of rotation. The time of relaxation was dependent on the angular velocity ω_0 and on the value of overcooling $(T_\lambda-T)$. An empirical formula was obtained in the following form (see Fig. 10.13):

$$\tau=\tau_0\exp\left[-(\omega_0-\omega_{0c})/\alpha\right], \qquad (10.3.1)$$

where $\alpha=1.18$ sec^{-1}, ω_{0c} is the critical angular velocity of rotation in the vessel with certain characteristic dimensions ($\omega_{0c}\ll\omega_0$), τ_0 is a parameter dependent on temperature, changing from 1100 sec when $T=2.165$°K to 500 sec, when $T=2.125$°K.

There can be in principle two situations at cooling below the point of the phase transition of rotating helium II: either vortex lines begin to form at once, or there can exist another type of motion, which can be called an intermediate or nonstable motion, which transforms into a stable form realized by an array of

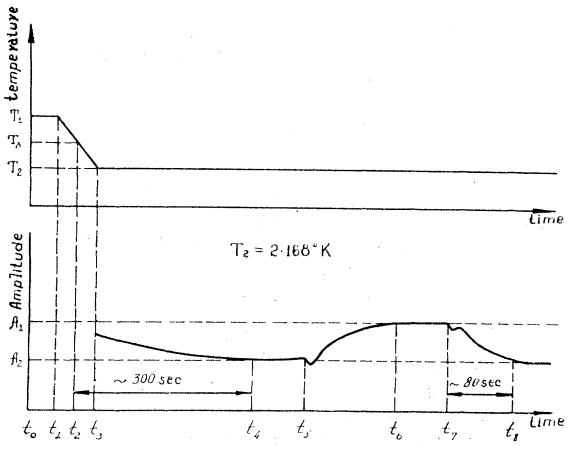

FIG. 10.12. Change of the amplitude of second sound in time in the radial mode resonator after the transition helium I–helium II taking place during rotation (Andronikashvili, Bablidze, and Tsakadze, 1965). The time notations: t_1 is the beginning of cooling; t_2 is the transition through the λ-point; t_3, the cooling has been finished; t_4, the amplitude of second sound has reached its equilibrium value ($t_4-t_2=\tau$); t_5, the termination of rotation; t_6, the amplitude of second sound has reached its resonance value; t_7, the repeated beginning of rotation; t_8, again the equilibrium (under the conditions of rotation) value of the amplitude has been reached. $\omega_0=1.76$ sec^{-1}.

vortex cores aligned parallel to the rotation axis. This transformation takes place both at a lowering of the temperature and in time.

A slow decrease of the second-sound amplitude with time, shown in Fig. 10.12, cannot solve this problem in favor of either assumption. It was necessary to construct another axial mode resonator to answer this question. In such a resonator the second-sound generator was fixed on the cover of the device and the receiver on its bottom.

From the papers of Hall and Vinen (1956a, b), it was known that propagation of second sound along vortex lines does not lead to an additional attenuation of its amplitude. Therefore if vortex lines, oriented along the rotation axis, were the only cause of an additional second-sound scattering (in a radial mode resonator), then rotating helium II in their presence would seem transparent for thermal waves propagating in an axial mode resonator.

The experiments made by Andronikashvili, Bablidze, and Tsakadze have shown that in the vicinity of the λ-point, rotating helium II is "opalescent" at its "translucence" by second sound along the axis of rotation (Fig. 10.14). In time or at removal from the λ-point, it becomes more and more translucent. And at last after ~200 sec, at the same velocity of rotation $\omega_0 = 1.76$ sec^{-1}, the second-sound amplitude reaches its resonance value.

The use of resonators of different geometrical shape

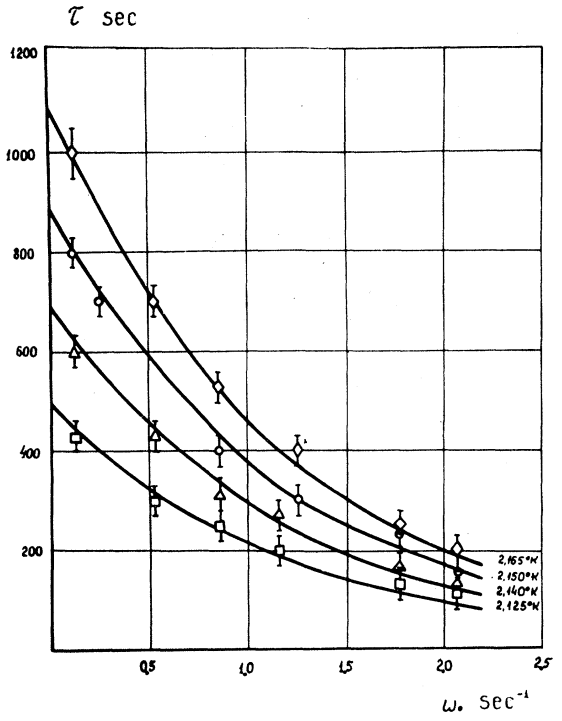

FIG. 10.13. Dependence of the relaxation time τ (equal to $t_4 - t_2$ in Fig. 10.12) on the velocity of rotation at different temperatures (Andronikashvili, Bablidze, and Tsakadze, 1965).

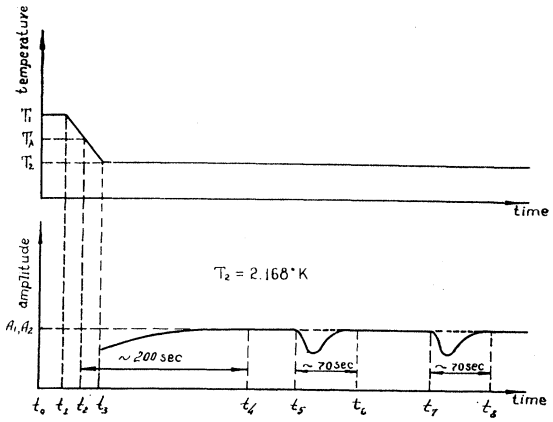

FIG. 10.14. The same as in Fig. 10.12, but with the use of an axial mode resonator (Andronikashvili, Bablidze, and Tsakadze, 1965).

shows that the change of an inner surface of a rotating vessel does not influence the formation of vortex lines.

Thus there can exist another intermediate type of motion than vortex lines, which makes rotating helium II isotropic with respect to second-sound propagation.

Evidently at such a stage vortex nuclei are generated in rotating helium II and vortex lines are formed gradually from them.

According to (10.3.1), the smaller the angular velocity is, i.e., the smaller the number of vortices, the longer the time is during which vortex nuclei can form a vortex line. This is clear, since the mean diffusion path of a nucleus, until it encounters a vortex core, is bigger for each nucleus when there are few vortex lines to be formed.

The time needed for a vortex line formation at the passage through the point of the phase transition (~300 sec) is comparable, by the order of the magnitude at the same ω_0, with the decay time and the time of vortex formation taking place at sudden switching on and off of the cylindrical container rotation (~70 sec).

This made us think that in this case as well vortex lines are formed from vortex line nuclei (or they decay on them). But the turbulent regime of the normal component leads in this case to reduction (3–4 time shorter) of the duration of the relaxation.

The idea of formation of vortex nuclei found its theoretical treatment in Iordanski's paper (1965a). It is shown there that in the presence of sufficiently high relative velocity of motion of the normal and the superfluid components, vortex formation begins in the latter, passing the initial stage of nucleus formation (the author considers the process of formation of ring vortices). The intensity of this process is calculated.

10.4. Change of Vortex Damping at the Variation of Temperature

We already know that at the change of temperature the number of vortex lines per unit of rotating liquid

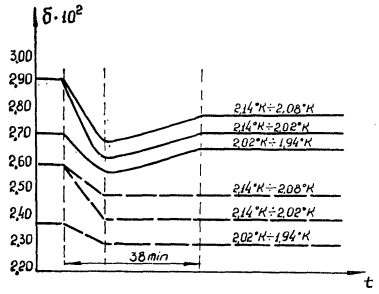

FIG. 10.15. Change in time of the disk oscillations damping in rotating helium II (solid lines) and in helium at rest (dashed lines) at its cooling (Gujabidze and Tsakadze, 1966).

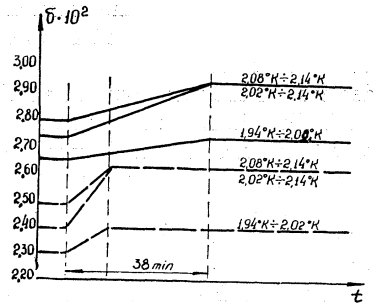

FIG. 10.17. Change in time of the disk oscillation damping in rotating helium II (solid lines) and helium II at rest (dashed lines) at its heating (Gujabidze and Tsakadze, 1966).

cross section does not change, but the amount of the superfluid component taking part in vortex motion does.

The study of relaxation processes at the change of temperature was made by Gujabidze and Tsakadze (1966). It was found that by lowering the temperature the normal component, having passed into the superfluid one, is dragged into the motion of already existing vortex lines during a very long time, in some cases reaching 40 min.

This process of enrichment of vortex lines by the superfluid component was studied by the time dependence of an additional damping of a disk oscillating in helium II and performing together with it a uniform rotation. As the tension of the vortex line according to formula (2.3.1) is porportional to ρ_s, then the projection of the tension on the plane of the disk causing an additional damping also depends on the amount of the superfluid component already dragged into a vortex motion. Figure 10.15 shows that there are two portions of the curve $\delta=f(t)$. One of them is associated directly with the process of temperature lowering, in particular, with the change in viscosity of the normal component. This process takes about 5 min. The other portion is associated only with the process of vortex line enrichment and it takes about 30–35 min.

The time necessary for a vortex line to drag the superfluid component into motion depends little on the value of the difference of the initial and finite temperatures, the same as on the absolute value of temperature. But it depends essentially on the angular velocity.

Figure 10.16 shows that the time of vortex enrichment is increased with an increase of the number of vortex lines and reaches the maximum when $2\omega_0/\Omega\approx 0.2$, i.e., when collectivization of vortex lines takes place. After that it begins to decrease. Beginning from the velocities $\omega_0\approx 0.25\,\Omega$, the time of vortex enrichment does not already depend on the angular velocity, remaining strictly constant. Thus a vortex line has the most stable configuration, with respect to dragging of new amounts of the superfluid component into motion, under the conditions of its strongest fastening.

The phenomenon of exclusion of the normal component from vortex motion at an increase of temperature was studied by the same authors. This process, connected with heating, proceeds more smoothly in comparison with the process taking place at cooling of rotating helium II. The same independence on the value of the difference of the initial and final temperatures and on the absolute value of the temperature as well is observed (Fig. 10.17). The dependence of the time of exclusion of the normal component on the angular velocity has the same character as at enrichment. And it has the same time characteristics as it is seen at the comparison of Fig. 10.18 with Fig. 10.16.

Again, the most stable are vortex lines existing under the conditions of the least sliding, when they decay in the slowest way. It is not excluded that a special role of the point $\omega_0=\tilde{\omega}_0$ in these phenomena is explained by the fact that the oscillation amplitude has its maximum

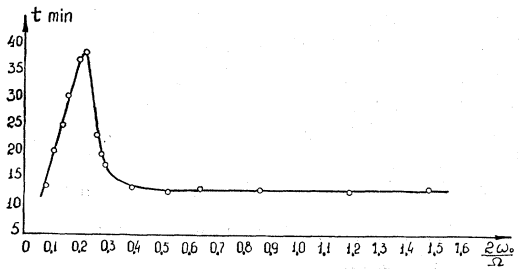

FIG. 10.16. Dependence of the duration of the process of vortex enrichment by the superfluid component (Fig. 10.15) on the velocity of rotation at a given rate of cooling (Gujabidze and Tsakadze, 1966).

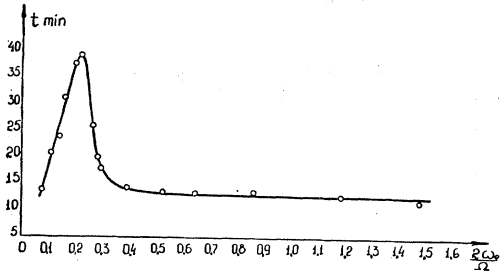

FIG. 10.18. Dependence of the duration of the process of vortex losing the superfluid component (Fig. 10.17) on the velocity of rotation (Gujabidze and Tsakadze, 1966), at a given rate of heating.

value at the best fastening of a vortex line. Being involved into such a vortex or "turned off" out of it the liquid should reconstruct most radically the character of its motion and that explains the maximum of relaxation time in Figs. 10.16 and 10.18.

The problem of the vortex decay at heating of rotating helium II was considered by Andreev (1964). He has shown that at heating two vortices (a superfluid and a normal one) with compatible cores are formed instead of one superfluid vortex. The newly formed normal vortex becomes more spread in time due to viscous forces. The duration of this process, estimated by Andreev on the basis of the analysis of dimensions is 10 min in the order of magnitude.

11. THE PHASE TRANSITION IN ROTATING HELIUM II

11.1. A Central Macroscopic Vortex

In Sec. 10.3 the phenomenon of delay at the vorticity formation was described at the phase transition helium I–helium II, under the conditions of rotation. A similar phenomenon of "overcooling" of the motion type is observed in the study of a central macroscopic vortex.

As early as 1948 Andronikashvili, studying rotation of liquid helium, found that under certain conditions in rapidly cooled rotating helium, there is observed a central macroscopic vortex piercing the whole liquid until the very bottom and forming something like a hollow rotation axis in helium II (Andronikashvili and Kaverkin, 1955). Andronikashvili's observations were confirmed by Donnelly, Chester, Walmsley, and Lane, (1956), who observed the central macroscopic vortex formation (see Fig. 11.1) not only in helium II, but in helium I as well.

A detailed study of this phenomenon was made by Tsakadze, who called it "Andronikashvili's vortex" (Tsakadze, 1963b,c,e, 1964a). He has found that this vortex is always formed in helium I. He has shown, by model experiments in water, that boiling of a rapidly rotating liquid leads to motion of vapor bubbles not in the direction to the surface, but in the direction to the axis of rotation. If boiling proceeds sufficiently intensively, then these bubbles are fused into a hollow axis, coinciding with the rotation axis.

In helium I, the central vortex forms a cord with the diameter 2 mm, which behaves restlessly, twisting and oscillating. Thus Andronikashvili's vortex is an essentially classical formation, having nothing in common with the quantum properties of the liquid. Tsakadze did not manage even once to observe formation of Andronikashvili's vortex in helium II.

But this vortex can be really observed in helium II, as reported by Andronikashvili. At the passage of the phase transition point this vortex, created in helium I, continues to exist for a sufficiently long time until the temperature 2.09°K. As soon as the temperature 2.17°K is passed, it stretches like a string and the meniscus of rotating helium II obtains the shape shown in Fig.

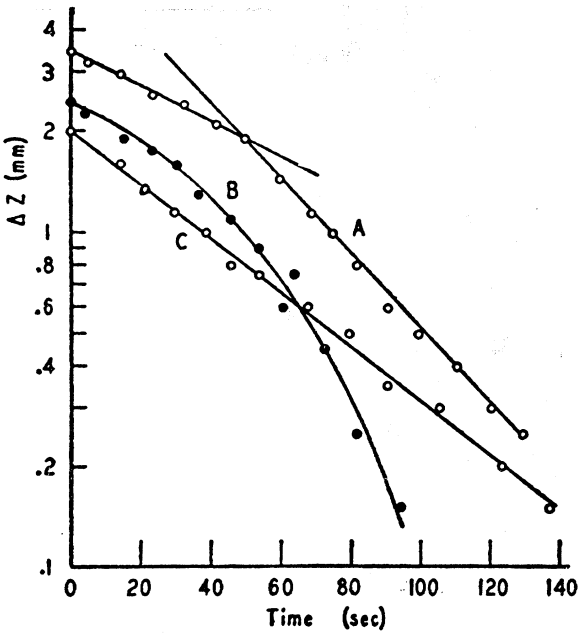

FIG. 11.1. The change in time of the meniscus depth of helium II brought into rotation (in the logarithmic scale), according to the data of Donnelly, Chester, Walmsley, and Lane (1956). Curve C shows the most frequently encountered case in these experiments. Sometimes the events develop as shown by curve B. Then the meniscus has a conic pit. In other cases the development of the pit is delayed. Then curve A is obtained. All these processes as well as the instability of the pit and formation of a central macroscopic vortex were observed both in helium I and in helium II. While according to Tsakadze (1964a) the curve of type A is possible only in helium I and B in helium II.

11.2. In time or at sufficiently low temperature, the central vortex tears off from the bottom of the container and begins to shorten gradually forming a conic deepening on the lower part of the parabolic meniscus.

It is a characteristic fact that this deepening, typical of a quantum liquid (see Sec. 3.6) remains in helium I for a long time. It can be observed there at a rapid heating from $T<T_\lambda$ until the temperature 3°K.

We dwell on these phenomena because they allow us to notice once more (compare Sec. 10.4) that at a transition from a classical liquid into a quantum one an overcooling is possible (though a temporary one) of classical kinds of motion, nonequilibrium for quantum systems. The similar phenomena—an overheating of quantum types of motion, nonequilibrium for classical liquids, can be observed at a reverse transition.

11.2. Peculiarities of the Phase Transition of Helium II into Helium I in the State of Rotation

It seemed evident that in the point of the phase transition, in which ρ_s becomes zero, the vortex damping described in detail in Secs. 5.1, 5.5, 6.2 should disappear.

Meanwhile the experiments of Andronikashvili, Mesoed, and Tsakadze (1964) have shown that the damping of an oscillating disk, rotating together with helium II and performing, in addition, axial oscillations remains constant by its character even above $T=$

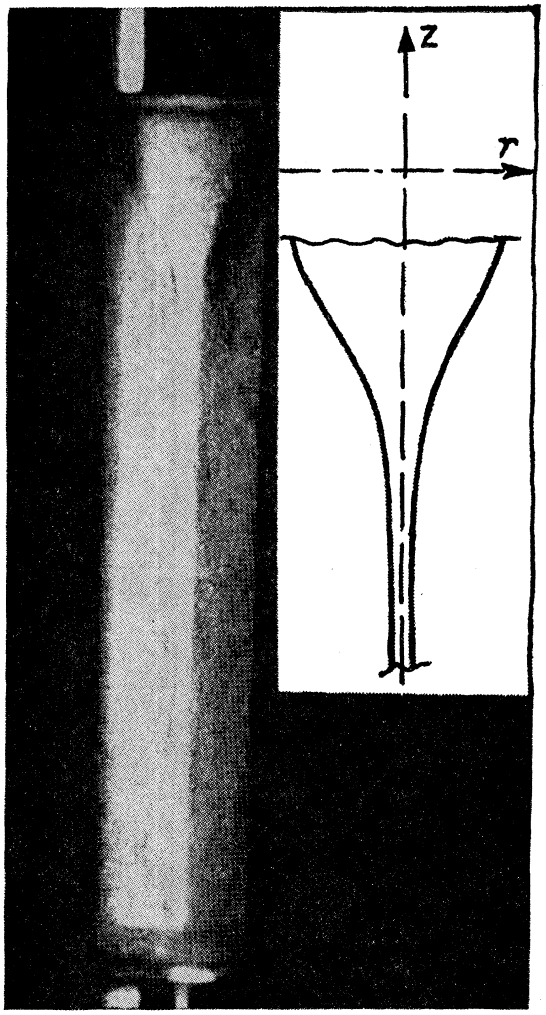

FIG. 11.2. The central macroscopic vortex in helium II: the photograph of the vortex and the result of the calculation according to the formula

$$z=-g^{-1}\left[\frac{1}{2}\left(\omega_0-\frac{\Gamma}{2\pi R^2}\right)^2(R^2-r^2)+\frac{\Gamma^2}{2\pi^2}\left(\frac{1}{r^2}-\frac{1}{R^2}\right)+\frac{\Gamma}{\pi}\left(\omega_0-\frac{\Gamma}{2\pi R^2}\right)\ln\frac{R}{r}\right],$$

when $\Gamma=10^2$ cm^2 sec^{-1} (Tsakadze, 1964a).

2.17°K, if only the phase transition of helium I into helium II takes place in the state of rotation (Fig. 5.12).

All attempts to find vortex damping in liquid helium brought into rotation above the λ-point and not cooled afterwards till temperatures corresponding to helium II, failed.

Thus it remained to assume that the existence of vortex lines in helium II is associated with extremely long relaxation time. The further experiments have confirmed these assumptions (Andronikashvili, Bablidze, Gujabidze, and Tsakadze, 1964a, b; Andronikashvili, Gujabidze, and Tsakadze, 1965, 1966).

It was natural to suppose that at the transition through 2.17°K, the whole superfluid component participating in the vortex motion, having passed into the normal state, begins to slow down sufficiently rapidly. This had to influence the energy of the vortex line, determining its tension. Thus if even the number of vortex lines would exist for some time at $T>2.17$°K and their number would be conserved constant, then due to a decrease of tension the vortex damping had to reduce.

But the obtained experimental data represent the time dependence of the logarithmic decrement of damping at the transition from rotating helium II into rotating helium I in the form shown in Fig. 11.3.

In a particular case when $\omega_0=\tilde{\omega}_0$, vortex lines, having passed through the λ-point, are conserved completely within the errors of the experiment during 18 min. Their existence causes the conservation of the corresponding maximum value of the decrement, characteristic of rotating helium II. This value of the decrement is associated, as we know, with the fact that the energy of the disk oscillations is carried away along the vortex lines. After 18 min a sudden vortex tearing off from the disk takes place during about one minute. This leads to a sharp decrease of the decrement and it decreases even lower than the value which should be expected for helium I, rotating as a solid body.

The latter circumstance can be understood by recalling that the logarithmic decrement of oscillation damping in helium II is expressed by formula (5.2.2), the main terms of which have the form:

$$\delta-(\Omega_0/\Omega)\,\delta_0\sim(\tfrac{1}{2}\eta_n\rho_n)^{\frac{1}{2}}[(\Omega+2\omega_0)^{\frac{1}{2}}+(\Omega-2\omega_0)^{\frac{1}{2}}]+(\eta_s\rho_s)^{\frac{1}{2}}(\Omega-2\omega_0)^{\frac{1}{2}} \quad (11.2.1)$$

and in helium I it should be:

$$\delta-(\Omega_0/\Omega)\,\delta_0\sim(\tfrac{1}{2}\eta\rho)^{\frac{1}{2}}[(\Omega+2\omega_0)^{\frac{1}{2}}+(\Omega-2\omega_0)^{\frac{1}{2}}]. \quad (11.2.2)$$

The first term of formula (11.2.1) is associated with the usual for a viscous liquid character of its interaction with an oscillating surface, which is realized between the disk and the normal component. The same process is described by formula (11.2.2) as well. As to the second term of formula (11.2.1), it is associated with the already mentioned mechanism of the disk energy loss by means of the waves, running along vortex lines.

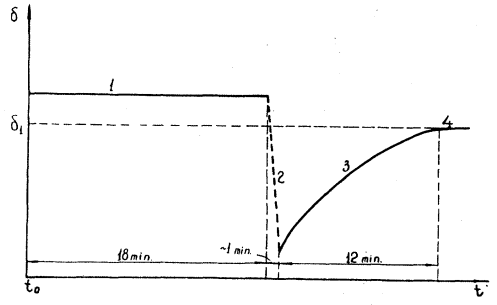

FIG. 11.3. The change in time of the disk oscillation damping in rotating helium I, after the phase transition has taken place at the moment t_0 in the state of rotation (Andronikashvili, Gujabidze, and Tsakadze, 1965).

In a metastable regime of rotation of helium I, when the system of vortex lines still continues to be connected with the disk, formula (11.2.1) has its initial meaning which is reflected by means of the first straight line portion of the given graph. At the moment of vortex tearing off, the second term of formula (11.2.1) decreases rapidly to zero. However, the amount of the liquid which participated in vortex motion is not dragged into the regime of the solid body rotation immediately. Therefore, beginning from the moment of vortex line tearing off, the decrement is expressed by formula (11.2.2) with the only difference that instead of the total density of the liquid ρ there is some effective density ρ' in it.

An increase of ρ' from the values near the value ρ_n, corresponding to the beginning of helium heating, until the total density ρ characteristic of the end of the experiment, represents the physical sense of the third portion of the graph in Fig. 11.3. The duration of this process is of the order of 12 min.

It was mentioned in Sec. 10.4 that superfluid vortex lines in helium II have the highest stability (in a sense of enrichment or losing the superfluid component) under the conditions of minimum sliding. The same is true in helium I as well: metastable vortex lines have the highest stability, i.e., the longest time until tearing off from the disk, when $\omega_0=\tilde{\omega}_0$. At the velocities larger or smaller than $\tilde{\omega}_0$, the time of vortex array tearing off from the disk surface becomes much shorter. It also becomes shorter at the temperature rise of helium I, at which the experiment takes place. Figure 11.4 illustrates this fact. At temperatures above 2.27°K one did not manage to observe the metastable vortex line array.

A question arises as to what reasons caused the sudden vortex array tearing off from the disk surface. The experiment shows that vortex lines of helium I,

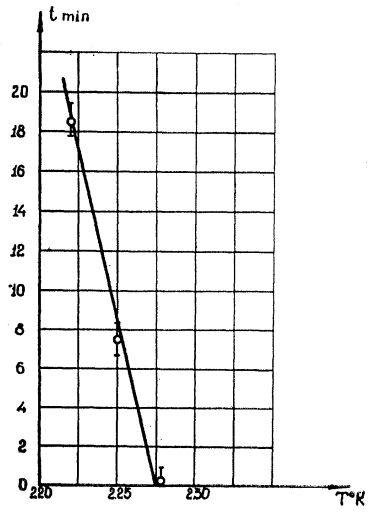

FIG. 11.4. Dependence of the duration of the first portion of Fig. 11.3 on the temperature (Andronikashvili, Gujabidze, and Tsakadze, 1965).

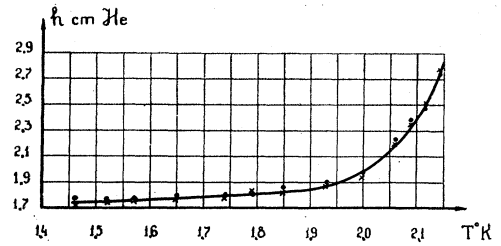

FIG. 11.5. Temperature dependence of the fountain effect in rotating helium II (crosses) and in helium II at rest (points) (Zamtaradze and Tsakadze, 1964).

stretched between two surfaces, are very stable and slowly damping formations until the moment of tearing off. Some decreases of the velocity of the liquid motion inside a vortex line, sufficiently small to escape the direct measurement, causes an increase of pressure along the vortex core. As a result of this pressure increase, a vortex separates from the solid surface and having become free decays. This explains the fact why the largest stability is observed in those vortex line arrays for which the coefficient of sliding is minimum.

This statement is confirmed by the fact that the relaxation time for vortex lines fixed to a smooth surface is four times as small as that for vortex lines fixed to a rough surface (when $\omega_0=\tilde{\omega}_0$).

11.3. Does the Point of the Phase Transition Shift in Rotating Helium II?

Some features of the phase transition in rotating helium described in two previous paragraphs, are very peculiar and extend to rather large temperature intervals.

The conservation of vortex damping in helium I, the delay of the vortex structure formation at the transition from rotating helium I into rotating helium II (9.3), and some other facts made it necessary to perform special investigations of the position of the phase transition point as a function of the angular velocity. With this aim Zamtaradze and Tsakadze (1964) studied the thermomechanical effect in rotating helium II and in helium II at rest near the phase transition point.

At first the experiment was made with a capillary filled with pressed rouge and equipped with an electrical heater, mounted along the rotation axis. The authors made another experiment as well, in which the thermomechanical effect was observed in a narrow annular gap near the cylindrical wall of the rotating container. As Fig. 11.5 shows, the curve of the thermomechanical effect in rotating helium II does not differ from that for helium II at rest.

Bablidze, Tsakadze, and Chanishvili (1964) made another attempt to find the phase transition point shift. With this aim they observed the break on the curve of cooling or heating of a phosphor–bronze thermometer placed in rotating helium and then in liquid helium at rest. This break was connected with a jump of thermal resistivity taking place while helium II

experienced the transition into helium I and vice versa. With the accuracy of 5×10^{-4} °K, the phase transition point remained unshifted until the velocity of rotation $\omega_0=0.56$ sec^{-1}. Later a theoretical estimation (formula 12.4.1) has shown that at maximum velocities of rotation, available at present, a shift of the phase transition could not exceed 10^{-9} °K.

11.4. The Order of the Phase Transition in Rotating Liquid Helium

Phenomena of "overcooling" and "overheating" of motion, characteristic of two states of liquid helium and observed at the phase transition in this liquid, suggested the idea that we are dealing with a first-order transition and not with a second-order one. However, to solve this problem, it was necessary to perform experiments of a thermodynamical and not hydrodynamical character.

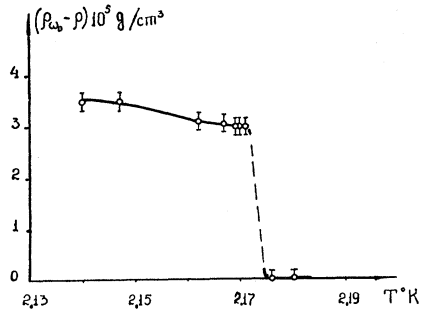

FIG. 11.6. A jump of the density in rotating helium. ρ_{ω_0} is the density at the velocity $\omega_0=30$ sec^{-1}; ρ is the density in helium at rest (Andronikashvili and Tsakadze, 1966).

For direct experiments undertaken with the aim to establish the order of the phase transition in rotating helium II, Andronikashvili and Tsakadze (1965b, 1966) have used the method of a rotating pyknometer. This device was sufficiently sensitive for registration of the slightest changes of the helium density taking place at the change of the temperature or angular velocity of rotation.

The character of the behavior of this magnitude which is the first derivative of the thermodynamical potential, determines the order of the phase transition unambigously.

A pyknometer with a volume of 37.093 cm³, representing a copper cylindrical reservoir, had a glass capillary with an inner diameter of 0.160 cm. In its upper part the capillary was blown into a small sphere and joined to a valve by means of which one could change the level of helium in the capillary. The observations were made by means of a cathetometer. At the rotation of the pyknometer with a velocity of $\omega_0=30$ sec^{-1}, in the temperature interval 2.18°—2.172°K, $\rho_{\omega 0}-\rho$ remains constant, at the further cooling a discontinuity appears, shown in Fig. 11.6. The comparison with the curve of the temperature dependence of density

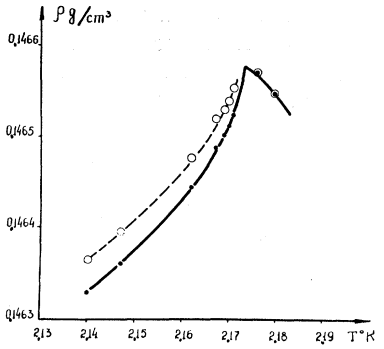

FIG. 11.7. Temperature dependence of densities of rotating helium and helium at rest (Andronikashvili and Tsakadze, 1966). The solid line is Kerr's curve (1957).

obtained by Kerr (1957) (Fig. 11.7) allows us to make the conclusion that the density of liquid helium changes at the phase transition point by a jump of about 0.02%.

That shows that in the state of rotation the order of the phase transition changes: liquid helium under such conditions experiences a phase transition of the first order superimposed on the transition of the second order (see Sec. 12.6).

Pyknometric studies (Andronikashvili and Tsakadze, 1965a,b, 1966) show that helium II brought into rotation increases its density appreciably. This fact contradicts the opinion of many physicists, who thought the vortex structure should reduce helium II density. As seen in Figs. 11.6, 11.7, 11.8 the density change is the higher, the lower in the temperature. An increase of the angular velocity also leads to an increase of helium II density. Naturally such effects are not observed in helium I.

Such experiments were made with a great accuracy (the relative error in the density determination is only 0.0009%).[13] The authors tried to explain the results by an action of the centrifugal pressure, tending to make the liquid more dense at the periphery. However, since the centrifugal pressure is small under the described conditions (it does not exceed 2×10^{-4} atm) the value of the effect $[(\Delta\rho/\rho)_{\max}\sim4\times10^{-4}]$ would

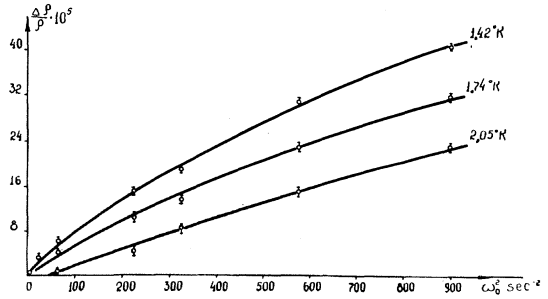

FIG. 11.8. Dependence of the density increase of rotating helium II on velocity and temperature (Andronikashvili and Tsakadze, 1966).

[13] In several experiments of Andronikashivli and Tsakadze (1965a, b) a pyknometer with the volume 52.57 cm³ and with the diameter of the capillary equal to 0.175 cm was used. The change of the level in the capillary was determined within the error ±0.02 cm.

require the value of the coefficient of compressibility exceeding the real value of this magnitude ($\sim 10^{-2}$ atm^{-1}) by two orders. (*Note added in proof.* Bablidze and Gavrilidi have measured the first sound velocity in rotating helium II and showed that its compressibility did not depend on the velocity of rotation.)

Besides, due to the known properties of the coefficient of compressibility, the effect of compression by centrifugal pressure should be increased with an increase of temperature, and the derivative $\partial\rho/\partial\omega_0^2$ should be decreased with an increase of the angular velocity. In reality only a decrease of $\partial\rho/\partial\omega_0^2$ at an increase of ω_0 is observed. But an increase of temperature decreases the observed packing.

12. PHENOMENOLOGICAL AND MICROSCOPIC THEORY OF QUANTUM LIQUID ROTATION

12.1. Phenomenological Quantum Theory of Helium II

The wave function, we mentioned in Sec. 2, while speaking on Feynman's ideas, is a function of coordinates of all the atoms of liquid helium. But a quantum liquid can be described phenomenologically by a simpler wave function depending only on three spatial coordinates (and may be on time). Ginzburg and Pitaevski (1958), proceeding from an analogy with the phenomenological theory of superconductivity of Ginzburg and Landau, suggested using a complex wave function for description of the superfluid component of helium II

$$\psi = f \exp(i\phi). \tag{12.1.1}$$

Its modulus f determines the density of the superfluid component

$$\rho_s = mf^2 \tag{12.1.2}$$

and the phase ϕ determines the velocity of the superfluid component

$$\mathbf{v}_s = (\hbar/m)\nabla\phi. \tag{12.1.3}$$

The condition curl $\mathbf{v}_s = 0$ is maintained automatically here.

A complete set of equations for the phenomenological quantum theory of helium II was obtained by Pitaevski (1958). Further we shall deal only with one equation of this set. It is the equation of equilibrium, valid in the static case. The equation of equilibrium has the following form:

$$\tfrac{1}{2}m[i(\hbar/m)\nabla + \mathbf{v}_n]^2\psi - \alpha\psi + \beta|\psi|^2\psi = 0, \tag{12.1.4}$$

where $\alpha \approx 4.5\times 10^{-17}\ (T_\lambda - T)$ erg and $\beta \approx 4\times 10^{-40}$ erg cm^3, T_λ is the temperature of the λ-transition in an infinite volume of helium at rest. The theory has a sufficient foundation only when $T_\lambda - T \ll T_\lambda$, but one may hope that its qualitative conclusions are valid when $T \ll T_\lambda$ as well.

It should be emphasized that the main peculiarity of this equation is the direct association between the motion of the normal component and the velocity and the density distributions of the superfluid component. This fact distinguishes the phenomenological quantum theory from hydrodynamics formulated in Sec. 4.2, which provides the association between motions of the components only when there are vortex lines (terms with $\mathbf{F}_{sn}$), while the density ρ_s is considered as the constant not dependent on $\mathbf{v}_n - \mathbf{v}_s$.[14]

12.2. Rotating Helium II in the Phenomenological Theory

Kiknadze, Mamaladze, and Cheishvili (1965) used Eq. (12.1.4) to consider uniform rotation of helium II. In this case the motion of the normal component is determined $\mathbf{v}_n = [\boldsymbol{\omega}_0, \mathbf{r}]$ and Eq. (12.1.4) has the form

$$\tfrac{1}{2}m\{i(\hbar/m)\nabla + [\boldsymbol{\omega}_0, \mathbf{r}]\}^2\psi - \alpha\psi + \beta|\psi|^2\psi = 0. \tag{12.2.1}$$

The other equations of the complete set of Pitaevski are reduced to the absence of the temperature gradient and to the requirement of a stationary distribution of all the physical magnitudes in the rotating frame of reference.

It was shown earlier (Ginzburg and Pitaevski, 1958) that Eq. (12.1.4) when $\mathbf{v}_n = 0$ has solutions describing a unit vortex line in an infinite liquid. Then in accordance with formula (2.2.3) the gradient of the wave function phase has the value $|\nabla\phi| = 1/r$ and it is directed along the tangent to the circumference $r =$ const. The same circumferences are the lines of the constant density ρ_s: the modulus of the wave function $f(\mathbf{r}) = f(r)$ is equal to zero on the vortex axis $r = 0$, $f(r) \approx 0.6(\alpha/\beta)^{\frac{1}{2}} r/a_0$, where $r \ll a_0 = \hbar/(2m\alpha)^{\frac{1}{2}}$ and $f(r) \approx (\alpha/\beta)^{\frac{1}{2}}(1 - a_0^2/2r^2)$, when $r \gg a_0$. The parameter a_0 is a characteristic dimension of the theory. It is equal to $a_0 \approx 4.3\times 10^{-8}(T_\lambda - T)^{-\frac{1}{2}}$ and appreciably exceeds interatomic distances in liquid helium only at temperatures very close to T_λ. This parameter represents simultaneously the radius of the vortex core; that is the reason why the symbol a_0 is used.

Kiknadze, Mamaladze, and Cheishvili (1965) have shown that Eq. (12.2.1) also has solutions similar to the just described one, with the only difference that the vortex axis, i.e., the line on which $f = 0$, moves together with the normal component (i.e., it takes part in the rotation of the vessel). Furthermore, it was found that Eq. (12.2.1) has solutions describing the existence of two-dimensional regular lattices of vortex lines in a rotating liquid, similar to vortex lattices of Abrikosov (1957). Such lattices can rotate together with the normal component without distortion of their motion. The distribution of the superfluid component density at the square or triangular symmetry of vortex arrangement coincides exactly with the distribution of superconducting electron density in the corresponding square

[14] The latter circumstance is associated with the fact that only the case of small $|\mathbf{v}_n - \mathbf{v}_s|$ was considered in Sec. 4.2. In the general case Landau's two fluid hydrodynamics and hydrodynamics of rotating helium II as well, take into account the dependence of ρ_n and ρ_s on $\mathbf{v}_n - \mathbf{v}_s$.

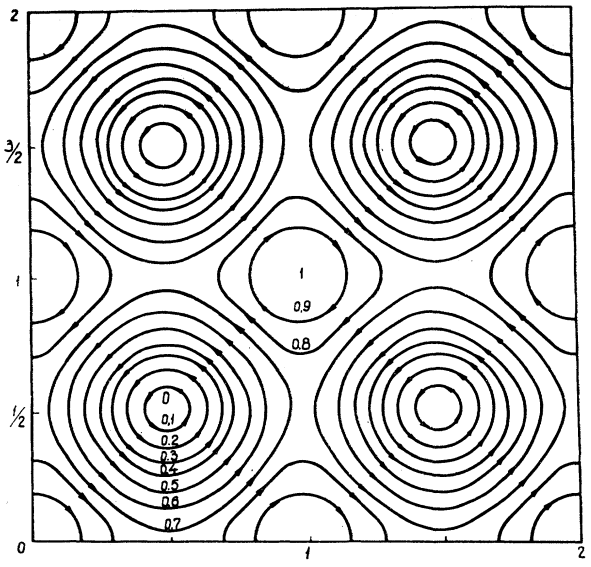

FIG. 12.1. Distribution of the superfluid component density when there is a square lattice of vortex lines in it. Vortex lines are situated in the points where the density is equal to zero. The lines of constant density are shown; values in units of maximum density ρ_s are shown on them. The same lines are the lines of the superfluid component curernt in the reference system rotating together with vortex lines, the normal component, and the vessel. Arrows show the direction of motion. The figure is plotted for the case when $\omega_0 \approx \alpha/\hbar \approx 4.3\times 10^{10}\ (T_\lambda - T)\,\mathrm{sec}^{-1}$ and is taken from Abrikosov's paper (1957).

(Abrikosov, 1957, Fig. 12.1) or triangular (Cleiner, Roth, and Autler, 1964, Fig. 12.2) lattices.[15]

The imaginary part of Eq. (12.2.1) has the form

$$(\nabla f,\ (\hbar/m)\nabla\phi - [\omega_0,\ \mathbf{r}]) = 0, \qquad (12.2.2)$$

and that means the lines of the constant density shown in Figs. 12.1, 12.2 are at the same time lines of a superfluid current in the rotating system of reference. On looking at Figs. 12.1 and 12.2 from this point of view, we cannot help but notice that near the points where f is maximum (we denote them $\mathbf{r}_m$), the superfluid component rotates in the opposite direction with respect to the direction of its rotation around vortex points (where $f=0$). A more detailed consideration shows that in the vicinity of $\mathbf{r}_m$ this rotation is performed according to the law $\mathbf{v}_s \approx -[\omega_0,\ \mathbf{r}-\mathbf{r}_m]$ (the next term of the expansion $\mathbf{v}_s$ over the powers of $\mathbf{r}-\mathbf{r}_m$ is equal to zero). At the transformation to the laboratory system of coordinates, we get $\mathbf{v}_s = [\omega_0,\ \mathbf{r}] - [\omega_0,\ \mathbf{r}-\mathbf{r}_m] = [\omega_0,\ \mathbf{r}_m]$, i.e., the vicinity of any point of $\mathbf{r}_m$ is a domain in which the linear velocity of rotation is constant. But the angular velocity is different for different domains (compare Fig. 12.3). Let us note that Pellam (1962) suggested a model of domains instead of the vortex model of rotating helium II.

The centers of these domains rotate together with the vessel and rotation of the superfluid liquid in the opposite direction takes place inside of them, that provides the constant linear velocity and the equality $\mathrm{curl}\ \mathbf{v}_s = 0$. It is interesting that Pellam's intuition was justified to some extent, but the existence of such domains in intervortex regions was a direct consequence of the vortex existence and there is no necessity to oppose it to the vortex model.

Thus the phenomenological quantum theory has confirmed and made somewhat more precise the quasiclassical considerations taken as the basis of rotating helium II hydrodynamics: the existence of vortex lines, their rotation together with the vessel, the validity of the equation $\mathrm{curl}\ \mathbf{v}_s = 0$ throughout the liquid at the mean velocity characterized by the curl equal to $2\omega_0$. Figure 2.2 given in Sec. 2.4, plotted on the basis of purely qualitative considerations have now obtained a deeper substantiation. In particular, it became known that the curve of the superfluid velocity crosses the line $v_s = \omega_0 r$ in each intervortex space (in the points $\mathbf{r}_m$) being parallel to the abscissa. This makes the velocity distribution closer to the law $v = \omega_0 r$, most favorable thermodynamically.

However, the statement on the advantages of liquid rotation as a solid body now requires a verification. Indeed, for the complex motion of the liquid consisting of two components, the densities of which depend on the character of motion, the variation problem on the minimum of the free energy should be formulated and solved anew.

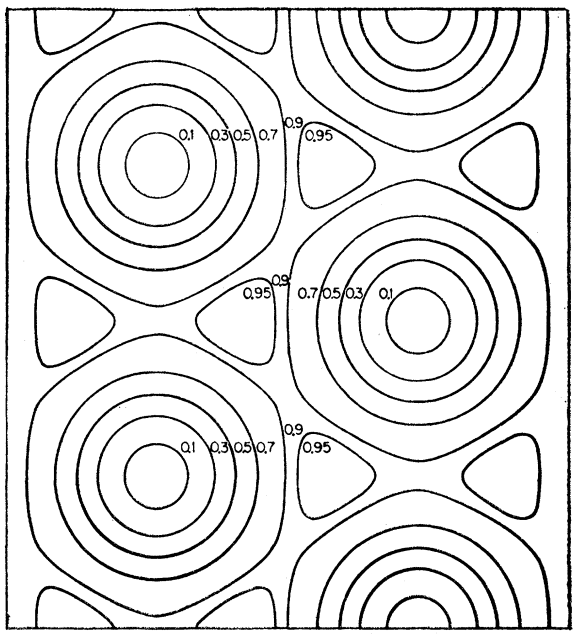

FIG. 12.2. The triangular lattice of vortex lines (compare Fig. 12.1). The figure is taken from the paper of Kleiner, Roth, and Autler (1964).

[15] The existence of Eq. (12.2.1) solutions describing regular systems of vortex lines, does not mean that all such systems are realized (compare Sec. 12.3). Some authors even state that only random, uniform in average, distribution of vortex lines is possible, in difference from superconductors of the second kind. But, we think that this problem is so far open. Ikachenko has shown that a two-dimension vortex lattice with a triangle symmetry is stable.

12.3. Free Energy of Rotating Helium II

The energy e and the angular momentum $\mathbf{l}$ of unit volume of liquid helium II are composed by means of equations

$$e=e_{s0}+\tfrac{1}{2}\rho_s v_s^2+\tfrac{1}{2}\rho_n v_n^2+(\hbar^2/8m^2)[(\nabla\rho_s)^2/\rho_s], \quad (12.3.1)$$

$$\mathbf{l}=[\mathbf{r},\ \rho_s\mathbf{v}_s+\rho_n\mathbf{v}_n], \quad (12.3.2)$$

where e_{s0} is the internal energy and the last term of formula (12.3.1) describes a purely quantum effect, connected with the contribution of any inhomogeneity into energy, due to the relation of uncertainties. The matter is that the statement on the existence of the density gradient is associated with the statement on the concentration of some additional number of particles in some volume, and an uncertainty of momentum, contributing into the kinetic energy, is associated with any restrictions of coordinates of particles.

Expressing ρ_s, $\mathbf{v}_s$, and $\rho_n=\rho-\rho_s$ by a phenomenological wave function ψ, and taking $\mathbf{v}_n=[\boldsymbol{\omega}_0, \mathbf{r}]$, and expanding e_{s0} in powers of ρ_s (Ginzburg and Pitaevski, 1958)

$$e_{s0}=e_{n0}-\alpha f^2+\tfrac{1}{2}\beta f^4 \quad (12.3.3)$$

then the free energy density will have the form

$$e-\mathbf{l}\cdot\boldsymbol{\omega}_0=e_{s0}+(\alpha^2/2\beta)-\alpha|\psi|^2+\tfrac{1}{2}\beta|\psi|^4$$
$$+(\hbar^2/2m)|\nabla\psi|^2-(\hbar/2i)(\psi^*\nabla\psi-\psi\nabla\psi^*, [\boldsymbol{\omega}_0, \mathbf{r}])$$
$$+\tfrac{1}{2}m|\psi|^2\omega_0^2r^2-\tfrac{1}{2}\rho\omega_0^2r^2. \quad (12.3.4)$$

Equation (12.2.1), which we had in Sec. 12.2 is just the solution of the variation problem on the minimum of the integral over the volume of expression (12.3.4). Substituting in its turn this equation into the minimized integral, we obtain the condition

$$\int(e-\mathbf{l}\cdot\boldsymbol{\omega}_0-e_{s0}+\tfrac{1}{2}\rho\omega_0^2r^2)\,dV=\frac{\alpha^2}{2\beta}\int\left(1-\frac{\beta^2}{\alpha^2}f^4\right)dV=\min, \quad (12.3.5)$$

which should be used with the purpose of choosing the most thermodynamically favorable solution of Eq. (12.2.1), when at given boundary conditions it has several solutions.

Let us note that the left-hand side of expression (12.3.5) is the difference of the "kinetic" free energy of rotating helium II and the free energy of rotation as a whole. In other words this condition describes the tendency of helium II to its inaccessible ideal, i.e., to solid body rotation. And the closeness of f to its maximum possible value $f=(\alpha/\beta)^{\frac{1}{2}}$ promotes the approach to such an "ideal."

The direct consequence of condition (12.3.5), which is reduced to the requirement $\int f^4\,dV=\max$, is the advantage of the superfluid component existence in the whole considered volume. The equality $f\equiv 0$ is very undesirable from the point of view of this consideration. Therefore the transition of the whole liquid into the normal state can be realized only because of the absence of nonzero solutions of Eq. (12.2.1) at given boundary conditions (or if there are no solutions with real positive f, which cannot be negative or complex by its definition). When $T=T_\lambda$ the coefficient $\alpha=4.5\times10^{-17}(T_\lambda-T)$ erg becomes zero and the density of the superfluid component vanishes as well, since this density in the stationary infinite liquid is equal to $m\alpha/\beta$ and is proportional to this magnitude in any other case. [The previous statement is connected with the circumstance that Eq. (12.2.1) can be rewritten in a dimensionless form with $|\psi|$ measured in the units $(\alpha/\beta)^{\frac{1}{2}}$.] In the moving liquid or in the presence of boundary surfaces reduction of ρ_s to zero takes place at $T\leq T_\lambda$ as well (a shift of the λ-point).

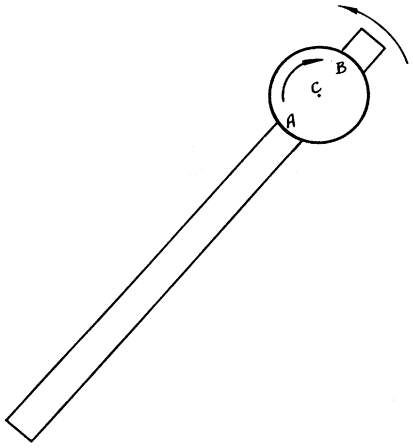

FIG. 12.3. A circle is placed on the rod rotating counter clockwise around the axis passing through one of its ends; the circle itself rotates clockwise. If the velocity at point C is equal to $\omega_0 R_C$, then the velocity at point A is equal to $\omega_0 R_A+\omega_0(R_C-R_A)=\omega_0 R_C$ and the velocity at point B is equal to $\omega_0 R_B-\omega_0(R_B-R_C)=\omega_0 R_C$. Similarly, one can be convinced that all the points of the circle have the same linear velocity $[\omega_0, R_C]$.

12.4. Critical Velocities and the λ-Point Shift

The possibility of reduction of ρ_s to zero [meaning the absence of solutions of Eq. (12.2.1)] is realized in the case of an infinite liquid, rotating with the angular velocity ω_0 which we shall denote as ω_{c2} [16]; $\omega_{c2}=(\alpha/\hbar)\approx 4.3\times10^{10}(T_\lambda-T)$ sec^{-1}. When ω_0 tends to ω_{c2}, the wave function of helium II, rotating in an infinite volume, tends to zero smoothly and disappears gradually (the phase transition of the second order). Thus rotation causes a shift of the point of the phase transition

$$\delta T_\lambda\approx-2.3\times10^{-11}\omega_0\ ^\circ\mathrm{K}, \quad (12.4.1)$$

where ω_0 is measured in sec^{-1}.

Calculations of Kiknadze, Mamaladze, and Cheishvili (1965) leading to the determination of the superfluid velocity near the points $\mathbf{r}_m$ which are the centers of the regions of rotation in the opposite direction were made

[16] The symbol ω_{c2} is introduced as an analogy with the second critical field H_{c2}, at which a superconductor of the second kind becomes normal.

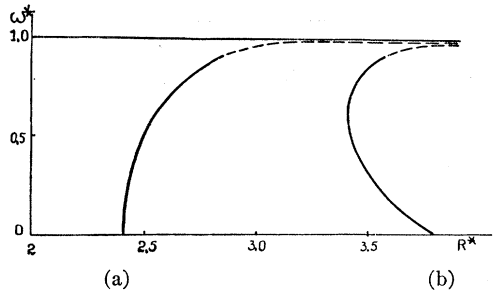

FIG. 12.4. The state diagram of rotating helium II. The symbols: $\omega^*=\hbar\omega_0/\alpha$ is the angular velocity in units $4.3\times10^{10}\,(T_\lambda-T)\,\mathrm{sec}^{-1}$, $R^*=R/a_0$ is the radius of the cylinder in units $4.3\times10^{-8}\,(T_\lambda-T)^{-\frac{1}{2}}$ cm. To the left and above line (a) there is a region of the normal state. To the right and below line (a) there is a region of the superfluid state. The density of the superfluid component is equal to zero on line (a). The existence of vortex lines between lines (a) and (b) is impossible. The existence of a vortex line is allowed to the right and below line (b). The density of the superfluid component on line (b) is equal to zero when there is one vortex line on the axis of the cylinder.

at $\omega_0 \lesssim \omega_{c2}$. The statement of these authors on the possibility of the description of the superfluid rotation picture by Figs. 12.1 and 12.2, also concerns the mentioned range of velocities. Condition (12.3.5) makes us prefer a two-dimensional lattice of vortex lines with the triangular symmetry in comparison with the square one.

Kiknadze and Mamaladze have also determined the critical velocities of rotating helium II at which the superfluid density becomes zero in vessels of finite size. These critical velocities at which helium II passes into the normal state depend on the dimensions of the vessel with a finite radius R (see Fig. 12.4). This figure determines in fact the region of the superfluid state existence on the diagram (ω_0, T), since the dimensionless radius R^* and the dimensionless angular velocity ω^*, used at its plotting are functions of temperature.

The family of curves on the diagram (ω_0, T) corresponds to one curve in Fig. 12.4, each of them is characterized by a definite value of the radius. The change of temperature at the constant radius corresponds to a shift from the right to the left in Fig. (12.4) along the line asymptotically tending to parallelity with the abscissa, when $T\to0$ and to the coincidence with the ordinate, when $T\to T_\lambda$ (see Fig. 12.7). Here since the wave function in the point of intersection of such a line with the curve (a) (taken from Fig. 12.4) becomes smoothly zero, then a shift of the λ-point should occur. As seen in Fig. 12.4 ,at relatively small velocities the phase transition takes place when $R^*\approx2.4$ (more accurately, when $R^*=j_{01}$, where j_{01} is the first root of the Bessel function J_0). Returning to usual units (cm, degree) we obtain

$$\delta T_\lambda \approx -(1.1\times10^{-14})/R^2\ ^\circ\mathrm{K}, \qquad (12.4.2)$$

where R is measured in centimeters. Independence of δT_λ from ω_0 takes place throughout the whole almost vertical portion of curve (a).

Because of a large value of the unit used in Fig. 12.4 of ω_0 measuring, the almost vertical portion of curve (a) overlaps practically the whole interval of the attainable velocities of rotation. At such velocities, an appreciable shift of the λ-point can be observed only in very narrow capillaries [formula (12.4.2)]. At a further increase of ω_0 the shift δT_λ depends both on R and on ω_0, and at last at extremely large ω_0, it hardly depends on R. The transition takes place at $\omega_0=\omega_{c2}$ in the vessel with an arbitrary large radius and δT_λ is determined by formula (12.4.1). As the magnitude a_0, used as a unit of the radius, is very small (if only T is not too close to T_λ), then ω_{c2} is the critical velocity of transition into the normal state for a vessel of any, but not extremely small size.

Using condition (12.3.5), it would be possible in principle to solve the problem of the lower critical velocity ω_{c1}, at which the first vortex line is formed. But in the process of such a calculation great difficulties arise.

An exception is the case of large radii R^*, which involves all practically interesting values of R, if only T is not too close to T_λ. When $R\gg a_0$, the structure of the vortex core has no special role. Therefore, to determine the critical velocity of vortex formation, the considerations which led to the Arkhipov–Vinen formula (2.6.1), for creation of the first vortex line

$$\omega_{c1}\approx(\hbar/mR^2)\ \ln\ (R/a_0) \qquad (12.4.3)$$

and to formula (2.6.4) for the velocity

$$\omega_{c1}'\approx(4\hbar/mR^2)\ \ln\ (\hbar/m\omega_{c1}'a_0^2)^{\frac{1}{2}} \qquad (12.4.4)$$

are sufficient. Here ω_{c1}' is the velocity starting from which the density of vortex lines corresponds to Feynman's formula (2.5.1). Keeping in mind the estimating character of given formulae, we neglect a_0^2 in comparison with R^2 in formula (2.6.1) and do not introduce the numerical factor, determined by Ginzburg and Pitaevski (1958), under the symbol of the logarithm.

As already noted, we could not manage to make these estimates more accurately on the basis of condition (12.3.5), but in spite of that, Kiknadze and Mamaladze having made a qualitative analysis of the problems of vortex formation in rotating helium II, came to certain conclusions discussed in the following paragraphs.

12.5. Why Are Vortex Lines Formed in Rotating Helium II?

According to a quasi-classical consideration, vortex lines are formed to make the superfluid component imitate to some extent the favorable rotation of the liquid as a whole. On the other hand, a vortex line is a node line of the wave function and the density of the superfluid is small in its core. It would seem to create an unfavorable situation from the point of view of condition (12.3.5). But now it will be shown that in reality, strange as it may seem, the existence of vortex lines increases the density of the superfluid component in a

rotating vessel. It should drop catastrophically if vortex lines were not formed or if they were not formed in sufficient number.

This statement is based on the analysis of solutions of two equations, which are the real parts of Eq. (12.2.1)[17] in two different cases: when there is no motion of the superfluid component ($\nabla\phi=0$) and when its motion is caused by the existence of one vortex line on the axis of rotation of the normal component ($|\nabla\phi|=1/r$). When there are no vortex lines, Eq. (12.2.1) has the form

$$(\hbar^2/2m)\Delta f+\alpha f-\beta f^3=\tfrac{1}{2}m\omega_0^2r^2f. \qquad (12.5.1)$$

Rotation, when there is one vortex line in the superfluid component, reduces Eq. (12.5.1) to the form

$$(\hbar^2/2m)\Delta f+\alpha f-\beta f^3=\tfrac{1}{2}m[\omega_0r-(\hbar/mr)]^2f. \qquad (12.5.2)$$

The analytical form of solutions of these equations is determined by the authors only for some particular cases. However, for the purposes of this section, the results of the qualitative analysis are sufficient. It is valid in the general case and it takes into account that an increase of $|\mathbf{v}_n-\mathbf{v}_s|$ leads to a decrease of ρ_s (see Fig. 12.5).

The density of the superfluid component is equal to zero on a solid surface, but at the distance of the order of a_0 from the wall the density of the superfluid component already reaches a value of the order of $m\alpha/\beta$, which is an equilibrium value for an infinite medium (curve 1 in Fig. 12.5; it is implied that $R\gg a_0$). As already noted in Sec. 12.2, $\rho_s=0$ on the vortex line and also reaches the order of $m\alpha/\beta$ at a distance of the order of a_0 from the vortex line axis (curve 3). Rotation of the normal component creates an action similar to that of a vortex line: the density of the superfluid component is smaller in regions where the velocity of rotation is higher. Therefore the difference between the character of rotation of the superfluid liquid taking place according to the law $1/r$ and the character of the rotation of the normal component, obeying the law ω_0r [the right-hand side of equation (12.5.1)] is very essential. In the first case the velocity is infinite when $r=0$ and there $\rho_s=0$, but with an increase of r the velocity drops rapidly and ρ_s increases (curve 3). In the second case when $r=0$, the velocity is equal to zero and ρ_s has its maximum value, but the velocity increases with an increase of r and ρ_s begins to decrease more rapidly. One may show that this decrease becomes especially pronounced at a distance from the axis of the order of $(\hbar/m\omega_0)^{\frac{1}{2}}$ [curve 2, Fig. 12.5 is given in arbitrary units for illustrative purposes, but one should keep in mind that at usual velocities of rotation $(\hbar/m\omega_0)^{\frac{1}{2}}\gg a_0$].

So if in a vessel, the radius R of which exceeds $(\hbar/m\omega_0)^{\frac{1}{2}}$, only the normal component would rotate, the density of the superfluid component in this vessel would be strongly reduced in the whole peripheral region $R>r>(\hbar/m\omega_0)^{\frac{1}{2}}$. In other words, at small velocities of the vessel rotation, the effect of the superfluidity depression by the rotation of the normal component is rarely seen. But when the angular velocity, equal by the order of the magnitude to $\omega_0\sim\hbar/mR^2$ is exceeded, this effect is stronger pronounced.

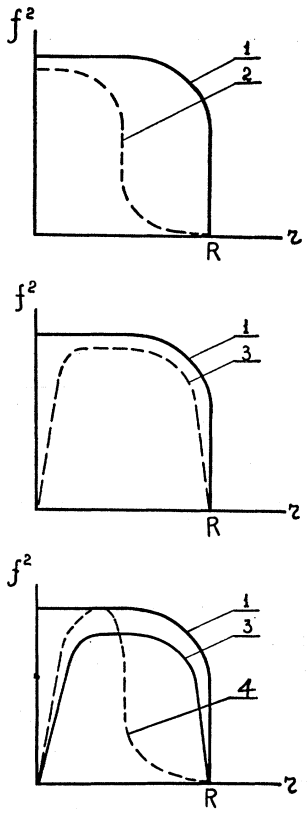

FIG. 12.5. Distribution of the superfluid component density ($\rho_s=mf^2$): (1) in the stationary cylindrical vessel; (2) with rotation of only the normal component ($v_n=\omega_0r$, $v_s=0$); (3) with rotation of the superfluid component caused by the presence of only one vortex line ($v_n=0$, $v_s=\hbar/mr$); (4) when the both components rotate ($v_n=\omega_0r$, $v_s=\hbar/mr$). The drawing is plotted in arbitrary units.

It would seem that the existence of a vortex line also decreasing ρ_s can only make this unfavorable situation still worse. But Eq. (12.5.2) (in the right-hand side of which we have *the difference* of ω_0r and $\hbar/mr$) shows that the effect of rotation of each of the components depressing superfluidity takes place only in the regions $r\ll(\hbar^2/m\omega_0)^{\frac{1}{3}}$ where a vortex line dominates or $r\gg(\hbar/m\omega_0)^{\frac{1}{2}}$, where the normal component dominates. In the region $r\approx(\hbar/m\omega_0)^{\frac{1}{2}}$ the mutual compensation of these influences takes place and the density of the superfluid component reaches the value characteristic of the liquid at rest (curve 4).

Hence two conclusions follow. Firstly, starting from the velocities of the order $\hbar/mR^2$ the formation of vortex lines on the rotation axis can be favorable (compare formula 12.4.3). Really, by decreasing the density ρ_s at the distance of the order of a_0 the vortex promotes its increase in a wider region. Thus it prevents the decrease of ρ_s at a distance from the axis of the order of $(\hbar/m\omega_0)^{\frac{1}{2}}$. Secondly, if the size of the vessel or the velocity of rotation is sufficiently large, then in the presence of a vortex line ρ_s will still decrease some-

[17] The real part of Eq. (12.1.4) has the form

$$(\hbar^2/2m)\Delta f+\alpha f-\beta f^3=\tfrac{1}{2}m(\mathbf{v}_n-\mathbf{v}_s)^2f.$$

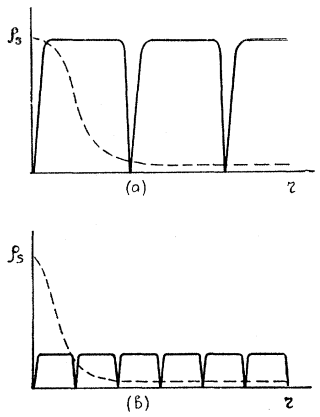

FIG. 12.6. Distribution of the density of the superfluid component in rotating helium II, containing an equilibrium number of vortex lines: (a) at relatively small velocity and (b) at relatively large velocity. The graph is plotted in arbitrary units. The dashed line shows the distribution that would be realized in the absence of vortex lines.

where at distances more than $r\approx(\hbar/m\omega_0)^{\frac{1}{2}}$. Only the appearance of new vortex lines can present this decrease of density ρ_s as they must be distributed apparently uniformly. This distribution should be such that the value of the velocity of the superfluid component would be close to that of the normal component in all the points, excluding those located in the vicinity of vortices. Indeed, the real part of Eq. (12.2.1) has the form

$$(\hbar^2/2m)\Delta f+\alpha f-\beta f^3=\tfrac{1}{2}m\{[\omega_0, \mathbf{r}]-(\hbar/m)\nabla\phi\}^2 \quad (12.5.3)$$

and if $\hbar\nabla\phi/m\approx[\omega_0, \mathbf{r}]$, considerations, treated just now can be repeated. According to them the value of the superfluid component density is close to its value in the liquid at rest. Let us consider an arbitrary point, not too near a vortex line. Such a point can be located at approximately equal distances from nearest vortices. Then their contribution to the magnitude $\nabla\phi$ in the point under consideration is mutually compensated. Or the condition, according to which, $\hbar/mr'$ is not too large in comparison with $\omega_0 r$ should be satisfied. Here r and r' are the distances from the mentioned point to the rotation axis and to the nearest vortex line, respectively. $\hbar\nabla\phi/m$ in such a point differs little from the mean velocity on a circumference with the radius r. That mean velocity is determined by the number of vortex lines N_r in this circumference in accordance with condition (2.2.2). Thus

$$\hbar/m\mid\nabla\phi\mid\approx N_r\Gamma_0/2\pi r, \quad (12.5.4)$$

where $N_r=\pi r^2N$, N is the density of vortex lines. If it is required that equality $\hbar\nabla\phi/m\approx\omega_0 r$ should be valid, then it follows from (12.5.4) that $N\approx 2\omega_0/\Gamma_0$.

That corresponds exactly to Feynman's formula (2.5.1), according to which an area $\pi\hbar/m\omega_0$ corresponds to each vortex line. This area if it were a circumference would have the radius $(\hbar/m\omega_0)^{\frac{1}{2}}$. At a square structure of a vortex lattice the vortex separation is then $(\pi\hbar/m\omega_0)^{\frac{1}{2}}$, at a triangular one it is $(8\pi\hbar/3\sqrt{3}m\omega_0)^{\frac{1}{2}}$. The distribution of ρ_s at such a vortex density is shown schematically in Fig. 12.6. More accurately "the topology" of this distribution was shown in Figs. 12.1 and 12.2 concerning the case when $\omega_0\leq\omega_{c2}$. In the latter case $(\hbar/m\omega_0)^{\frac{1}{2}}$ is comparable with a_0 and maximum values of ρ_s are small (as it was noted $\rho_s\to 0$ when $\omega_0\to\omega_{c2}$). But when $(\hbar/m\omega_0)^{\frac{1}{2}}\gg a_0$, that is valid at any practically achieved velocities ω_0, ρ_s has almost everywhere the value very close to the superfluid component density in an infinite liquid at rest.

Thus vortex lines formed in rotating helium II were found to be the means preventing the breakdown of the superfluidity by rotation of the normal liquid.

12.6. The Character of the Phase Transition in Rotating Helium II

It has already been noted in Sec. 12.4 that a change of temperature of rotating helium II on the diagram (ω^*, R^*) may be represented by a line tending to parallelity with the abscissa when $T\to 0$ and to a coincidence with the ordinate when $T\to T_\lambda$. In Fig. 12.7 there are shown, in addition to the mentioned line, the boundaries of the existence for vortexless and single vortex solutions of Eq. (12.2.1). They are given by curves (a) and (b), which were earlier shown in Fig. 12.4. (Figure 12.7, in contrast to Fig. 12.4, is plotted in an arbitrary scale to the more illustrative.) Curve (c) is also given there, it is a boundary of thermodynamical advantages of the vortex existence. It has been already noted that the curve is computed only in the region $R^*\gg 1$ and $\omega^*\ll 1$, where it is given by formula (12.4.3). The other portion of the curve is plotted (in arbitrary units) on the basis of the following simple considerations. In the immediate vicinity of curve (b), below it, in spite of the fact that here the solution of Eq. (12.5.2) exists, the presence of a vortex line cannot be thermodynamically favorable, because the function f of a single vortex is small. Condition (12.3.5) gives preference to a vortexless situation here. Therefore curve (c) should turn back and repeat in its upper part the outline of curve (b). A similar shape should have the curves confining the regions of thermodynamical advantages of existence of two vortex lines, etc. When $R^*\to\infty$ their upper branches tend to a straight line

$$\omega^*=1 \qquad (\omega_0=\omega_{c2}).$$

Let us now move from the left to the right along the line of helium cooling. Superfluidity will appear in the

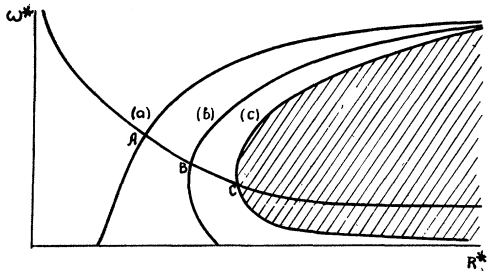

FIG. 12.7. Curve of heating and cooling of rotating helium II on its state diagram. The symbols ω^* and R^* are the same as in Fig. 12.4. The hatched region is the region of the thermodynamical advantages of the existence of vortex lines. The boundary of this region represented by curve (c) is given rather conventionally. The figure is plotted in arbitrary units.

point of intersection with curve (a), and the function f which is the solution of Eq. (12.5.1) increases, beginning from the zero value, i.e., it is continuous in this point. It is the phase transition of the second order, taking place with the shift of the λ-point, that was mentioned in Sec. 12.4. In contrast to the intersection with curve (a), the intersection with curve (b) does not cause any essential consequences. The superfluid liquid remains at rest. Its state changes only at the intersection with the curve (c), when a vortex appears and a new state of the superfluid component is described by the solution of Eq. (12.5.2). This change of the function f takes place by a jump, as only the integrals taken of the fourth power of the modulus of vortexless and single vortex functions ψ are equal to each other on curve (c) [because of condition (12.3.5)], but the functions themselves are different. It is already the phase transition of the first order.

Let us consider this problem in more detail. $\int f_0^4\,dV$ and $\int f_1^4\,dV$ will denote contributions into the free energy of rotating helium II, which are generally speaking different for a vortexless and single vortex states. When point C is approached from the left, the first of these integrals decreases [vortexless state becomes less favorable (12.7)], the second integral increases. In point C itself, the integral $\int f^4\,dV$ is continuous, as $\int f_0^4\,dV=\int f_1^4\,dV$. But here the transition from a decrease of the integral $\int f^4\,dV$ to its increase takes place and hence the derivative ot the integral $\int f^4\,dV$ along the curve of cooling experiences a discontinuity. If we calculate the first derivative of the free energy with respect to temperature, there appears a term

$$\frac{\partial}{\partial T}\int f^4\,dV=\frac{\partial R^*}{\partial T}\frac{\partial}{\partial R^*}\int f^4\,dV+\frac{\partial \omega^*}{\partial T}\frac{\partial}{\partial \omega^*}\int f^4\,dV,$$

i.e., this derivative experiences a discontinuity, and that characterizes the phase transition of the first order. The consideration of the processes of formation of the following vortex lines will lead, apparently, to similar results.

But one should keep in mind, firstly, that the considerations just mentioned are purely qualitative ones, as they are not based on the treatment of the computed portion of the phase diagram. Secondly, only the principal importance should be ascribed to the statement on the character of the phase transition. It means, for instance, that relaxation phenomena connected with vortex formation are possible. But thermodynamical effects of the type of the latent heat can be too insignificant for direct measurement (see, however, Sec. 11.4).

Relaxation effects can significantly influence the character of the considered phenomena. Even at not very rapid cooling, the state of liquid can be vortexless until the values R^* corresponding to a rather large equilibrium number of vortex lines at a given ω^*.

At heating of the liquid, processes proceed in the reverse succession. Here also relaxation phenomena connected with the vortex disappearance are unavoidable. But at an intersection with curve (a) the superfluidity disappears instantaneously.

Under the real conditions of the experiment with the passage through the λ-point, intersections with curves (a) (the point A) and with curve (c) (the point C) and also with the curves confining the regions of two-, three- and many-vortex states, take place almost simultaneously. Thus, some transitions of the first order coincide with the phase transition of the second order. However these transitions of the first order may not take place because of the great probability of overcooling or overheating.

12.7. Rotation of the Ideal Bose Gas

Since at present the microscopic theory of helium II cannot give a complete answer to all the problems encountered by it, the consideration of simplified models becomes especially interesting. Such models are an ideal Bose gas, a rarefied Bose gas, or a system of weakly interacting Bose particles. In particulai only in the theory of these systems is there a microscopic consideration of such problems as vortex core structure, the spectrum of vortex line oscillations, interaction of vortex lines with thermal excitations, determination of the moment of inertia (or the angular momentum) of the rotating substance, etc. A short review of the results of such a type directly concerning the topic of our paper is given in this and the following section.

The problem of rotation of the ideal Bose gas was considered by Blatt and Butler (1955), who have shown that at low velocities of the vessel rotation, the particles, having experienced Bose–Einstein condensation in the state with the zero momentum, do not take part in the rotation and the angular momentum is expressed by the formula

$$L=(T/T_{cr})^{\frac{3}{2}}L_c, \qquad (12.7.1)$$

where T_{cr} is the temperature at which condensation begins, L_c is the classical angular momentum of the liquid rotation as a whole. When $T<T_{cr}$, $L<L_c$ (superfluidity). Beginning from $T=T_{cr}$, $L=L_c$ always (a classical behavior).

When the angular velocity is increased, there arises such a situation, when particles of condensate are involved into rotation. Here the angular momentum experiences a jump with the value $N_0\hbar$, where N_0 is the number of particles in the condensate. The internal energy changes by a jump as well. That takes place at the angular velocity of rotation

$$\omega_1=4.45\hbar/mR^2. \qquad (12.7.2)$$

The further increase of the angular velocity causes again and again such jumps, which are the phase transitions of the first order. As the states of the condensate are described by Bessel functions $J_n(j_{1n}r/R)$ the expression for critical velocity ω_n of each nth transition is connected with the first roots of these functions j_{1n} (compare Sec. 12.4, Fig. 12.4). Having used the

asymptotic expression for j_{1n}, Blatt and Butler have received the following formula for the velocity ω_n, at which the transition into the state with the angular momentum of the condensate $N_0 n\hbar$ takes place:

$$\omega_n \approx [n+2.47n^{\frac{1}{3}}-0.5+O(m^{-\frac{1}{3}})]\hbar/mR^2. \quad (12.7.3)$$

All these phase transitions are very close to each other and *coincide* in fact. At very large n we have $\omega_n \approx n\hbar/mR^2$ and

$$L_n = N_0 n\hbar + \tfrac{1}{2}m(N-N_0)R^2\omega_n \approx \tfrac{1}{2}m(N+N_0)R^2\omega_n$$
$$= [1+(N_0/N)]L_c = [2-(T/T_{cr})^{\frac{3}{2}}]L_c. \quad (12.7.4)$$

The analogy with the behavior of helium II finishes here. At large velocities of rotation the ideal Bose gas has a smoothed angular momentum, even larger than at rotation as a whole. In this association Blatt and Butler spoke of the gas "infrafluidity." The physical reason for such a behavior of the system is the following: because of the properties of the function $J_n(j_{n1}r/R)$, the particles of the condensate are concentrated near the walls of the cylinder and then contributions of each of them into the moment of inertia are close to mR^2. That distinguishes the rotating condensate from the rotating substance with the uniform distribution of particles, in which the mean contribution of a particle into the moment of inertia is $0.5mR^2$.

12.8. Vortex Lines in the Gas of Weakly Interacting Bose Particles and Rotation of Nonideal Bose Gas

The fundamental work of Bogolubov (1947) formed the basis of the microscopic theory of a nonideal Bose gas. It influenced decisively all the following development of the theory. Unfortunately we cannot dwell on those aspects of that theory which do not directly concern the topic of our review. As to its connection with the problem of rotating helium II, it is sufficient to note that the wave function of the condensate in the theory of nonideal Bose gas satisfies, under the conditions of equilibrium, the equation quite similar to Eq. (12.1.4) when $v_n=0$ (Pitaevski, 1961; Gross, 1961).[18]

$$(\hbar^2/2m)\Delta\psi + n_0V_0\psi - V_0|\psi|^2\psi = 0. \quad (12.8.1)$$

Here the modulus and the phase of ψ determine the density and the velocity of the condensate flow similarly as in formulas (12.1.2), (12.1.3), n_0 is the density of the condensate particles in an infinite and stationary liquid. The characteristic dimension in this case is expressed as $a_0=\hbar(2mn_0V_0)^{-\frac{1}{2}}$ and the region of application of the theory is restricted by the requirement of smallness of the product n_0V_0 sufficient that the parameter a_0 would be much larger than interatomic distances.

In the connection of the similarity of Eqs. (12.2.1) and (12.8.1), it is quite clear that the latter of them as well as the former one has solutions describing a single vortex line.

Fetter (1965) has described the array of vortex lines formed in a rotating vessel by an approximate function

$$\psi(\mathbf{r}) = n_0^{\frac{1}{2}}\prod_k \frac{|\mathbf{r}-\mathbf{r}_k|}{[(\mathbf{r}-\mathbf{r}_k)^2+a_0^2]^{\frac{1}{2}}}\exp(i\theta_k), \quad (12.8.2)$$

where $\mathbf{r}_k$ is the coordinate of the kth vortex line, $\theta_k=\arctan[(y-y_k)/(x-x_k)]$. In this approximation he made the minimization of the magnitude $E-L\omega_0$ and became convinced that vortex lines should be distributed with the density corresponding to Feynman's formula (2.5.1) and $L=L_c$ [compare formula (2.6.3)]. The angular momentum value per each particle is equal to $0.5N_R\hbar$, where N_R is the total number of vortex lines in the cylinder with the radius R.

The difference between the results of Blatt and Butler (12.7.4) and those of Fetter ($L=L_c$) is due not only to the circumstance that the former ones considered in fact one vortex line with a large circulation and the latter a lot of vortex lines. The nonlinearity of Eq. (12.8.1) is also very essential. It takes into account the interaction of the particles, due to which the modulus of the wave function is maintained at the constant level equal to $n_0^{\frac{1}{2}}$ everywhere besides the immediate vicinity of vortex lines and that of solid boundaries. Therefore even at consideration of an intensive ($\Gamma=n\Gamma_0$) single vortex line on the axis of the vessel with sufficiently large radius ($R\gg na_0$), the double contribution of condensate particles to the moment of inertia because of their "centrifuging" is not obtained. The expression of the type $J_n(j_{n1}r/R)$ does not already describe the distribution of the condensate particles. $\psi\to 0$ only near the vortex line, but almost throughout the whole vessel $|\psi|\approx n_0^{\frac{1}{2}}$ (see curves 1 and 3 in Fig. 12.5).

Scattering of thermal excitations on vortex lines in a rotating nonideal Bose gas was considered by Iordanski (1964) as well as the force of mutual friction caused by this scattering. Having made more accurate calculations Tordanski (1965b) has shown that the force of mutual friction is not expressed directly by the transport cross section of scattering of thermal excitations on vortex lines as it was assumed in papers of Hall and Vinen (1965b), Lifshitz and Pitaevski (1957), and Pitaevski (1958c). It was found that a model of a weak ideal Bose gas indicates the existence of the Magnus force (see footnote 4), which was not taken into account before the expression for which contains ρ_n and $\mathbf{v}_n$ instead of ρ_s and $\mathbf{v}_s$. As the final results contain only the density ρ_n and the relative velocity $\mathbf{v}_L-\mathbf{v}_n$, they depend little on the model of the substance, Iordanski has calculated the coefficients B and B' for helium II. He has obtained the temperature dependence of B (Iordanski 1965b) similar to that shown in Fig. 7.2 at the symmetric cross section of absorption of exitation

[18] Equation (12.8.1) is put down in the form corresponding to a short-range, repulsive interaction, with the potential

$$U_{12}(\mathbf{r}_1-\mathbf{r}_2) = V_0\delta(\mathbf{r}_1-\mathbf{r}_2).$$

momentum equal to 8.5 Å. The temperature dependence of B' was then greatly different from that shown in Fig. 7.2. The value of $(-B')$ increases monotonously practically from zero at $T=1.1°K$ to about 0.05 at $T=1.7°K$.

12.9. The Rotating Helium II Problem and the Microscopic Theory of Superfluidity

The phenomenological theory of helium II, used in Secs. 12.1–12.6, as has been noted, has a restricted region of application. The quantitative results of this theory are valid only in the region $T_\lambda - T \ll T_\lambda$, when the characteristic dimension a_0 is much larger than interatomic distances. The assumption on, at least, qualitative validity of the conclusions of the phenomenological theory in the whole range of temperatures $0 < T < T_\lambda$, though it seems rather plausible, still awaits its substantiation by the microscopic theory.[19] The microscopic theory of an ideal and even nonideal Bose gas is not sufficient for a complete solution of this problem.

The description of the situation existing nowadays in the microscopic theory of helium II is beyond the scope of this review. Therefore we shall limit ourselves with a short statement on some facts. (See for more detail Chester, 1963.) Papers of Onsager and Penrose (Penrose 1951, Penrose and Onsager 1956, Penrose 1957) allow us to consider superfluidity of helium II as a result of Bose–Einstein condensation of some macroscopic part of atoms in this liquid into the state with zero momentum. The velocity of the superfluid liquid can be considered as the gradient of the wave function phase of the condensate. So far the question of the physical interpretation of the density of the superfluid component is not clear. This density, apparently, does not coincide with the relative density of the condensate. In this connection one cannot consider that the question on the sense of the wave function describing the superfluid component is solved completely. Strictly speaking even the possibility of introduction of such a function at any temperatures is not clear.

The latter question has a direct relation to the conception of Landau–Onsager–Feynman, according to which the superfluid component is an ideal liquid, which can perform only potential ($\operatorname{curl} \nabla\phi \equiv 0$) motions. If the conclusions just mentioned here from the Onsager and Penrose papers obtain sufficiently general basis, then possible doubts in the validity of the conception of Landau–Onsager–Feynman will have no grounds at all and the equations of Landau's two-liquid hydrodynamics will not be considered as only one of the possibilities allowed by a more general consideration (Lin, 1963).

[19] The phenomenological theory of superconductivity, as is known, has received such a substantiation in Gorkov's investigations. The wave function of superconducting electrons was found to be directly connected with the width of the gap in the energy spectrum of a superconductor.

SUMMARY

A rapid and successful development of ideas on the nature of rotating helium II has allowed us, during less than a decade, to obtain a more or less clear understanding of the mechanisms of the phenomena taking place in this liquid, instead of accumulation of paradoxical facts.

A vast experimental material has been collected and a lot of theoretical studies were made, confirming the ideas of curl-free rotation of the superfluid component accompanied by quantization of circulation. Thus a new confirmation was obtained for the assumption of Landau's theory ($\operatorname{curl} \mathbf{v}_s = 0$), the violation of which was the first impression obtained from the experiments on rotation of helium II.

At present much is known on properties of Onsager–Feynman vortex lines which are formed in rotating helium II. Studies of irrotational motion of the superfluid liquid, leading to the creation of gyroscopes, are developed successfully.

Apparently, in the near future one should expect further great successes both in the study of quantized vortex lines and in the study of persistent currents. We think that the main directions, in which such advances are possible and especially desirable, are connected with the problems of the mechanism of vortex formation, stability of vortex arrays, quantum coherence, and the microscopic basis of the theory.

It should be believed that solution of these problems will lead not only to the necessary basis and confirmation of the complete validity of the conception of Landau–Onsager–Feynman, but to the further development of the ideas on the nature of superfluidity as well.

ACKNOWLEDGMENT

The authors wish to acknowledge their gratitude to Mrs. A. R. Azo for her valuable assistance in the preparation of the manuscript of this review, the last chapter of which was written without the participation of E. L. Andronikashvili.

REFERENCES

Abrikosov, A. A., 1957, Zh. Eksperim. i Teor. Fiz. **32,** 1442 [English transl.: Soviet Phys.—JETP **5,** 1174 (1957)].

Andreev, A. F., 1964, Zh. Eksperim. i Teor. Fiz. **46,** 1456 [English transl.: Soviet Phys.—JETP **19,** 983 (1964)].

Andronikashvili, E. L., 1946, J. Phys. USSR **10,** 201.

——, 1948a, Zh. Eksperim. i Teor. Fiz. **18,** 424.

——, 1948b, dissertation, Inst. Fiz. Problem Akad. Nauk SSSR (unpublished).

——, 1948c, Zh. Eksperim. i Teor. Fiz. **18,** 429.

——, 1952, Zh. Eksperim. i Teor. Fiz. **22,** 62.

——, R. A. Bablidze, G. V. Gujabidze, and J. S. Tsakadze, 1964a, Second All Union Congress on Theoretical and Applied Mechanics (Summaries of papers), Moscow, edited by Acad. Sci. USSR, p. 16.

——, R. A. Bablidze, G. V. Gujabidze, and J. S. Tsakadze, 1964b, preprint, Institute of Physics, Akad. Nauk GSSR (unpublished).

——, J. S. Tsakadze, and R. A. Bablidze, 1962, Zh. Eksperim. i Teor. Fiz. **43,** 1562 [English transl.: Soviet Phys.—JETP **16,** 1103 (1963)].

——, R. A. Bablidze, and J. S. Tsakadze, 1965, *Proceedings of the Ninth International Conference on Low Temperature Physics*, J. G. Daunt, D. V. Edwards, F. J. Milford, and M. Yaqub, Eds. (Plenum Press, Inc., New York), p. 155.
——, R. A. Bablidze, and J. S. Tsakadze, 1966, Zh. Eksperim. i Teor. Fiz. **50,** 46 [English transl.: Soviet Phys.—JETP **23,** 31 (1966)].
——, G. V. Gujabidze, and J. S. Tsakadze, 1965, *Proceedings of the Ninth International Conference on Low Temperature Physics*, J. G. Daunt, D. V. Edwards, F. J. Milford, and M. Yaqub, Eds. (Plenum Press, Inc., New York), p. 159.
——, G. V. Gujabidze, and J. S. Tsakadze, 1966, Zh. Eksperim. i Teor. Fiz. **50,** 51 [English transl.: Soviet Phys.—JETP **23,** 34 (1966)].
——, and I. P. Kaverkin, 1955, Zh. Eksperim. i Teor. Fiz. **28,** 126 [English transl.: Soviet Phys.—JETP **1,** 174 (1955)].
——, Yu. G. Mamaladze, S. G. Matinyan, and J. S. Tsakadze, 1961, Usp. Fiz. Nauk **73,** 3 [English transl.: Soviet Phys.—Usp. **4,** 1 (1961)].
——, K. B. Mesoed, and J. S. Tsakadze, 1964, Zh. Eksperim. i Teor. Fiz. **46,** 157 [English transl.: Soviet Phys.—JETP **19,** 113 (1964)].
——, and J. S. Tsakadze, 1958, Bull. Acad. Sci. GSSR **20,** 667.
——, and J. S. Tsakadze, 1959a, Zh. Eksperim. i Teor. Fiz. **37,** 322 [English transl.: Soviet Phys.—JETP **10,** 227 (1960)].
——, and J. S. Tsakadze, 1959b, Zh. Eksperim. i Teor. Fiz. **37,** 562 [English transl.: Soviet Phys.—JETP **10,** 397 (1960)].
——, and J. S. Tsakadze, 1962, Tr. Inst. Fiz. Akad. Nauk Gruz. SSR **8,** 209.
——, and J. S. Tsakadze, 1965a, Phys. Letters **18,** 26.
——, and J. S. Tsakadze, 1965b, ZhETF Pis' ma **2,** 278 [English transl.: JETP Letters **2, 177** (1965)].
——, and J. S. Tsakadze, 1966, Phys. Letters **20,** 446.
——, J. S. Tsakadze, and K. B. Mesoed, 1961, *Proceedings of the Seventh International Conference on Low Temperature Physics* (University of Toronto Press, Toronto), p. 454.
Arkhipov, R. G., 1957, Zh. Eksperim. i Teor. Fiz. **33,** 116 [English transl.: Soviet Phys.—JETP **6,** 90 (1958)].
Atkins, K. R., 1963, *Proceedings of the International School of Physics, "Enrico Fermi"* (Academic Press Inc., New York), p. 403.
Bablidze, R. A., 1965, dissertation, Tbilissi State University.
——, J. S. Tsakadze, and G. V. Chanishvili, 1964, Zh. Eksperim. i Teor. Fiz. **46,** 843 [English transl.: Soviet Phys.—JETP **19,** 577 (1964)].
Bekarevich, I. L., and I. M. Khalatnikov, 1961, Zh. Eksperim. i Teor. Fiz. **40,** 920 [English transl.: Soviet Phys.—JETP **13,** 643 (1961)].
Bendt, P. J., 1961, *Proceedings of the Seventh International Conference on Low Temperature Physics* (University of Toronto Press, Toronto), p. 576.
——, 1962, Phys. Rev. **127,** 1441.
——, R. D. Cowan and J. L. Yarnell, 1959, Phys. Rev. **113,** 1386.
——, and J. A. Oliphant, 1961, Phys. Rev. Letters **6,** 213.
Blatt, J. M., and S. T. Butler, 1955, Phys. Rev. **100,** 476.
Careri, G., 1961, *Progress in Low Temperature Physics* (North-Holland Publ. Co., Amsterdam), Vol. III, Chap. II.
——, 1963, *Proceedings of the International School of Physics. "Enrico Fermi"* (Academic Press Inc., N.Y.), p. 423.
——, W. D. McCormick and F. Scaramuzzi, 1961, *Proceedings of the Seventh International Conference on Low Temperature Physics* (University of Toronto Press, Toronto), p. 502.
——, W. D. McCormick and F. Scaramuzzi, 1962, Phys. Letters **1,** 61.
——, W. D. McCormick and F. Scaramuzzi, 1963, *Proceedings of the Eighth International Conference on Low Temperature Physics* R. O. Davies, Ed. (Butterworths Scientific Publications Ltd., London), p. 88.
Chandrasekhar, S., and R. J. Donnelly, 1957, Proc. Roy. Soc. (London) **A241,** 9.
Chase, C. E., 1960a, Phys. Rev. Letters **4,** 220.
——, 1960b, *Proceedings of the Seventh International Conference on Low Temperature Physics* (University of Toronto Press, Toronto), p. 438.
Cheishvili, O. D., and Yu. G. Mamaladze, 1965, Phys. Letters **18,** 278.
Chester, G. V., 1963, *Proceedings of the International School of Physics. "Enrico Fermi"* (Academic Press Inc., New York), p. 51.
Clow, J. R., D. A. Depatie, J. C. Weaver, and J. D. Reppy, 1965, *Proceedings of the Ninth International Conference on Low Temperature Physics*, J. G. Daunt, D. V. Edwards, F. J. Milford, and M. Yaqub, Eds. (Plenum Press, Inc., New York), p. 328.
Craig, P. P., 1961, Phys. Rev. Letters **7,** 331.
——, 1964, Phys. Rev. Letters **13,** 708.
——, and J. R. Pellam, 1957, Phys. Rev. **108,** 1109.
Depatie, D., J. D. Reppy, and C. T. Lane, 1963, *Proceedings of the Eighth International Conference on Low Temperature Physics*, R. O. Davies, Ed. (Butterworths Scientific Publications Ltd., London), p. 75.
Donnelly, R. J., 1959, Phys. Rev. Letters **3,** 507.
——, 1965, Phys. Rev. Letters **14,** 39.
——, G. V. Chester, R. H. Walmsley, and C. T. Lane, 1956, Phys. Rev. **102,** 3.
Douglass, R. L., 1964, Phys. Rev. Letters **13,** 79.
Eselson, B. N., B. G. Lazarev, K. D. Sinelnikov, and A. D. Shvets, 1956, Zh. Eksperim. i Teor. Fiz. **31,** 912 [English transl.: Soviet Phys.—JETP **4,** 774 (1957)].
Feynman, R. P., 1955, *Progress in Low Temperature Physics* (North-Holland Publ. Co., Amsterdam), Vol. 1, Chap. 2.
——, 1957, Rev. Mod. Phys. **29,** 205.
Gamtsemlidze, G. A., Sh. A. Japaridze, Ts. M. Salukvadze, and K. A. Turkadze, 1966, Zh. Eksperim. i Teor. Fiz. **50,** 323 [English transl.: Soviet Phys.—JETP **23,** 214 (1966)].
——, Sh. A. Japaridze and K. A. Turkadze, 1966, Zh. Eksperim. i Teor. Fiz. **50,** 327 [English transl.: Soviet Phys.—JETP **23,** 217 (1966)].
Ginzburg, V. L., and L. P. Pitaevski, 1958, Zh. Eksperim. i Teor. Fiz. **34,** 1240 [English transl.: Soviet Phys.—JETP **7,** 858 (1958)].
Gopal, E. S. Raja, 1963, Ann. Phys. (N.Y.) **25,** 196.
——, 1964a, Phys. Letters **9,** 230.
——, 1964b, Ann. Phys. (N.Y.) **29,** 350.
Griffiths, D. J., 1964, Proc. Roy. Soc. (London) **A277,** 214.
Gujabidze, G. V., and J. S. Tsakadze, 1966, Zh. Eksperim. i Teor. Fiz. **50,** 55 [English transl.: Soviet Phys.—JETP **23,** 37 (1966)].
Hall, H. E., 1955, Conference de Phusique des Basses Temperature (Paris), p. 63.
——, 1957, Phil. Trans. Roy. Soc. London **A250,** 359.
——, 1958a, Proc. Roy. Soc. (London) **A245,** 546.
——, 1958b, *Proceedings of the Kamerlingh-Onnes Conference on Low Temperature Physics* (Suppl. to Physica **24,** 141).
——, 1960, Phil. Mag. Suppl. **9,** 89.
——, and W. F. Vinen, 1955, Phil. Mag. **46,** 546.
——, and W. F. Vinen, 1956a, Proc. Roy. Soc. (London) **A238,** 204.
——, and W. F. Vinen, 1956b, Proc. Roy. Soc. (London) **238,** 215.
Heikkila, W. J., and A. C. Hollis-Hallett, 1955, Can. J. Phys. **33,** 420.
Hollis-Hallett, A. C., 1953, Proc. Cambridge Phil. Soc. **49,** 717.
Iordanski, S. V., 1964, Ann. Phys. (N.Y.) **29,** 335.
——, 1965a, Zh. Eksperim. i Teor. Fiz. **48,** 708 [English transl.: Soviet Phys.—JETP **21,** 467 (1965)].
——, 1965b, Zh. Eksperim. i Teor. Fiz. **49,** 225 [English transl.: Soviet Phys.—JETP **22,** 160 (1966)].
Kapitza, P. L., 1938a, Dokl. Akad. Nauk SSSR **18,** 21.
——, 1938b, Nature **141,** 74.
——, 1941a, J. Phys. USSR **4,** 181.
——, 1941b, J. Phys. USSR **5,** 59.
Kelvin, W., 1880, Phil. Mag. **10,** 155.
Kemoklidze, M. P., and Yu. G. Mamaladze, 1964a, Zh. Eksperim. i Teor. Fiz. **46,** 165 [English transl.: Soviet Phys.—JETP **19,** 118 (1964)].
——, and Yu. G. Mamaladze, 1964b, Zh. Eksperim. i Teor. Fiz. **46,** 804 [English transl.: Soviet Phys.—JETP **19,** 547 (1964)].
——, and I. M. Khalatvikov, 1964, Zh. Eksperim. i Teor. Fiz. **46,** 1677 [English transl.: Soviet Phys.—JETP **19,** 1134 (1964)].
Kerr, E. C., 1957, J. Chem. Phys. **26,** 511.
Kiknadze, L. V., Yu. G. Mamaladze, and O. D. Cheishvili, 1965, Zh. Eksperim. i Teor. Fiz. **48,** 1520 [English transl.: Soviet Phys.—JETP **21,** 1018 (1965)].
Kleiner, W. H., Z. M. Roth, and S. H. Autler, 1964, Phys. Rev. **133,** A1226.
Kitchens, T. A., W. A. Steyert, R. D. Taylor, and P. P. Craig, 1965, Phys. Rev. Letters **14,** 942.

Koehler, T. R., and J. R. Pellam, 1962, Phys. Rev. **125,** 791.
Landau, L. D., 1941, J. Phys. USSR **5,** 71.
——, 1944, J. Phys. USSR **8,** 1.
——, 1947, J. Phys. USSR **11,** 91.
——, and E. M. Lifshitz, 1953, *Mechanics of Continuum Media* (Gostekhizdat, Moscow).
Lifshitz, E. M., and E. L. Andronikashvili, 1959, *A Supplement to "Helium"* (Consultants Bureau Enterprises, Inc., N.Y.; Chapman and Hall, Ltd., London).
——, and L. P. Pitaevski, 1957, Zh. Eksperim. i Teor. Fiz. **33,** 535 [English transl.: Soviet Phys.—JETP **6,** 418 (1958)].
Lin, C. C., 1959, Phys. Rev. Letters **2,** 245.
——, 1963, *Proceedings of the International School of Physics. "Enrico Fermi"* (Academic Press Inc., New York), p. 93.
Mamaladze, Yu. G., 1960a, Zh. Eksperim. i Teor. Fiz. **39,** 859 [English transl.: Soviet Phys.—JETP **12,** 595 (1961)].
——, 1960b, Seventh All Union Congress on Low Temperature Physics, theses of papers, Kharkov, edited by Acad. Sci. Ukr.SSR, p. 7.
——, 1964, Prikl. Mat. Mekhan. USSR **28,** 952.
——, 1965, Collected papers on Low Temperature Physics, Publishing House "Metsniereba".
——, and S. G. Matinyan, 1960a, Zh. Eksperim. i Teor. Fiz. **38,** 184 [English transl.: Soviet Phys.—JETP **11,** 134 (1960)].
——, and S. G. Matinyan, 1960b, Zh. Eksperim. i Teor. Fiz. **38,** 656 [English transl.: Soviet Phys.—JETP **11,** 471 (1960)].
——, and S. G. Matinyan, 1960c, Prikl. Mat. Mekhan. USSR **24,** 473.
——, and S. G. Matinyan, 1961, *Proceedings of the Seventh International Conference on Low Temperature Physics* (University of Toronto Press, Toronto).
——, and S. G. Matinyan, 1963, Zh. Eksperim. i Teor. Fiz. **44,** 2118 [English transl.: Soviet Phys.—JETP **17,** 1424 (1963)].
——, K. B. Mesoed and J. S. Tsakadze, 1964, Second All Union Congress on Theoretical and Applied Mechanics, summaries of the papers, Moscow, edited by Acad. Sci. USSR, p. 144.
Mehl, J. B., and W. Zimmerman, Jr., 1965, Phys. Rev. Letters **14,** 815.
Meservey, R., 1964, Phys. Rev. **133,** 1471.
Mesoed, K. B., and J. S. Tsakadze, 1961, Bull. Acad. Sci. GSSR **26,** 145.
——, and J. S. Tsakadze, 1963, Tr. Inst. Fiz. Akad. Nauk Gruz. SSR **9,** 147.
Onsager, L., 1949, Nuovo Cimento, Suppl. 2, 249.
Osborne, D. V., 1950, Proc. Phys. Soc. (London) **A63,** 909.
——, 1961, *Proceedings of the Seventh International Conference on Low Temperature Physics* (University of Toronto Press, Toronto), p. 449.
Pellam, J. R., 1960, Phys. Rev. Letters **5,** 189.
——, 1962, Phys. Rev. Letters **9,** 281.
——, 1965, *Proceedings of the Ninth International Conference on Low Temperature Physics,* J. G. Daunt, D. V. Edwards, F. J. Milford, and M. Yaqub, Eds. (Plenum Press, Inc., New York), p. 191.
Penrose, O., 1951, Phil. Mag. **42,** 1373.
——, and L. Onsager, 1956, Phys. Rev. **104,** 576.
Pitaevski, L. P., 1958a, Zh. Eksperim. i Teor. Fiz. **35,** 408 [English transl.: Soviet Phys.—JETP **8,** 282 (1959)].
——, 1958b, dissertation, Institut Fiz. Problem Akad. Nauk SSSR (unpublished).
——, 1958c, Zh. Eksperim. i Teor. Fiz. **35,** 1271 [English transl.: Soviet Phys.—JETP **8,** 888 (1959)].
Rayfield, G. W., and F. Reif, 1963, Phys. Rev. Letters **11,** 305.
——, and F. Reif, 1965, Phys. Rev. **136,** 1194.
Reppy, J. D., 1965, Phys. Rev. Letters **14,** 733.
——, and D. Depatie, 1961, *Proceedings of the Seventh International Conference on Low Temperature Physics* (University of Toronto Press, Toronto), p. 442.
——, and D. Depatie, 1964, Phys. Rev. Letters **12,** 187.
——, D. Depatie and C. T. Lane, 1960, Phys. Rev. Letters **5,** 541.
——, and C. T. Lane, 1961, *Proceedings of the Seventh International Conference on Low Temperature Physics* (University of Toronto Press, Toronto), p. 443.
——, and C. T. Lane, 1965, Phys. Rev. **140,** A106.
Rayleigh, Lord, 1916, *Scientific Papers* (Cambridge University Press, New York), Vol. 6, p. 447.
Snyder, H. A., 1963, Phys. Fluids **6,** 755.
Springett, B. E., D. J. Tanner, and R. J. Donnelly, 1965, Phys. Rev. Letters **14,** 585.
Steyert, W. A., R. D. Taylor, and T. A. Kitchens, 1965, Phys. Rev. Letters **15,** 546.
Tanner, D. J., B. E. Springett, and R. J. Donnelly, 1965, *Proceedings of the Ninth International Conference on Low Temperature Physics,* J. G. Daunt, D. V. Edwards, F. J. Milford, and M. Yaqub, Eds. (Plenum Press, Inc., N.Y.), p. 346.
Taylor, G. I., 1923, Phil. Trans. Roy. Soc. London **A223,** 289.
Tsakadze, J. S., 1962a, Zh. Eksperim. i Teor. Fiz. **42,** 985 [English transl.: Soviet Phys.—JETP **15,** 681 (1962)].
——, 1962b, *Eighth International Conference on Low Temperature Physics,* Preprints of Papers, London, p. 388.
——, 1963a, Zh. Eksperim. i Teor. Fiz. **44,** 103 [English transl.: Soviet Phys.—JETP **17,** 70 (1963)].
——, 1963b, Zh. Eksperim. i Teor. Fiz. **44,** 105 [English transl.: Soviet Phys.—JETP **17,** 72 (1963)].
——, 1963c, Tr. Inst. Fiz. Akad. Nauk Gruz. SSR **9,** 151.
——, 1963d, *Proceedings of the Eighth International Conference on Low Temperature Physics,* R. O. Davies, Ed. (Butterworths Scientific Publications Ltd., London), p. 104.
——, 1963e, Bull. Acad. Sci. GSSR **30,** 25.
——, 1964a, Zh. Eksperim. i Teor. Fiz. **46,** 153 [English transl.: Soviet Phys.—JETP **19,** 110 (1964)].
——, 1964b, Zh. Eksperim. i Teor. Fiz. **46,** 1553 [English transl.: Soviet Phys.—JETP **19,** 1050 (1964)].
——, 1964c, Zh. Eksperim. i Teor. Fiz. **46,** 505 [English transl.: Soviet Phys.—JETP **19,** 343 (1964)].
——, and L. V. Cheremisina, 1966, Zh. Eksperim. i Teor. Fiz. **50,** 58 [English transl.: Soviet Phys.—JETP **23,** 39 (1966)].
——, and I. M. Chkheidze, 1960, Zh. Eksperim. i Teor. Fiz. **38,** 637 [English transl.: Soviet Phys.—JETP **11,** 457 (1960)].
——, and K. B. Mesoed, 1962, Tr. Inst. Fiz. Akad. Nauk Gruz. SSR **8,** 213.
——, and L. Shanshiashvili, 1965, ZhETF Pis' ma **2,** 305 [English transl.: JETP Letters **2,** 194 (1965)].
——, and T. M. Shults, 1960, Tr. Tbil. Gos. Univ. **86,** 51.
Turkington, R. E., J. B. Brown, and D. V. Osborne, 1963, Can. J. Phys. **41,** 820.
Vinen, W. F., 1957a, Proc. Roy. Soc. (London) **A240,** 114.
——, 1957b, Proc. Roy. Soc. (London) **A240,** 128.
——, 1957c, Proc. Roy. Soc. (London) **A242,** 493.
——, 1958a, Nature **181,** 1524.
——, 1958b, Proc. Roy. Soc. (London) **A243,** 400.
——, 1961a, *Progress in Low Temperature Physics* (North-Holland Publ. Co., Amsterdam), Vol. 3, Chap. 1.
——, 1961b, Proc. Roy. Soc. (London) **A260,** 218.
Walmsley, R. H. and C. T. Lane, 1958, Phys. Rev. **112,** 1041.
Wheeler, R. C., C. U. Blakewood, and C. T. Lane, 1955, Phys. Rev. **99,** 1667.
Whitmore, S. C. and W. Zimmerman, 1965, Phys. Rev. Letters **15,** 389.
Woods, A. D. B. and A. C. Hollis-Hallett, 1958, *Low-Temperature Physics and Chemistry,* J. R. Dillinger, Ed. (University of Wisconsin Press, Madison, Wisc.), p. 16.
Zamtaradze, L. A. and J. S. Tsakadze, 1964, Zh. Eksperim. i Teor. Fiz. **46,** 162 [English transl.: Soviet Phys.—JETP **19,** 116 (1964)].

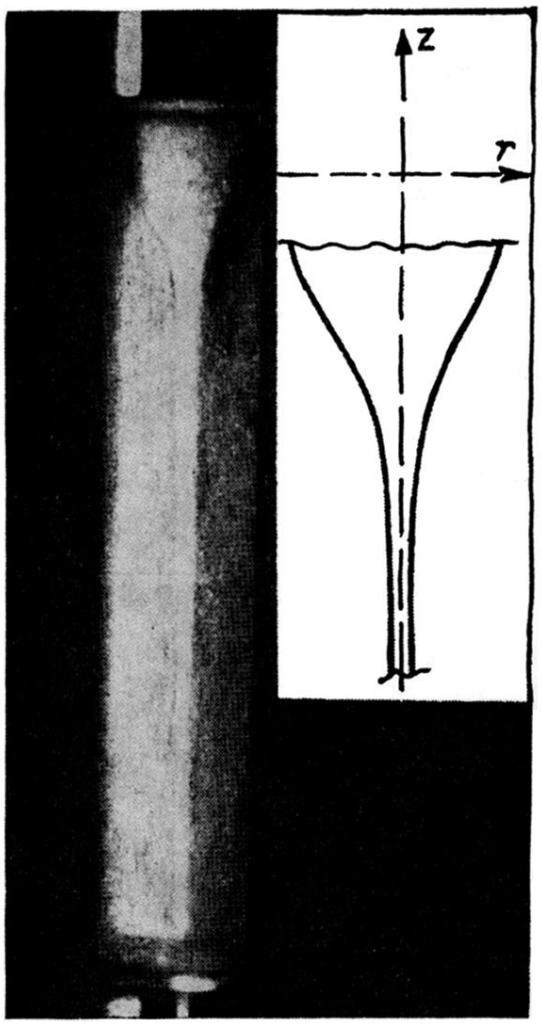

FIG. 11.2. The central macroscopic vortex in helium II: the photograph of the vortex and the result of the calculation according to the formula